Port of Abbot Point Ambient Marine Water Quality Monitoring Program (July 2018 – July 2019)

Nathan Waltham, Christina Buelow, Jordan Iles, James Whinney, Blake Ramsby, and Rachael Macdonald

Report No. 19/30

December 2019

Port of Abbot Point Ambient Marine Water Quality Monitoring Program (July 2018 – July 2019)

A Report for North Queensland Bulk Ports Corporation

Report No. 19/30

December 2019

Prepared by Nathan Waltham, Christina Buelow, Jordan Iles, James Whinney, Blake Ramsby, and Rachael Macdonald

Centre for Tropical Water & Aquatic Ecosystem Research (TropWATER)
James Cook University
Townsville
Phone : (07) 4781 4262
Email: TropWATER@jcu.edu.au
Web: www.jcu.edu.au/tropwater/

Information should be cited as:
Waltham N, Buelow C, Iles, J.A., Whinney J, Ramsby B, & Macdonald R, 2019, 'Port of Abbot Point Ambient Marine Water Quality Monitoring Program (July 2018 – July 2019)', Centre for Tropical Water & Aquatic Ecosystem Research (TropWATER) Publication 19/30, James Cook University, Townsville, 110 pp.

For further information contact:
Dr Nathan Waltham
Centre for Tropical Water & Aquatic Ecosystem Research (TropWATER)
James Cook University
Nathan.waltham@jcu.edu.au

This publication has been compiled by the Centre for Tropical Water & Aquatic Ecosystem Research (TropWATER), James Cook University.

EXECUTIVE SUMMARY

Background

1. In November 2017, North Queensland Bulk Ports implemented an ambient marine water quality monitoring program surrounding the Port of Abbot Point. The objective of the program is to collect a long term water quality dataset to characterise marine water quality conditions within the Abbot Point region, and to support future planned Port activities. This document reports on data collected from July 2018 to July 2019.
2. This program has incorporated a combination of approaches to collect ambient water quality data from the coastal ocean. The approaches adopted include spot field measurements and water sample collection, acquisition of data via deployment of high frequency continuous loggers, and laboratory analysis of samples for a range of nutrients, herbicides and heavy metals.
3. The Port of Abbot Point has five established sites for ambient water quality monitoring whose locations align with key sensitive receptor habitats (e.g. corals or seagrass), along with key features in the study region (e.g. river flow points).

Climatic conditions

1. The total wet season rainfall within the study area during 2018/2019 was above average compared to wet season totals since 1961. Data also shows that there has been high inter-annual variability in rainfall; for example total wet season rainfall in the previous year (2017/2018) was considerably less, and therefore catchment discharge was also considerably less.
2. Inter-annual variability of wet season rainfall and catchment discharge to the coastal ocean highlights the necessity for a long-term commitment to ambient marine monitoring programs, as continued monitoring will allow changes in ambient environmental conditions due to differences in annual rainfall to be better understood and characterised, rather than monitoring and evaluation supported by much shorter time series data sets.
3. The daily average wind speed and direction recorded at Abbot Point for the reporting period was predominantly from the south east, with 30 % of days having wind speeds greater than 24 km hr^{-1}. Wind rarely came from the northwest direction during this reporting period (< 5 % of the days), which is different to other ports under NQBP management.

Water chemistry

1. Field water quality conditions were measured at all sites on a ~6 weekly basis. Parameters collected were water temperature, electrical conductivity, pH, and dissolved oxygen at three depths (surface, mid-water and bottom), along with secchi disk depth and light attenuation.
2. Seasonal differences in water quality were minor, except for temperature which was highest during the summer months; a similar pattern to previous years' reporting.
3. There was little difference in temperature among the three depths examined, indicating that the water column are persistently well mixed on a vertical plane.
4. Particulate nitrogen concentrations exceeded the guidelines throughout most of the 2018-2019 monitoring period, this pattern has remained over previous years monitoring, which outlines the need for a closer examination of sources of particulate nitrogen
5. Chlorophyll-*a* concentrations exceeded the GBRMPA (2010) Water Quality Guideline in most months and all sites surveyed during the 2018-2019 monitoring period.
6. Copper, nickel, and arsenic were detected in water samples collected in August 2018, although the concentrations continue to be below relevant guideline values. No other metals were detected throughout the reporting period.
7. Atrazine, Diuron, Hexazinone, and Tebutryn were detected during all survey in the 2018/2019 period although their concentrations continue to not exceed relevant guideline values. All other pesticides and herbicides tested for during ambient monitoring surveys were below analytical limits of detection.

8. An assessment of the plankton community (both phytoplankton and zooplankton) was completed during this reporting period. Phytoplankton abundance was high over the 2018/19 wet season, while diversity was lowest in February 2018. As the dataset grows, relationships between the plankton community and other physiochemical/nutrient parameters can be statistically evaluated. Evidence of Trichodesmium blooms were again observed during the reporting period, a common phytoplankton that occurs during the warm summer months when conditions are suitable.

Sediment deposition and turbidity

1. RMS water height values were mostly driven by weather events and this is clearly evident in the data as peaks in RMS water heights were observed at the same times at all sites over the survey year. Variation in the magnitude of RMS water height values during peak events and during non-event periods differs among sites due to differences in water depth and site exposure to wave energy.
2. The NTUe/SSC time series data at each site followed a typical pattern of low background values with recurring peak events. These peak events occurred at the same times at each site and coincided with peaks in RMS water height. This is a typical pattern which is similar to data collected in coastal locations in north Queensland
3. Time series deposition data shows that deposition tends to peak following high RMS water height events but with a lag so that peak deposition occurs at a time when RMS water height has decreased to near background levels. An explanation for this lag is that as waves resuspend sediment, little deposition is expected because the energy in the system will keep the sediment in suspension. It is only when waves decrease and there is no longer enough energy in the system to keep the same quantity of sediment in suspension that deposition begins to occur.
4. Current meter data indicates the prominent current direction and velocity at each site and shows that coastal current, tidal current or a combination of both influence current direction and magnitude.

Light attenuation (Photosynthetically active radiation; PAR)

1. Benthic PAR was highly variable within sites throughout the year, with peaks and troughs occurring both regularly and intermittently over time. Semi-regular oscillations between low and high PAR levels were overridden by larger episodic events caused by storm or rainfall events experienced in the region. The data series here continues to increase, which is slowly providing a greater insight into trends, and whether these be tidally influenced or dependent on seasonality and cloud cover. Benthic PAR is also important to assess and validate NTUe sensor data.

Recommendations

1. The program thus far includes five monitoring sites, and it is recommended that these same five sites remain for the 2019/20 period in order to continue to capture local water quality conditions, which will then provide 3 full years of data to thereby base further recommendations on ratiocinations to the ambient water monitoring program.

TABLE OF CONTENTS

TABLE OF FIGURES

1 INTRODUCTION

1.1 Port operations

The Port of Abbot Point is situated in naturally deep waters off the central Queensland Coast (Figure 1.1). The Port of Abbot Point is located approximately 25 kilometres north of Bowen, and North Queensland Bulk Ports Corporation (NQBP) is the Port Authority. The Port has one operating terminal

and provides important services for the surrounding region.

1.2 Program outline

Routine maintenance dredging is periodically required at the Port of Abbot Point to maintain vessel navigational depths, and has only been triggered once in the last 25 years. In order to better define the potential impacts associated with port operations and to characterise the natural variability in key water quality parameters within the adjacent sensitive habitats, NQBP committed to an ambient marine water quality monitoring program in and around the coastal waters of the Port of Abbot Point (Figure 1.1; Table 1.1). As part of this program, water quality parameters are being investigated at a range of sites. This monitoring program contains a range of ambient water quality components that collectively continue to characterise the natural variability in key water quality parameters, including those experienced at the nearest sensitive receiving habitats.

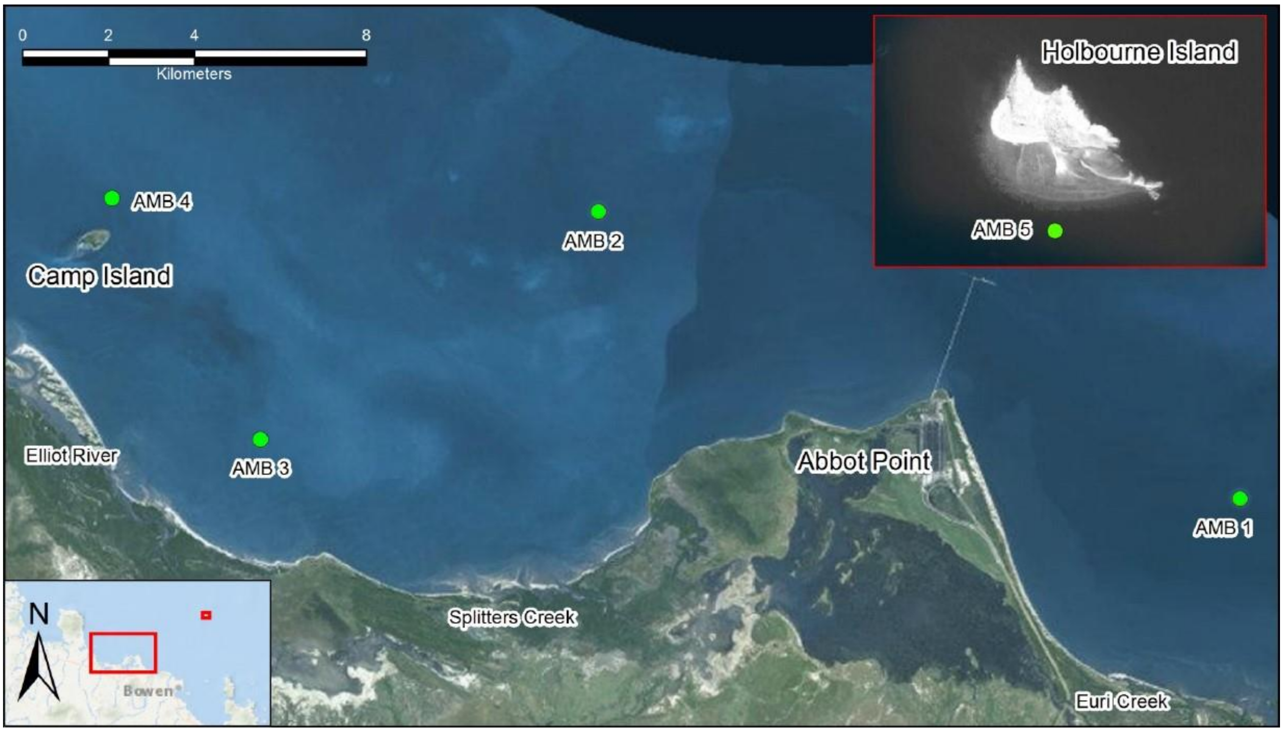

Figure 1.1 Geographical positions for the locations of the ambient marine water quality monitoring program sites at the Port of Abbot Point

Table 1.1 Descriptions for the locations of the ambient marine water quality monitoring program sites

Location	AMB site no.	Lat.	Long.	Water quality	Deposition/PAR logger
Euri Creek	1	-19.9047	148.1418	Yes	Yes
Spoil Grounds	2	-19.8444	148.0077	Yes	Yes
Elliot River	3	-19.8922	147.9368	Yes	Yes
Camp Island	4	-19.8417	147.9058	Yes	Yes
Holbourne	5	-19.7358	148.3593	Yes	Yes

1.3 Rainfall and river flows

Total rainfall during the 2018/2019 wet season period was high in comparison to wet season rainfall totals since 1961/1962 (Figure 1.2). Rainfall in recent years has also been highlighted (Figure 1.2), indicating that the influence of rainfall, and therefore catchment flow, can have high inter-annual variability. This highlights the necessity for long term commitment to ambient marine monitoring programs.

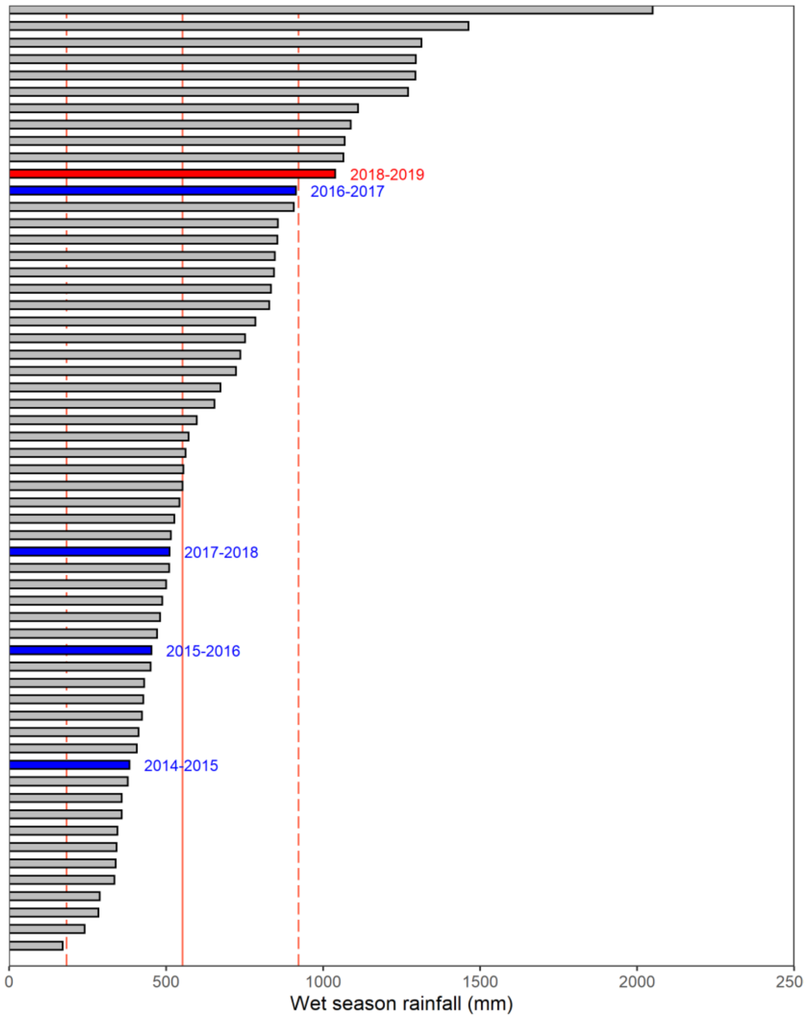

Figure 1.2 Wet season rainfall for the Bowen region ranked in order of decreasing total wet season rainfall (mm). Daily rainfall data was obtained from the Bureau of Meteorology Mount Danger weather station (Station number 033096). Totals were calculated for the wet season period 1st November to 31st March for each reporting year. Red bar represents the current 2018/19 ambient marine water quality monitoring period, blue bars show total rainfall over the previous four years. Solid red line represents median wet season rainfall 1961/62 to 2018/19 and dashed red line represents one standard deviation from the median.

A hydrograph for Euri River near Abbot Point (Figure 1.3) shows a large increase in river discharge at the end of February 2019 due to high rainfall runoff originating from a monsoonal low pressure system (Figure 1.4). River discharge associated with this rainfall event was higher than the maximum flow rate (22,640 ML d^{-1}) recorded during TC Debbie in 2016/2017.

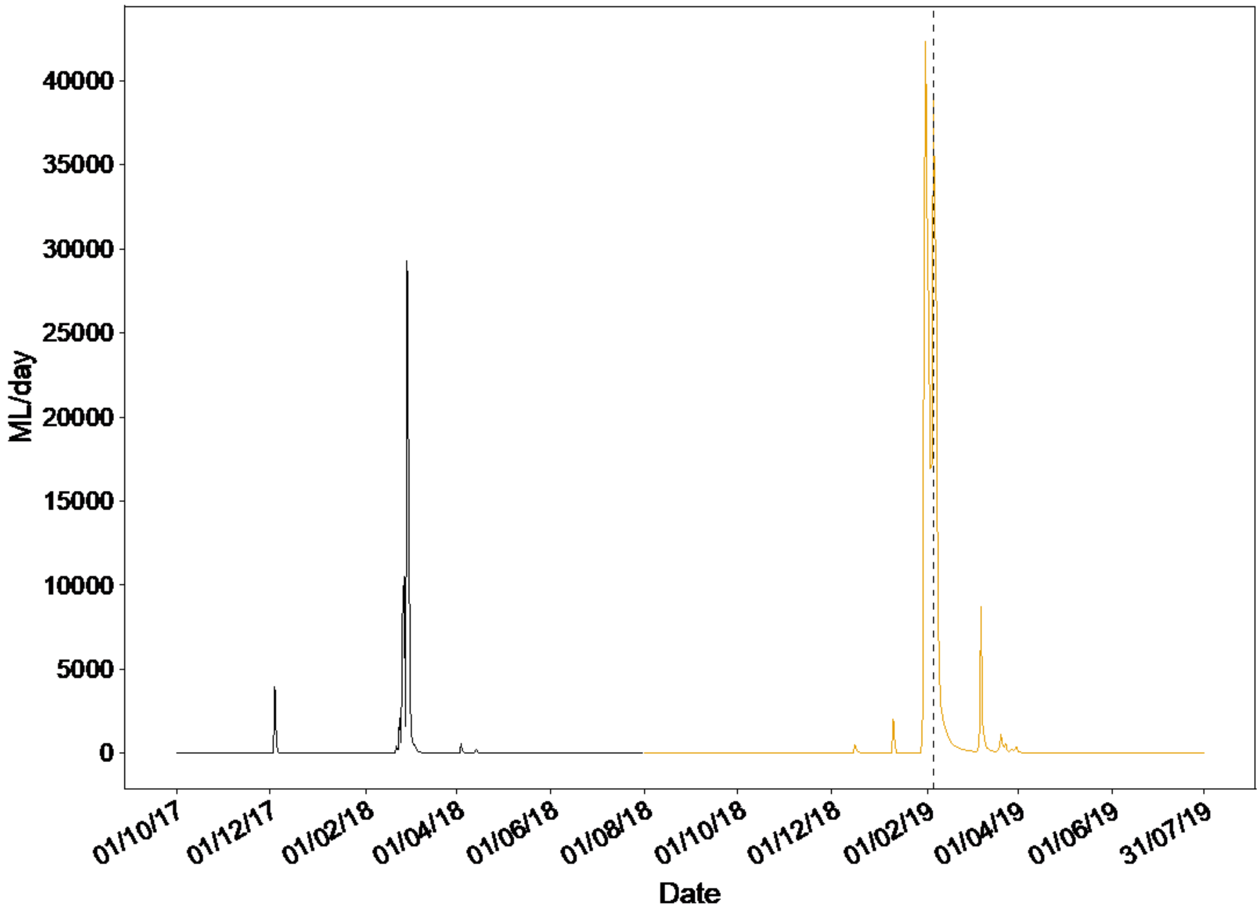

Figure 1.3 Flow (ML d^{-1}) recorded for Euri River (station number: 121004A) during October 2017 – July 2019. The vertical dashed line indicates a period of heavy rainfall due to convergence of a monsoon and low-pressure system (see Figure 1.4).

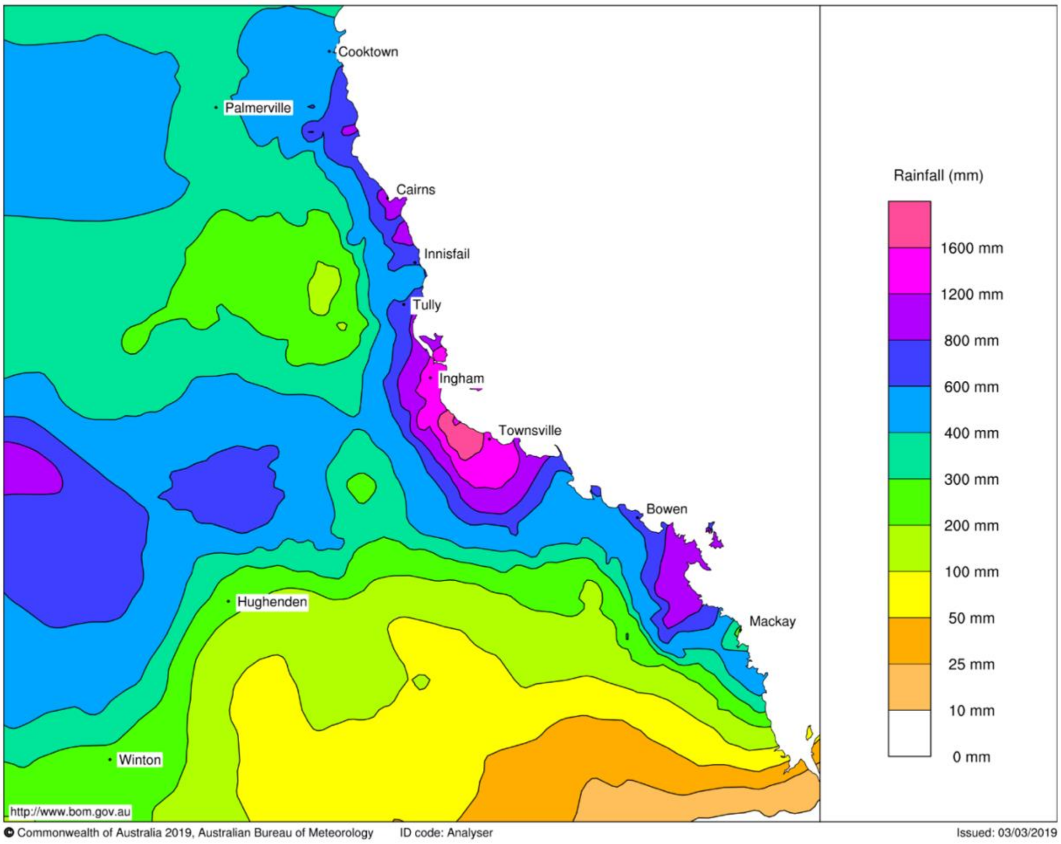

Figure 1.4 Heavy rainfall occurred in the region during 26 January to 9 February 2019 due to convergence of an active monsoon trough and slow-moving low pressure system. Rainfall map sourced from Commonwealth of Australia 2019, Special Climate Statement 69 – an extended period of heavy rainfall and flooding in tropical Queensland.

1.4 Wind for Abbot Point

The daily average wind speed and direction recorded at Abbot Point airport for the reporting period was predominantly from the south east, and ~30 % of days had wind speeds greater than 24 km h^{-1} (Figure 1.5). Wind rarely came from the northwest direction during this reporting period (< 5 % of the days).

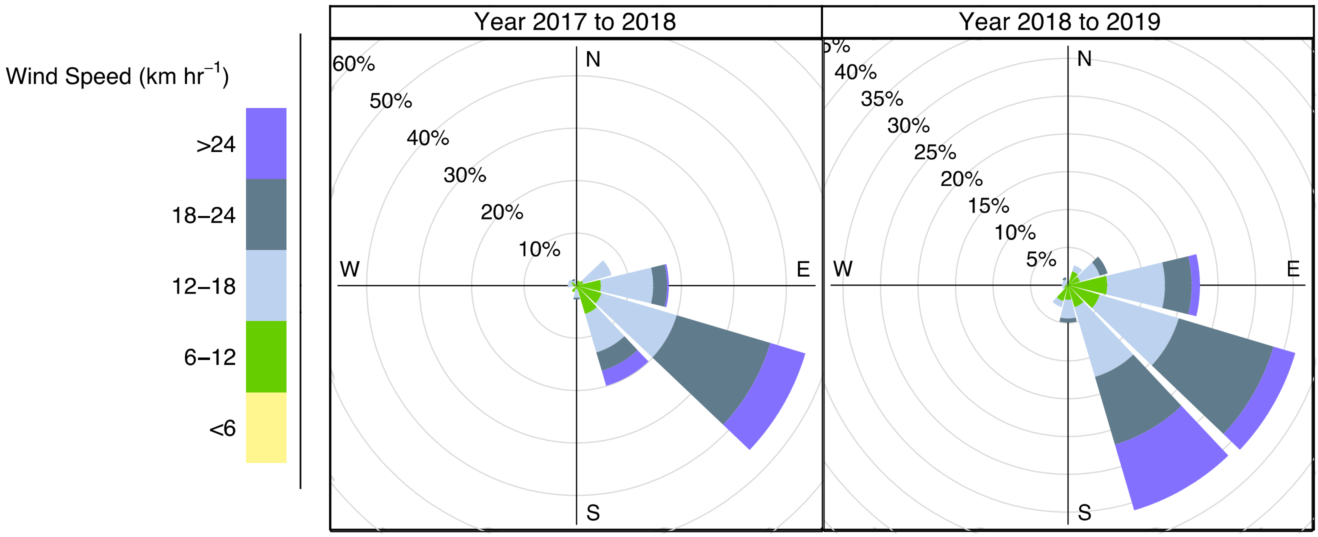

Figure 1.5 Daily average wind direction and strength recorded at Abbot Point in each monitoring period

1.5 Project objectives

The goal of the program is to characterise the ambient marine water quality monitoring within the region and adjacent to the Port of Abbot Point. This report provides a review and analysis of data collected between November 2018 and July 2019. These data are part of a longer-term commitment to monitor and characterise receiving water quality conditions, in particular to support future planned asset management and protection for both these ports.

2 METHODOLOGY

2.1 Ambient water quality

Spot water quality samples were collected at sites approximately on a 6 week basis (Table 1.1) from a research vessel. At each site, a calibrated multiprobe is used to measure water temperature, salinity, dissolved oxygen (%sat), pH, and turbidity (Figure 2.1). In addition to spot measurements, secchi disk depth is recorded, as a measure of the optical clarity of the water column, along with light attenuation using a LiCor meter. These field in-situ measurements are recorded at three depth horizons: a) surface (0.25m); b) mid-depth; and c) bottom horizon. The measurements assist in characterising water quality conditions in the water column.

In considering key priority outcomes outlined in recently published Coastal Strategic Assessment and Marine Strategic Assessments for the Great Barrier Reef World Heritage area (DEHP, 2013; GBRMPA, 2013), the water quality program design below was completed. The list of parameters examined consisted of:

- Ultra-trace dissolved metals : arsenic (As), cadmium (Cd), copper (Cu), mercury (Hg), nickel (Ni), lead (Pb), and zinc (Zn);
- Nutrients (particulate nitrogen and phosphorus);
- Chlorophyll-a;
- Pesticides/herbicides (Low LOR suite (EP234(A-I)) including: diuron, ametryn, atrazine, terbutryn. Note that pesticides are suspected to be in low concentrations during periods of low rainfall runoff, and only detectable following rainfall. As a consequence sampling of only two events at all sites for pesticides, one during the dry and a wet season – though note that the timing of sample collection are dependent on prevailing weather conditions, so the timing of each survey will differ from year to year; and
- Phytoplankton and zooplankton collection occurred four times across this reporting period. The timing of sample collection, similar to pesticides/herbicides, is dependent on prevailing weather conditions, to capture a range of different conditions ranging from wet, dry, late dry, late wet, post wet etc. This strategy maximises the opportunity to sample under different conditions, and overtime a stronger understanding of the variability of plankton communities is possible.

Figure 2.1 TropWATER staff conducting field water quality sampling

Table 2.1 Summary of instrument maintenance and water quality surveys completed during the 2018/19 reporting period

Date	Nutrients, Chloro	Metals, herbicides	Plankton	Logger maintenance
August 2018	Yes	Yes	Yes	Yes
October 2018	Yes	-	-	Yes
November 2018	Yes	-	Yes	Yes

February 2019	Yes	Yes	-	Yes
March 2019	Yes	-	Yes	Yes
May 2019	Yes	-	Yes	Yes
July 2019	Yes	-	-	Yes

Sampling methodology, sample bottles, preservation techniques and analytical methodology (NATA accredited) were in accordance with standard methods (i.e., DEHP 2010; Standards Australia 1998). Field collected water samples were stored on ice in eskies immediately during field trips aboard the vessel, and transported back to refrigeration, before delivery to the TropWATER laboratory. For chlorophyll analysis, water was placed into a 1L dark plastic bottle and placed on ice for transportation back to refrigeration. For dissolved metals and nutrients, water was passed through a 0.45 µm disposable membrane filter (Sartorius), fitted to a sterile 60 mL syringe (Livingstone), and placed into 60 mL bottles (metals) and 10 mL bottles (nutrients) for posterior analysis in the laboratory. (The use of these field sampling equipment and procedures have been previously shown to reduce the risk of contamination of samples, contributing to false positive results for reporting; TropWATER, 2015). Unfiltered sample for total nitrogen and total phosphorus analysis were frozen in a 60 mL tube. All samples are kept in the dark and cold until processing in the laboratory, except nutrients which are stored frozen until processing.

Water for chlorophyll determination was filtered through a Whatman 0.45 µm GF/F glass-fibre filter with the addition of approximately 0.2 mL of magnesium carbonate within (less than) 12 hours after collection. Filters are then wrapped in aluminium foil and frozen. Pigment determinations from acetone extracts of the filters were completed using spectrophotometry, method described in 'Standard Methods for the Examination of Water and Wastewater, 10200 H. Chlorophyll'.

Water samples are analysed using the defined analysis methods and detection limits outlined in Table 2.2. In summary, all nutrients were analysed using colorimetric method on OI Analytical Flow IV Segmented Flow Analysers. Total nitrogen and phosphorus and total filterable nitrogen and phosphorus are analysed simultaneously using nitrogen and phosphorous methods after alkaline persulphate digestion, following methods as presented in 'Standard Methods for the Examination of Water and Wastewater, 4500-NO3- F. Automated Cadmium Reduction Method' and in 'Standard Methods for the Examination of Water and Wastewater, 4500-P F. Automated Ascorbic Acid Reduction Method'. Nitrate, Nitrite and Ammonia were analysed using the methods 'Standard Methods for the Examination of Water and Wastewater, 4500-NO3- F. Automated Cadmium Reduction Method', 'Standard Methods for the Examination of Water and Wastewater, 4500-NO2- B. Colorimetric Method', and 'Standard Methods for the Examination of Water and Wastewater, 4500-NH3 G. Automated Phenate Method', respectively. Filterable Reactive Phosphorous is analysed following the method presented in 'Standard Methods for the Examination of Water and Wastewater, 4500-P F. Automated Ascorbic Acid Reduction Method'. Filterable heavy metals, and herbicides are analysed by Australian Laboratory Service (ALS).

For all water quality plots, boxes are 20th and 80th quantile, centre line is median, and whiskers represent the 5th and 95th percentile.

Table 2.2 Water analyses performed during the program

Parameter	APHA method number	Reporting limit
Routine water quality analyses		
pH	4500-H^+ B	-
Conductivity (EC)	2510 B	5 µS/cm
Total Suspended Solids (TSS)	2540 D @ 103 - 105°C	0.2 mg/L
Turbidity	2130 B	0.1 NTU
Salinity		
Dissolved Oxygen		

Light Attenuation			
Pesticides/herbicides			
Organophosphate pesticides	In house LC/MS method: EP234A	0.0002-0.001 µg/L	
Thiocarbamates and Carbamates	In house LC/MS method: EP234B	0.0002 µg/L	
Thiobencarb			
Dinitroanilines	In house LC/MS method: EP234C	0.001 µg/L	
Pendimethalin			
Triazinone Herbicides	In house LC/MS method: EP234D	0.0002 µg/L	
Hexazinone			
Conazole and Aminopyrimidine Fungicides	In house LC/MS method: EP234E	0.0002 µg/L	
Propiconazole, Hexaconazole, Difenoconazole, Flusilazole, Penconazole			
Phenylurea Thizdiazolurea Uracil and Sulfonylurea Herbicides	In house LC/MS method: EP234F	0.0002 µg/L	
Diuron, Ametryn, Atrazine, Cyanazine, Prometryn, Propazine, Simazine, Terbuthylazine, Terbutryn			
Nutrients			
Total Nitrogen and Phosphorus (TN/TP)	Simultaneous 4500-NO_3^- F and 4500-P F analyses after alkaline persulphate digestion		25 µg N/L
			5 µg P/L
Filterable nutrients (nitrate, nitrite, ammonia, Nox)	4500-NO_3^- F		1 µg N/L
Ammonia	4500- NH_3 G		1 mg N/L
Filterable Reactive Phosphorus (FRP)	4500-P F		1 µg P/L
Chlorophyll	10200-H		0.1 µg/L
Trace Metals			
Arsenic, Cadmium, Copper, Lead, Nickel, Silver, Zinc, Mercury	3125B ORC/ICP/MS		0.05 to 100 µg/L

2.2 Plankton community

At all sites, a 60 µm plankton net (for phytoplankton) and a 500 µm plankton net (for zooplankton) was towed behind the survey vessel for approximately 100 m (Figure 2.2). The nets were towed at a speed of approximately 6 kts, with the position recorded by GPS at the start and end of each plankton tow. At the end of each plankton tow, the nets were retrieved, and the contents retained in the plastic jar attached to the net was immediately transferred to preservation containers. Samples were identified to the lowest possible taxon.

a) b)

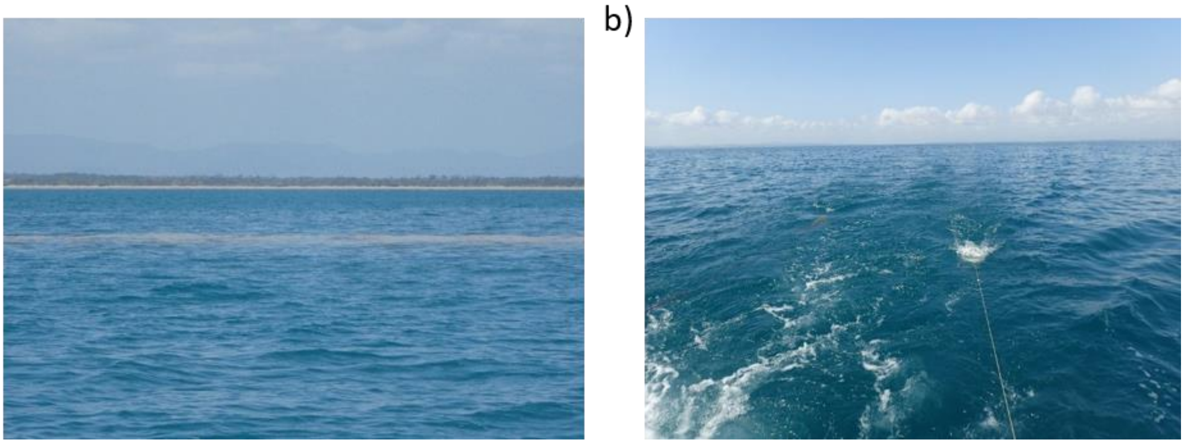

Figure 2.2 Example plankton sample. a) Trichodesmium bloom on sea surface; b) phytoplankton (60µm) tow behind the survey vessel

2.3 Multiparameter water quality logger

Sediment deposition, turbidity, Photosynthetically Available Radiation (PAR), water depth, Root Mean Squared (RMS) water depth and water temperature were measured at seven sites using multiparameter water quality instruments manufactured at the Marine Geophysics Laboratory, School of Engineering and Physical Sciences, James Cook University (Figure 2.3). These instruments are based on a Campbell's Scientific 1000 data logger that has been programmed to measure and store these marine physical parameters using specifically designed sensors.

2.3.1 Turbidity

The turbidity sensor provides data in Nephelometric Turbidity Unit's equivalent (NTUe) and can be calibrated to Suspended Sediment Concentration (SSC) in mg/L (Larcombe et al., 1995). The sensor is located on the side of the logger, pointing parallel light-emitting diodes (LED) and transmitted through a fibre optic bundle. The backscatter probe takes 250 samples in an eight second period to attain an accurate turbidity value. The logger is programmed to take these measurements at 10 minute intervals. The sensor interface is cleaned by a mechanical wiper at a two hour interval allowing for long deployment periods where bio-fouling would otherwise seriously affect readings.

It must be noted the international turbidity standard ISO7027 defines NTU only for 90 degree scatter, however, the Marine Geophysics Laboratory instruments obtain an NTUe value using 180 degree backscatter as it allows for much more effective cleaning. Because particle size influences the angular scattering functions of incident light (Ludwig and Hanes 1990; Conner and De Visser 1992; Wolanski et al., 1994; Bunt et al., 1999), instruments using different scattering angles can provide different measurements of turbidity (in NTU). This has to be acknowledged if later comparison between instruments collecting NTUe and NTU are to be made. To enhance the data, all sites were calibrated to provide a measure of SSC (mg L^{-1}) and enable for the accurate comparison between 90 degree backscatter and 180 degree backscatter measurements.

2.3.2 Sediment deposition

Deposition is recorded in Accumulated Suspended Sediment Deposition (ASSD) (mg cm^{-2}). The sensor is wiped clean of deposited sediment at a 2 hour interval to reduce bio-fouling and enable sensor sensitivity to remain high. The deposition sensor is positioned inside a small cup shape (16 mm diameter x 18 mm deep) located on the flat plate surface of the instrument facing towards the water surface. Deposited sediment produces a backscatter of light that is detected by the sensor. Deposited sediment is calculated by subtracting, from the measured data point, the value taken after the sensor was last wiped clean. This removes influence of turbidity from the value and re-zeros the deposition sensor every 2 hours.

If a major deposition event is in progress, the sensor reading will increase rapidly and will be considerably above the turbidity sensor response. Gross deposition will appear as irregular spikes in the data where the sediment is not removed by the wiper but by re-suspension due to wave or current stress. When a major net deposition event is in progress the deposited sediment will be removed by the wiper and the deposition sensor reading should fall back to a value similar to the turbidity sensor. The data will have a characteristic zigzag response as it rises, perhaps quite gently, and falls dramatically after the wipe (see Ridd et al., 2001).

Deposition data is provided as a measurement of deposited sediment in mg cm^{-2} and as a deposition rate in mg cm^{-2} d^{-1}. The deposition rate is calculated over the 2 hour interval between sensor wipes and averaged over the day for a daily deposition rate. The deposition rate is useful in deposition analysis as it describes more accurately the net deposition of sediment by smoothing spikes resulting from gross deposition events.

2.3.3 Pressure

A pressure sensor is located on the horizontal surface of the water quality logging instrument. The pressure sensor is used to determine changes in water depth due to tide and to produce a proxy for wave action. Each time a pressure measurement is made the pressure sensor takes 10 measurements over a period of 10 seconds. From these 10 measurements, average water depth (m) and Root Mean Square (RMS) water height are calculated. RMS water height, D_{rms}, is calculated as follows:

$$D_{rms} = \sqrt{\sum_{n=1}^{10} (D_n - \overline{D})^2 / n}$$

Equation 1 : where D_n is the nth of the 10 readings and $\overline{D}$ is the mean water depth of the n readings.

The average water depth and RMS water depth can be used to analyse the influence that tide and water depth may have on turbidity, deposition and light levels at an instrument location. The RMS water height is a measure of short term variation in pressure at the sensor. Changes in pressure over a 10 second time period at the sensor are caused by wave energy. RMS water height can be used to analyse the link between wave re-suspension and SSC. It is important to clearly establish that RMS water height is not a measurement of wave height at the sea surface. What it does provide is a relative indication of wave shear stress at the sea floor that is directly comparable between sites of different depths. For example, where two sites both have the same surface wave height, if site one is 10 m deep and has a measurement of 0.01 RMS water height and site two is 1m deep and has a measurement of 0.08 RMS water height. Even though the surface wave height is the same at both sites, the RMS water height is greater at the shallower site and we would expect more re-suspension due to wave shear stress at this site.

2.3.4 Water temperature

Water temperature values are obtained with a thermistor that records every 10 minutes. The sensor is installed in a bolt that protrudes from the instrument and gives sensitive temperature measurements.

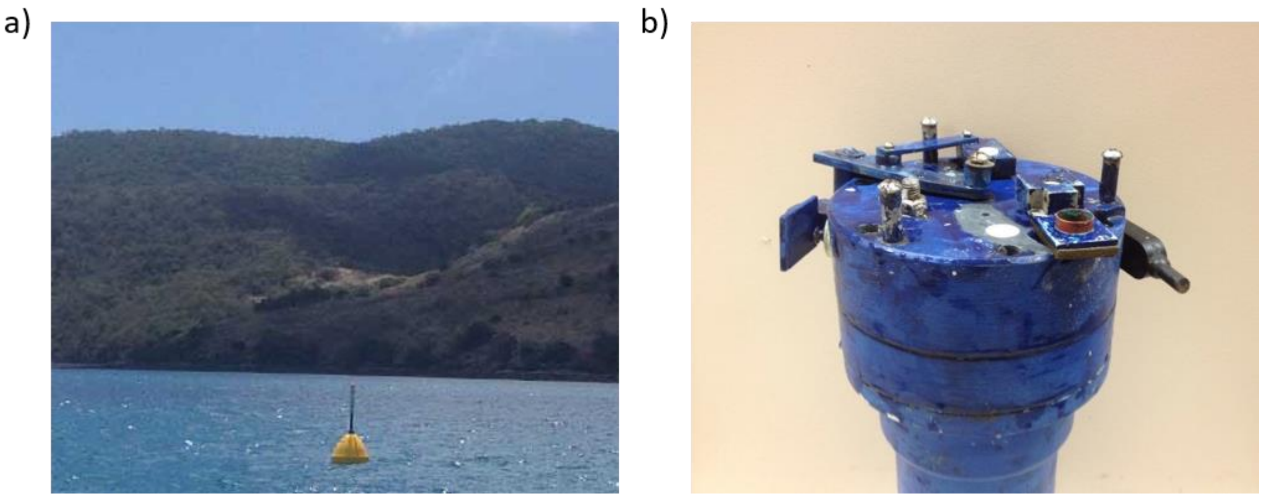

Figure 2.3 Example coastal multiparameter water quality instrument: a) site navigation beacon for safety and instrument retrieval; b) instrument showing sensors and wiping mechanisms

2.3.5 Photosynthetically Active Radiation (PAR)

A PAR sensor, positioned on the horizontal surface of the water quality logging instrument, takes a PAR measurement at ten (10) minute intervals for a one second period. To determine total daily PAR (mol m^{-2} d^{-1}) the values recorded are multiplied by 600 to provide an estimate of PAR for a 10 minute period and then summed for each day.

2.4 Marotte current meter

The Marotte HS (High Sampling Rate) is a drag-tilt current meter invented at the Marine Geophysics Laboratory (Figure 2.4). The instrument records current speed and direction with an inbuilt accelerometer and magnetometer. The current speed and direction data are smoothed over a 10-minute period. The instruments are deployed attached the nephelometer frames and data is download when the instruments are retrieved. Inclusion of this current meter has been added to the program as a way to trial new technology, gather new data and to add value to the project outcomes and deliverables.

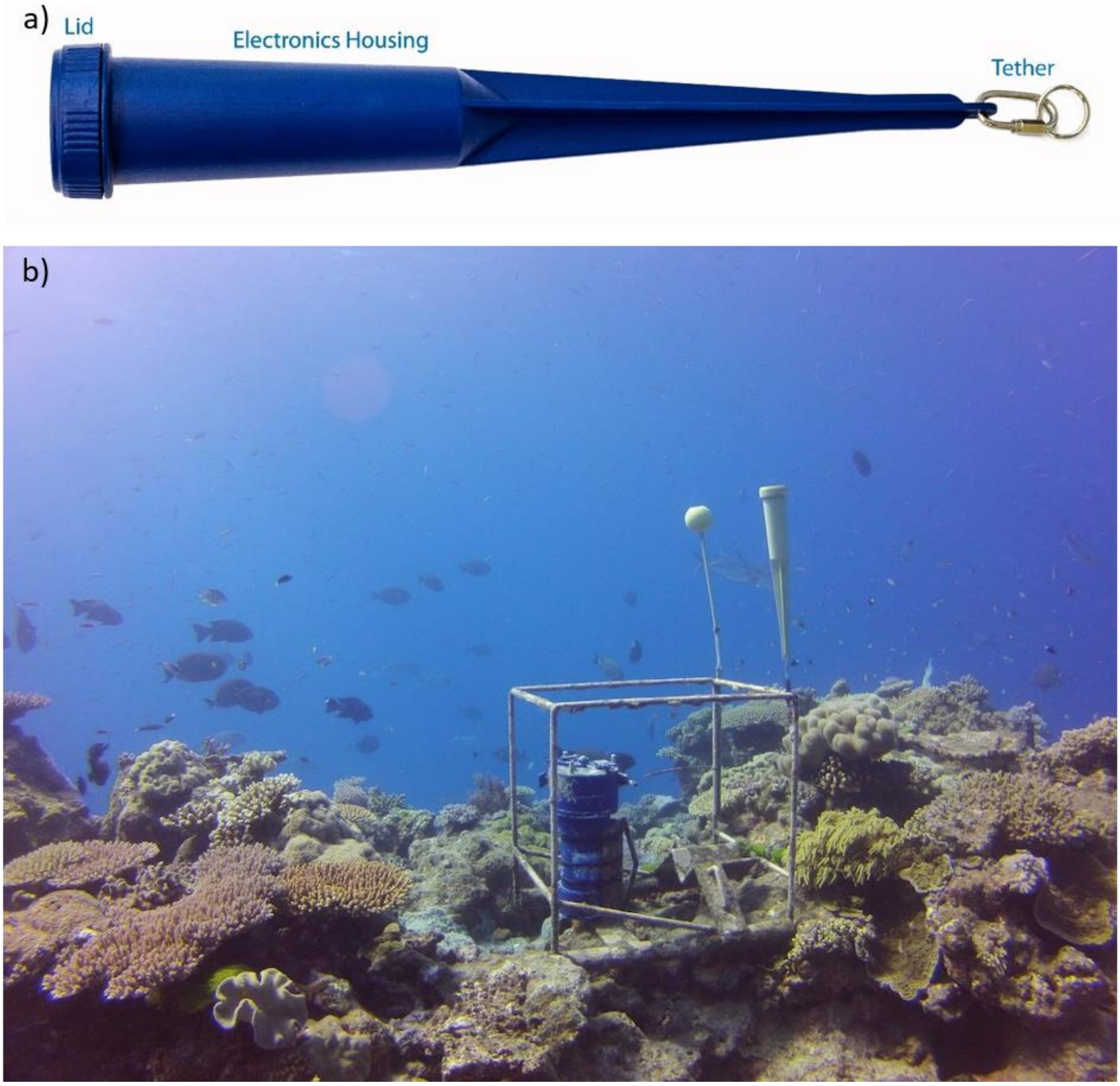

Figure 2.4 a) Basic schematic of Marotte HS current meter; and b) Marotte HS alongside Marotte at Moore Reef. Image courtesy of Eric Fisher

2.4.1 Measuring environmental controls on SSC

Stepwise regression analysis was used to investigate the environmental controls on SSC at the ambient sites, with data selected including:

(a) Ambient sites:

[1] "AMB1"[2] "AMB2"

[3] "AMB3"[4] "AMB4"

[5] "AMB5"

(b) River Gauge Station:

[1] "Euri"[2] "Don"

(c) Wind Station:

[1] "Station 33327 – Bowen"

(d) Tide Gauge Station:

[1] "Bowen"

In this assessment, the environmental parameters with control on SSC were analysed by stepwise regression analysis followed by relative importance analysis (Grömping, 2006) using R language (R Core Team, 2015). The stepwise analysis allowed the selection of the environmental variables that explain the SSC variability in the water column. The relative importance analysis allowed these selected variables to be ranked based on their overall explanation of the SSC variability. In order to visualize the effect of each environmental parameter selected in the stepwise analysis, a partial plot analysis (Crawley, 2007) was carried out. These partial plots indicate the dependence between SSC and each selected variable when all the other variables in the model are kept constant (Crawley, 2007). The data set used in the stepwise analysis was log-transformed, if needed, in order to satisfy requirements for regression analysis. For each site, all the following variables were tested in an initial model against SSC: RMS of water depth, mean daily wind, maximum tide amplitude and the Don and Euri River discharges. These rivers were selected due to their proximity to the sampling sites. Mean daily wind was calculated from 8 daily readings decomposed into NE-SW and NW-SE components. Maximum tide amplitude was calculated as the maximum absolute difference between two consecutive maximum or minimum tide readings. Wind components were calculated as the mean value of 8 daily measurements decomposed to in two diagonals, NE-SW and NW-SE. Variables presenting autocorrelation were excluded based on a variance inflation test (Fox and Monett, 1992) > 4 and outliers were removed based on Bonferroni Outlier Test (Cook and Weisberg 1982).

3 RESULTS AND DISCUSSION

3.1 Ambient water quality

3.1.1 Spot water quality physio-chemical

For the reporting period between July 2018 and July 2019 water temperature ranged between 21 and 30 °C (Figure 3.1). There is a strong seasonal effect on water temperatures in the region, with the highest water temperatures observed during surveys in the summer months, and cool water temperatures observed during the winter months (Figure 3.1). These patterns are consistent throughout the water column, indicating that the water column profile is vertically well mixed. There are no guidelines for water temperature in coastal areas, however, temperature is an essential interpretative aid for ecological assessment in environments. For example, species such as fish and other animals have thermal stress point which causes discomfort and could be misconstrued as being a toxicological impact (example are the coral trout; Johansen et al. 2015). There were no observed or known impacts on aquatic species in the region during this monitoring period.

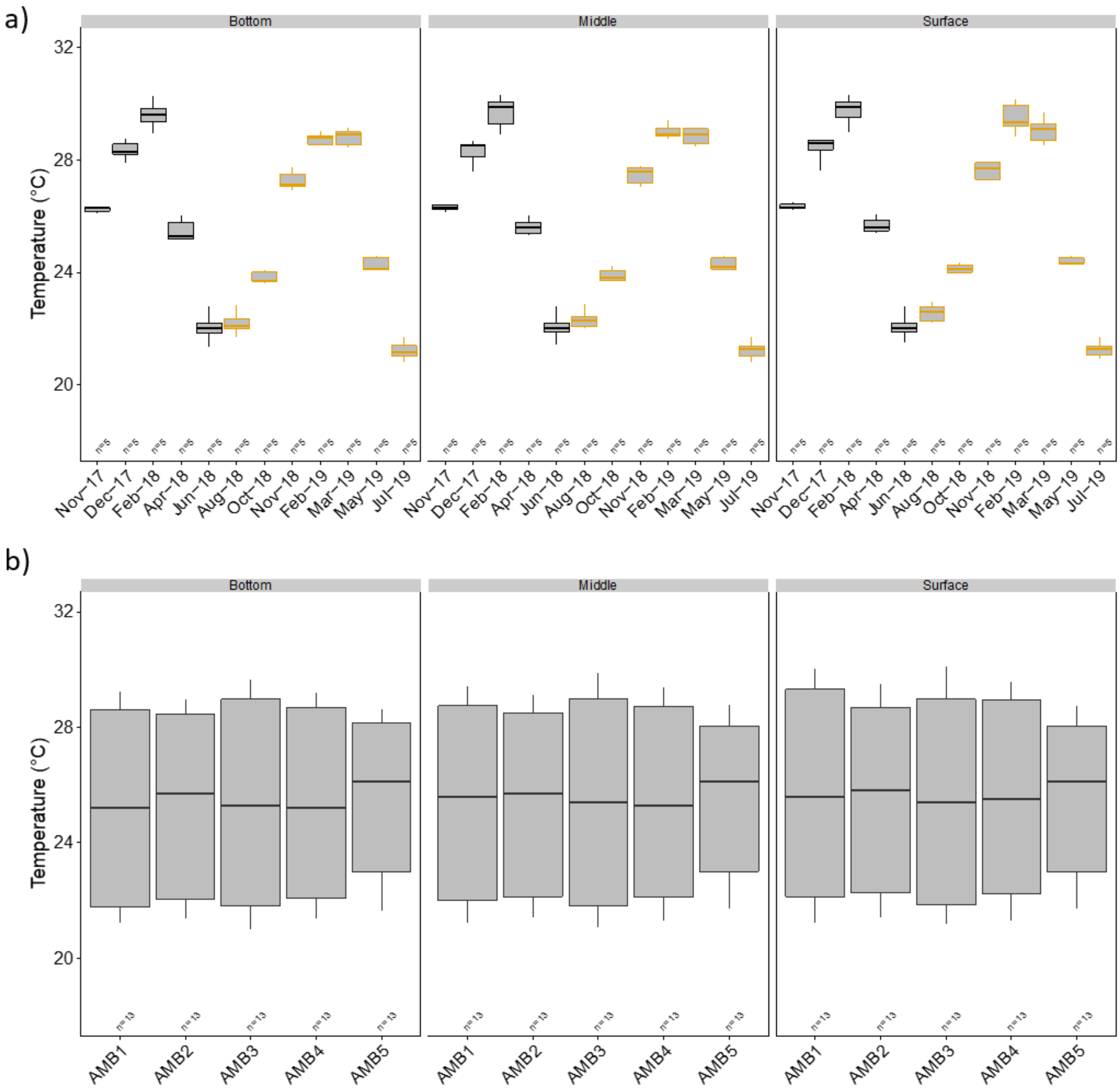

Figure 3.1 Water temperature box plots recorded: (a) the three depth horizons during each survey (sites pooled) where colour indicates monitoring period: black = 2017/2018 and orange = 2018/2019; and (b) the three depth horizons for each site (pooled across all monitoring periods 2017-2019)

Electrical conductivity (EC) values (i.e. November 2018 – July 2019) show higher variability, but overall EC has remained between 51 mS cm^{-1} and 55 mS cm^{-1}, generally indicating oceanic conditions (Figure 3.2a). EC is stable among sites, with little evidence of changing conditions throughout the water column, and across surveys (Figure 3.2).

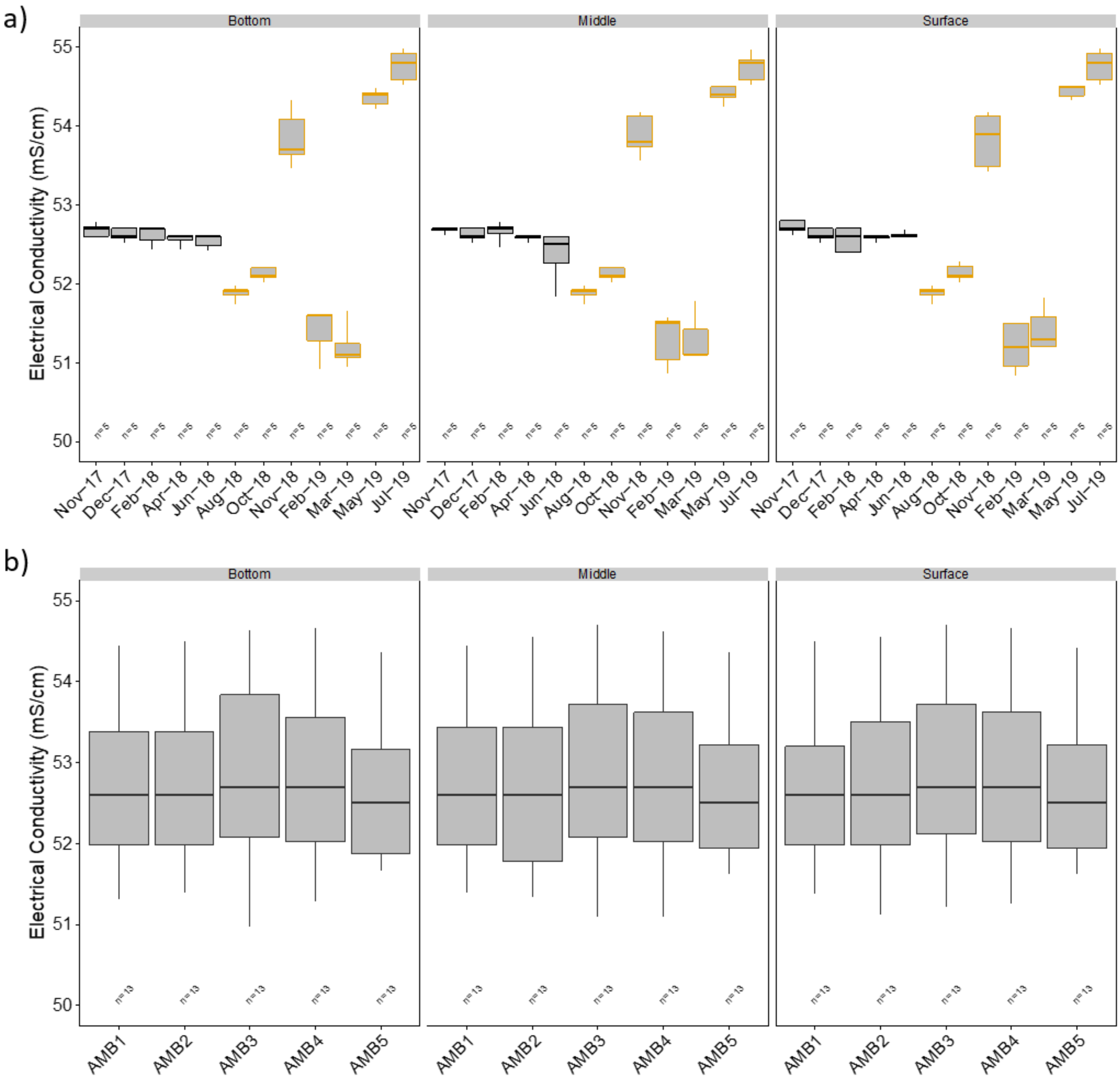

Figure 3.2 Electrical conductivity box plots recorded: (a) the three depth horizons during each survey (sites pooled) where colour indicates monitoring period: black = 2017/2018 and orange = 2018/2019; and (b) the three depth horizons for each site (pooled across all monitoring periods 2017-2019)

Dissolved oxygen saturation ranged between 83 to 109 % (Figure 3.3) and were similar across sites (Figure 3.3b). There was some variability among sampling months, with the lowest concentrations recorded in November 2017 (Figure 3.3a). The water column continues to be well mixed although there is a subtle oxycline with dissolved oxygen concentrations decreasing with depth (Figure 3.3). Field pH measurements were also similar across sites and depths, primarily ranging between 7.4 and 9.0 (Figure 3.4). However, higher variability in pH measurements was recorded during the current monitoring period in comparison to the previous monitoring period (Figure 3.4a).

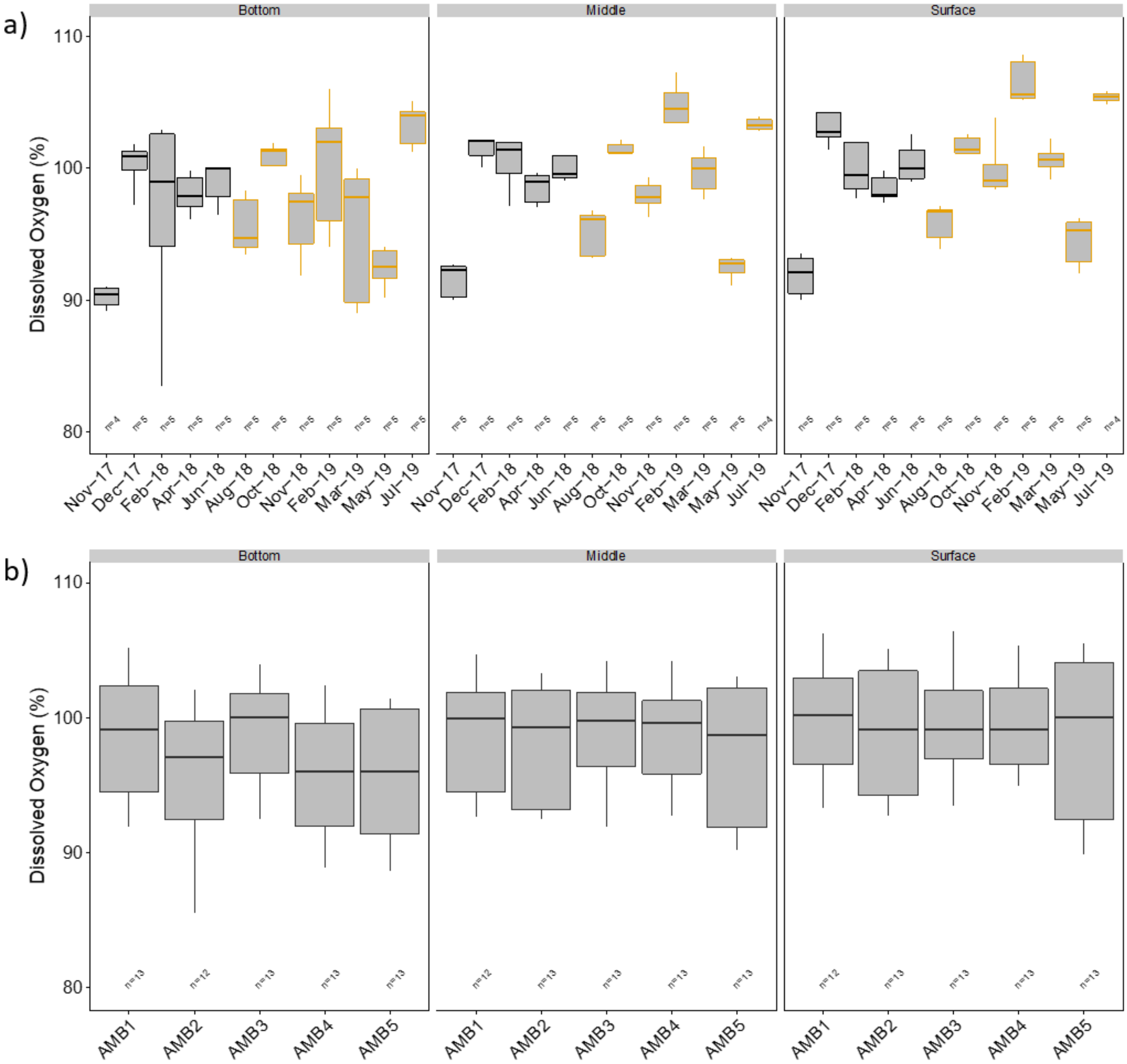

Figure 3.3 Dissolved oxygen box plots recorded: (a) the three depth horizons during each survey (sites pooled) where colour indicates monitoring period: black = 2017/2018 and orange = 2018/2019; and (b) the three depth horizons for each site (pooled across all monitoring periods 2017-2019)

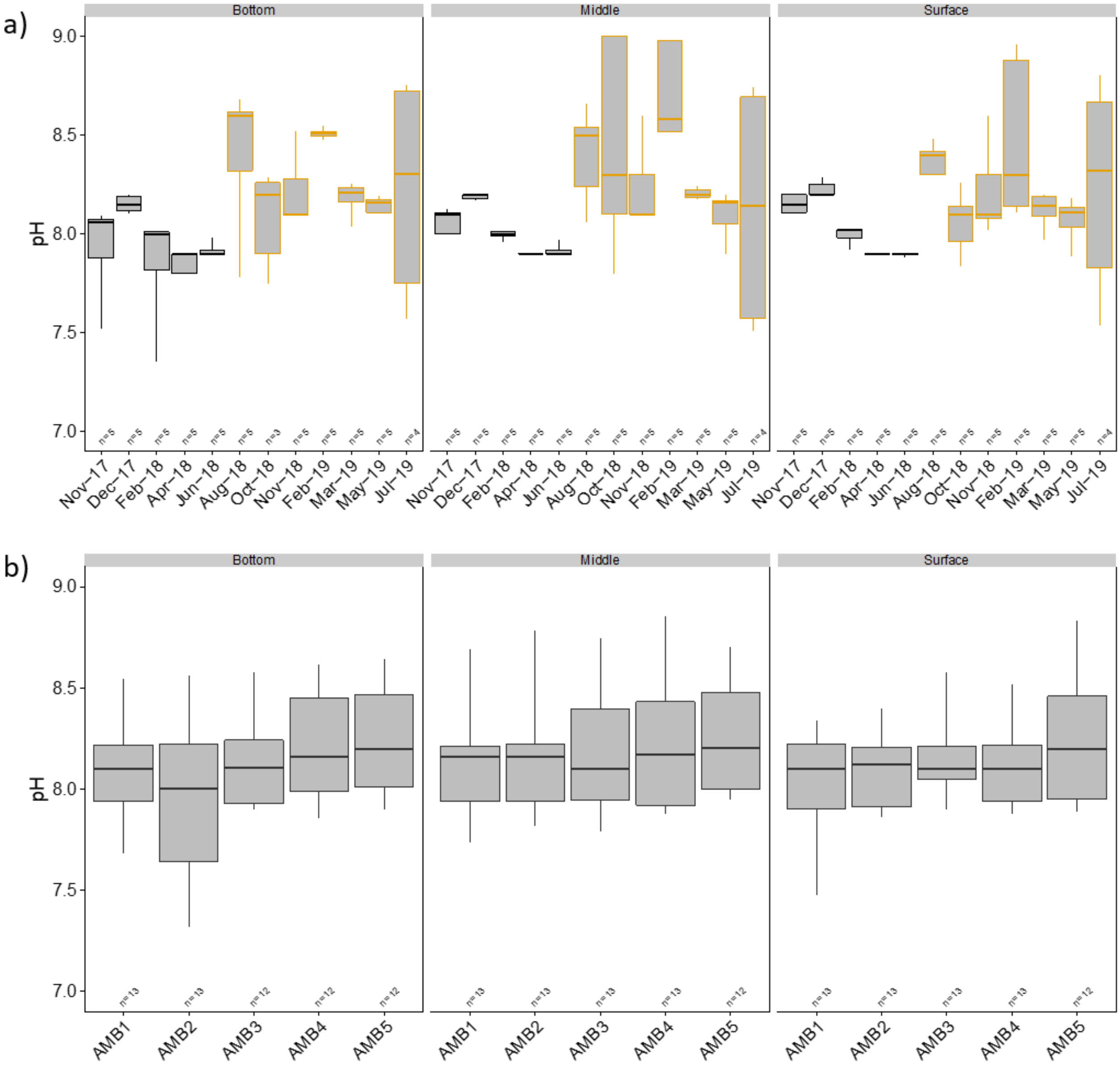

Figure 3.4 pH box plots recorded: (a) the three depth horizons during each (sites pooled) where colour indicates monitoring period: black = 2017/2018 and orange = 2018/2019; and (b) the three depth horizons for each site (pooled across all monitoring periods 2017-2019)

Field turbidity measurements ranged between < 1 to 120 NTU (Figure 3.5a). Turbidity was similar among sites and relatively consistent throughout the water column (Figure 3.5b). Secchi disk depth (m) is a vertical measure of the optical clarity of the water column and ranged between 1 and 10 m (Figure 3.6b). The range measured is a response to localised variation in water quality, most likely a difference in tidal stage among sites during a survey, short term localised changes in turbidity that is associated with tide or algal blooms that reduce vertical clarity. The secchi disk depth to depth ratio (Z_{sd}:Z, Figure 3.6b) was calculated for each site and survey. This ratio corrects the secchi disk depth for water depth, and ranged between 10 and 100% of the water column.

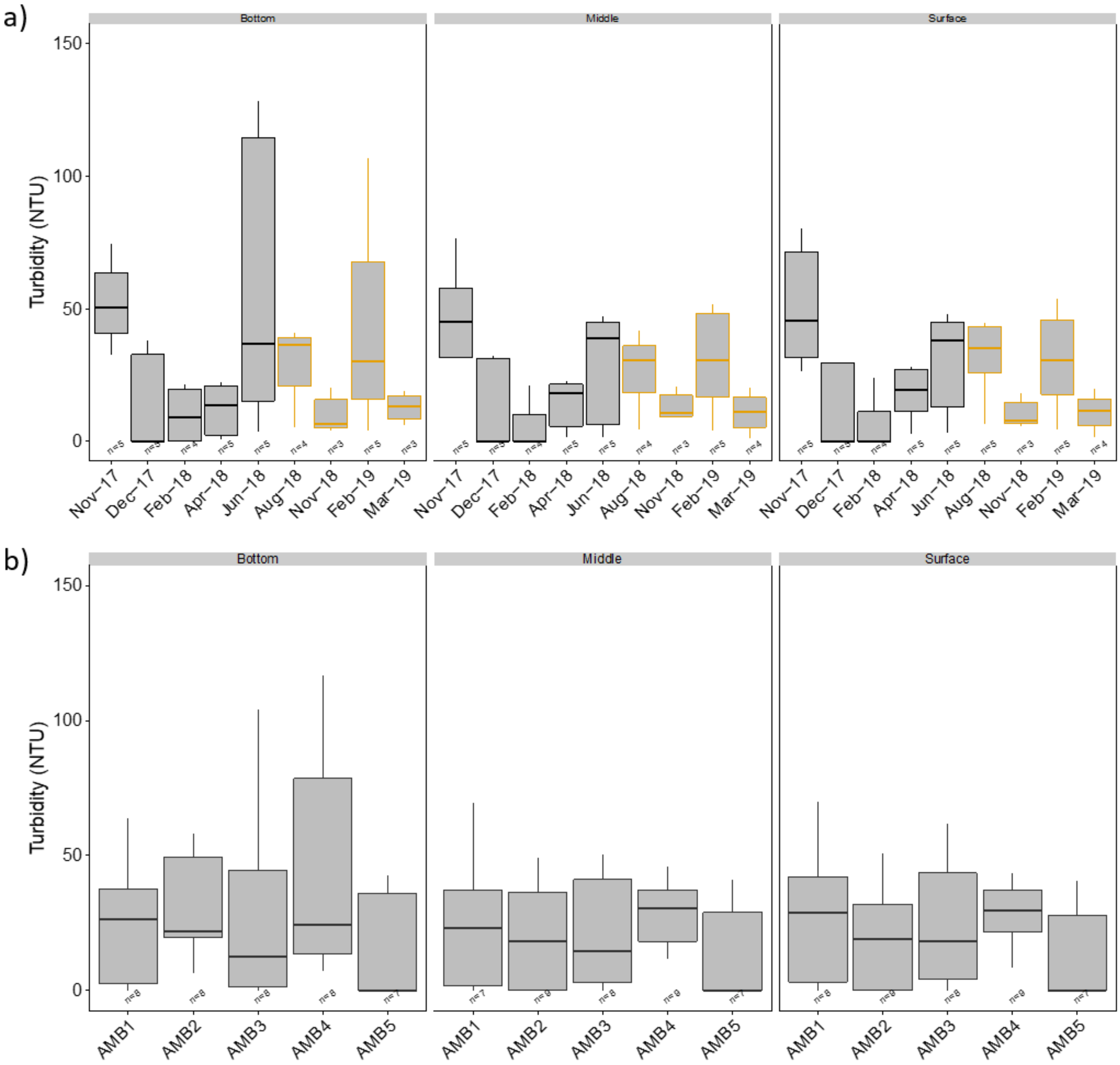

Figure 3.5 Turbidity box plots recorded: (a) the three depth horizons during each survey (sites pooled) where colour indicates monitoring period: black = 2017/2018 and orange = 2018/2019; and (b) the three depth horizons for each site (pooled across all monitoring periods 2017-2019).

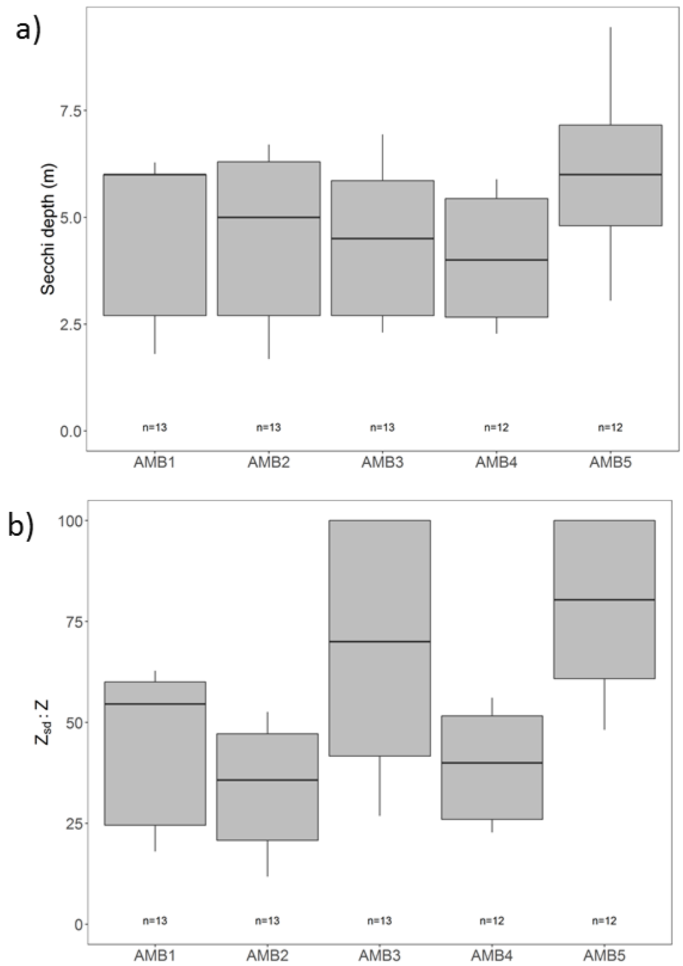

Figure 3.6 (a) Water secchi disk depth for all sites (surveys pooled for all monitoring periods 2017-2019); and (b) secchi depth depth to depth ratio (Z_{sd}:Z) for sites (surveys pooled for all monitoring periods 2017-2019)

3.1.2 Nutrients and chlorophyll-*a*

Particulate nitrogen (PN) and phosphorus (PP) concentrations were compared to the Water Quality Guidelines for the Great Barrier Marine Park Authority (GBRMPA, 2010). Particulate nitrogen concentrations exceeded the guidelines throughout most of the 2018-2019 monitoring period (Figure 3.7a). Also, when pooled across all surveys, concentrations exceeded guidelines at all sites. High concentrations of PN might be associated with the contribution from local land use activities, as base flow from rivers and local rainfall is known to contribute to nutrient loadings to coastal regions (Brodie et al. 2012; Kroon et al. 2012; Schaffelke et al. 2012; Logan et al. 2014). In addition, other sources of the nutrients might be via remobilisation of coastal sediments, and release of available nutrients adsorbed to coastal sediments (Devlin et al. 2012). Elevated nutrients may also be related to reprocessing of nutrients with algal blooms, where there has been an obvious trichodesmium (a marine cyanobacteria; Capone et al. 1997) bloom across the region during most surveys, but most notably during late spring and early summer.

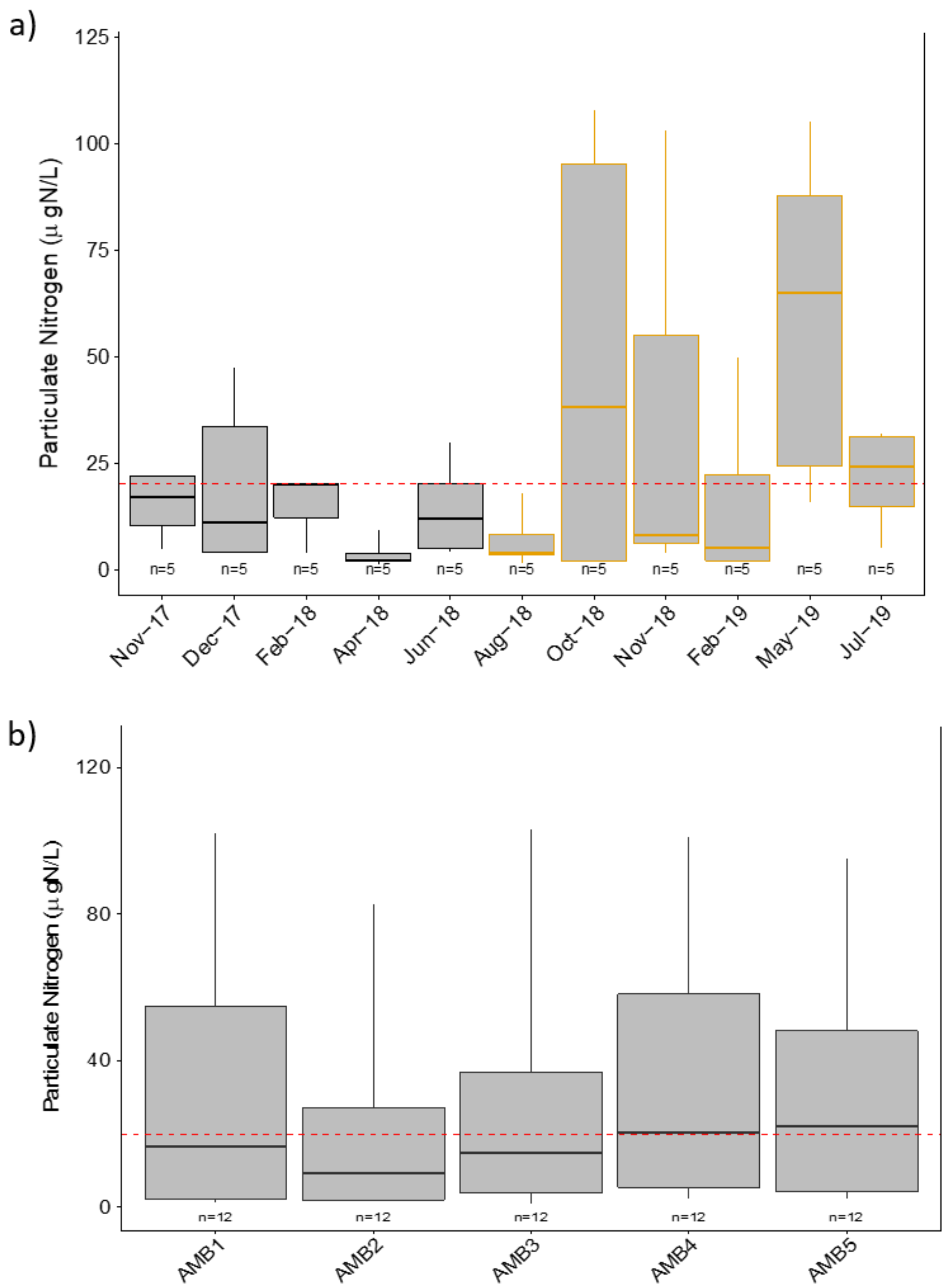

Figure 3.7 Particulate nitrogen box plots: (a) during each survey (sites pooled) where colour indicates monitoring period: black = 2017/2018 and orange = 2018/2019; and (b) pooled at each site across all monitoring periods 2017-2019. Horizontal red-dash indicates the guideline value.

Particulate phosphorus concentrations were similar across seasons and sites and exceeded the GBRMPA (2010) Water Quality Guideline between November 2018 – May 2019 (Figure 3.8). AMB3 had the highest concentration of particulate phosphorus (Figure 3.8b). Chlorophyll-*a* concentrations exceeded the GBRMPA (2010) Water Quality Guideline in most months and all sites surveyed (Figure 3.9). Relationships between nutrient levels (i.e. PN, PP, Chlorophyll-*a*, and Phaeophytin-*a*) across all sites and sampling periods were weak (correlation coefficients (r) ranged between -0.01 – 0.3; Figure 3.10).

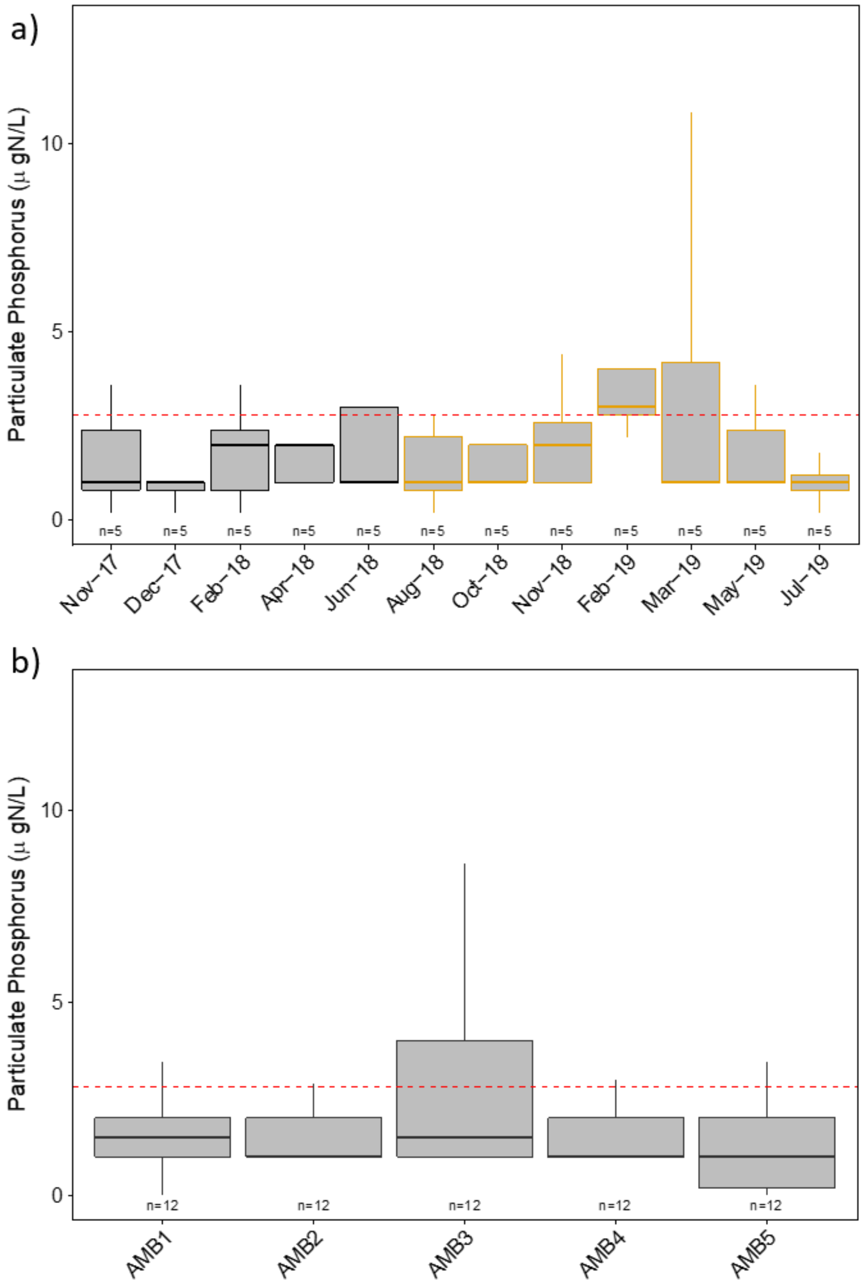

Figure 3.8 Particulate phosphorus box plots: (a) during each survey (sites pooled) where colour indicates monitoring period: black = 2017/2018 and orange = 2018/2019; and (b) pooled at each site across all monitoring periods 2017-2019. Horizontal red-dash indicates the guideline value.

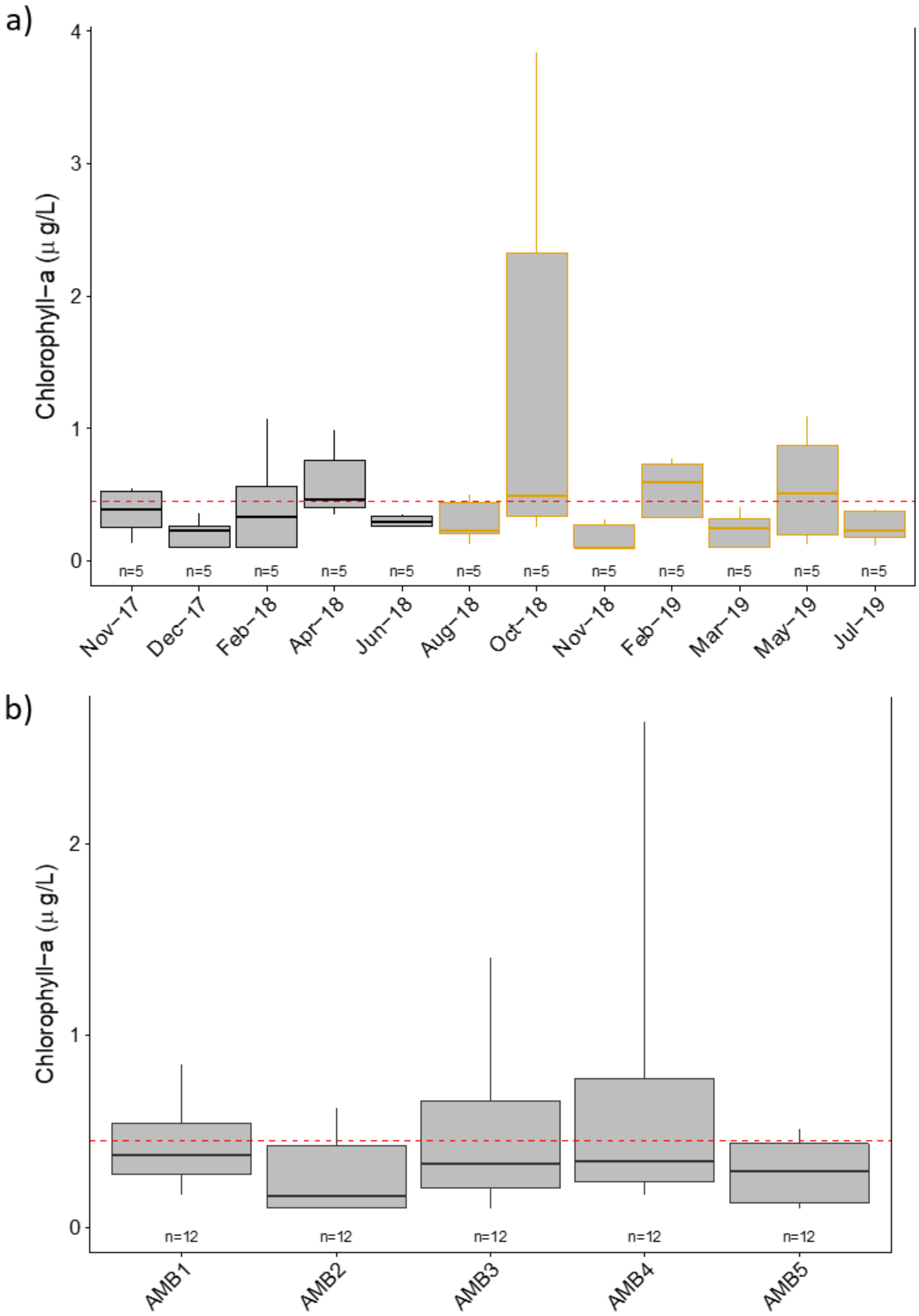

Figure 3.9 Chlorophyll-*a* box plots: (a) during each survey (sites pooled) where colour indicates monitoring period: black = 2017/2018 and orange = 2018/2019; and (b) pooled at each site across all monitoring periods 2017-2019. Horizontal red-dash indicates the guideline value.

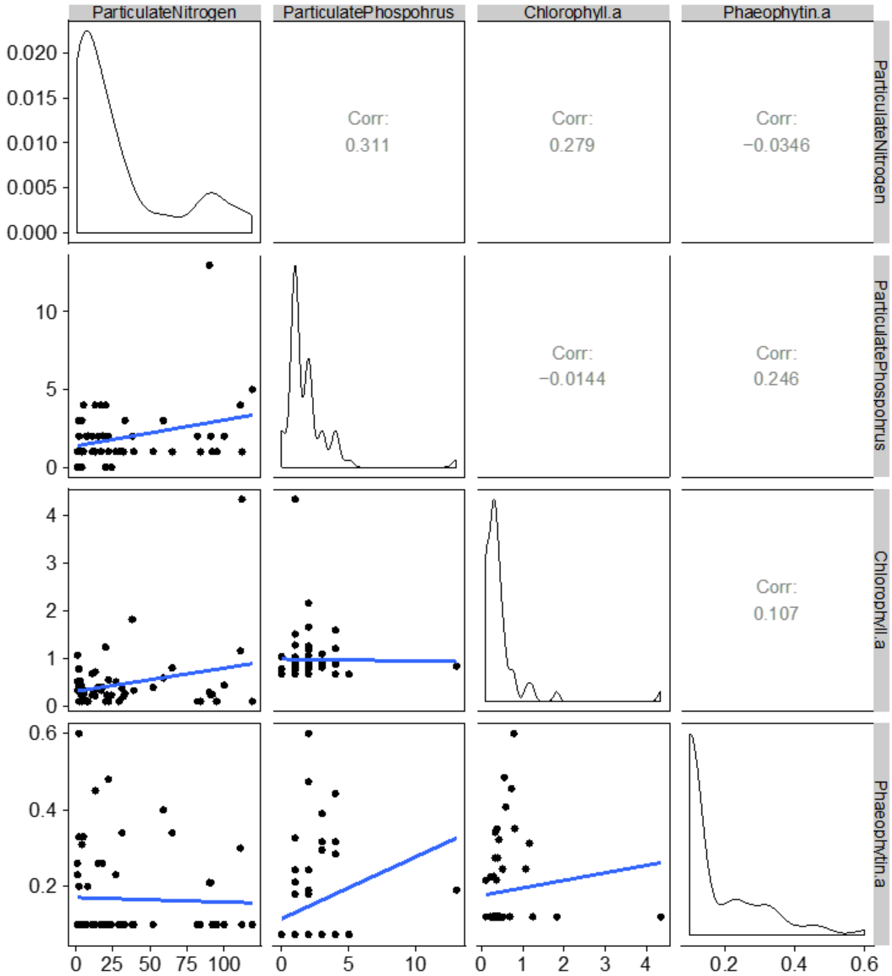

Figure 3.10 Scatterplot of nutrient relationships at pooled across all sites and surveys. Lines of best fit with 95% confidence intervals are displayed in blue, and correlation coefficients are shown in corresponding plots. Density plots show log-normal distribution of the data, and therefore non-parametric spearman correlation was used.

3.1.3 Ultra-trace water heavy metals

Ultra-trace heavy metal concentrations were compared to the ANZECC and ARMCANZ 2000 water quality guidelines (ANZECC, 2000). Most filterable metals were not detected above the Limit of Reporting (LOR), except for copper and nickel in August 2018 (Table 3.1). Note that ANZECC guidelines have not been established for arsenic. Arsenic is released into the environment naturally by weathering of arsenic-containing rocks and volcanic activity. It can be in the form of As (III) or As (V), which can be toxic to marine aquatic life. A low reliability marine guideline trigger value of 4.5 µg/L for As (V) and 2.3 µg/L for As (III) has been derived (ANZECC, 2000), however, these trigger guidelines are only an indicative interim working level. Although Arsenic was detected, the measured concentrations were below low reliability guidelines, and similar values have recorded consistently at these sites since mid-2016.

Table 3.1 Summary statistics for metals data recorded at all sites during the program. Values are pooled across sites. Values are compared to the ANZECC 95% protection guideline values (2000).

		Arsenic	Cadmium	Copper	Lead	Nickel	Silver	Zinc	Mercury
	Unit	ug/L	ug/L	ug/L	ug/L	ug/L	ug/L	ug/L	mg/L
	LOR	-	0.2	1	0.2	0.5	0.1	5	0.001
	ANZECC	-	5.5	1.3	4.4	70	1.4	15	0.4
Apr-18	Mean	1.64	<0.2	<1	<0.2	<0.5	<0.1	<5	<0.001
	Min	1.5	<0.2	<1	<0.2	<0.5	<0.1	<5	<0.001
	Max	1.7	<0.2	0.5	<0.2	<0.5	<0.1	6	<0.001
Aug-18	Mean	1.64	<0.2	1.6	<0.2	<0.5	<0.1	<5	<0.001
	Min	1.5	<0.2	<1	<0.2	<0.5	<0.1	<5	<0.001
	Max	1.7	<0.2	4	<0.2	0.7	<0.1	<5	<0.001
Feb-19	Mean	1.64	<0.2	<1	<0.2	<0.5	<0.1	<5	<0.001
	Min	1.5	<0.2	<1	<0.2	<0.5	<0.1	<5	<0.001
	Max	1.7	<0.2	0.5	<0.2	<0.5	<0.1	<5	<0.001

3.1.4 Water pesticides and herbicides

The major pesticides and herbicides were not detected at concentrations exceeding water quality improvement guidelines for the Great Barrier Reef Marine Park (GBRMPA, 2010) and all detected concentrations were below the 95% protection level (Table 3.2).

Table 3.2 Average concentrations of pesticides/herbicides recorded at all sites during the program (all values are µg/L). Values are pooled across sites for each survey and compared to the Water Quality Guidelines for the Great Barrier Reef Marine Park (GBRMPA, 2010) 95% protection level.

Survey	Guideline	Atrazine ug/L	Ametyn ug/L	Diuron ug/L	Hexazinone ug/L	Tebutryn ug/L
	GBRMPA (2010)	1.4	1.0	1.6	1.2	-
April 2018		0.0005	<0.0002	0.0065	0.0015	0.0001
August 2018		0.0001	<0.0002	0.0055	0.0001	0.0001
February 2019		0.0028	<0.0002	0.004	0.001	0.0001

3.1.5 Ordination of data

Spot water quality measurements have been collected at all sites for: water temperature, electrical conductivity, dissolved oxygen (%), pH, nutrients (particulate nitrogen and phosphorus), and chlorophyll-*a*. In addition to these spot measurements, secchi depth has also been recorded, as a measure of the optical clarity of the water column. These measurements continue to assist in characterising water quality conditions within the water column, among sites and surveys.

Principal components analysis (PCA) was used to explore relationships between physiochemical and nutrient data collected at the water surface at each site during each month of sampling. The PCA determined that 40.6 % of the variability among sites and sampling months is explained by physiochemical and nutrient parameters (Figure 3.11). There are no inter-annual differences in physiochemical parameters among sites, except for higher variability in 2019 (Figure 3.11a). However, there physiochemical parameter differ seasonally, with higher temperatures and dissolved oxygen levels in the wet season months (Figure 3.11b).

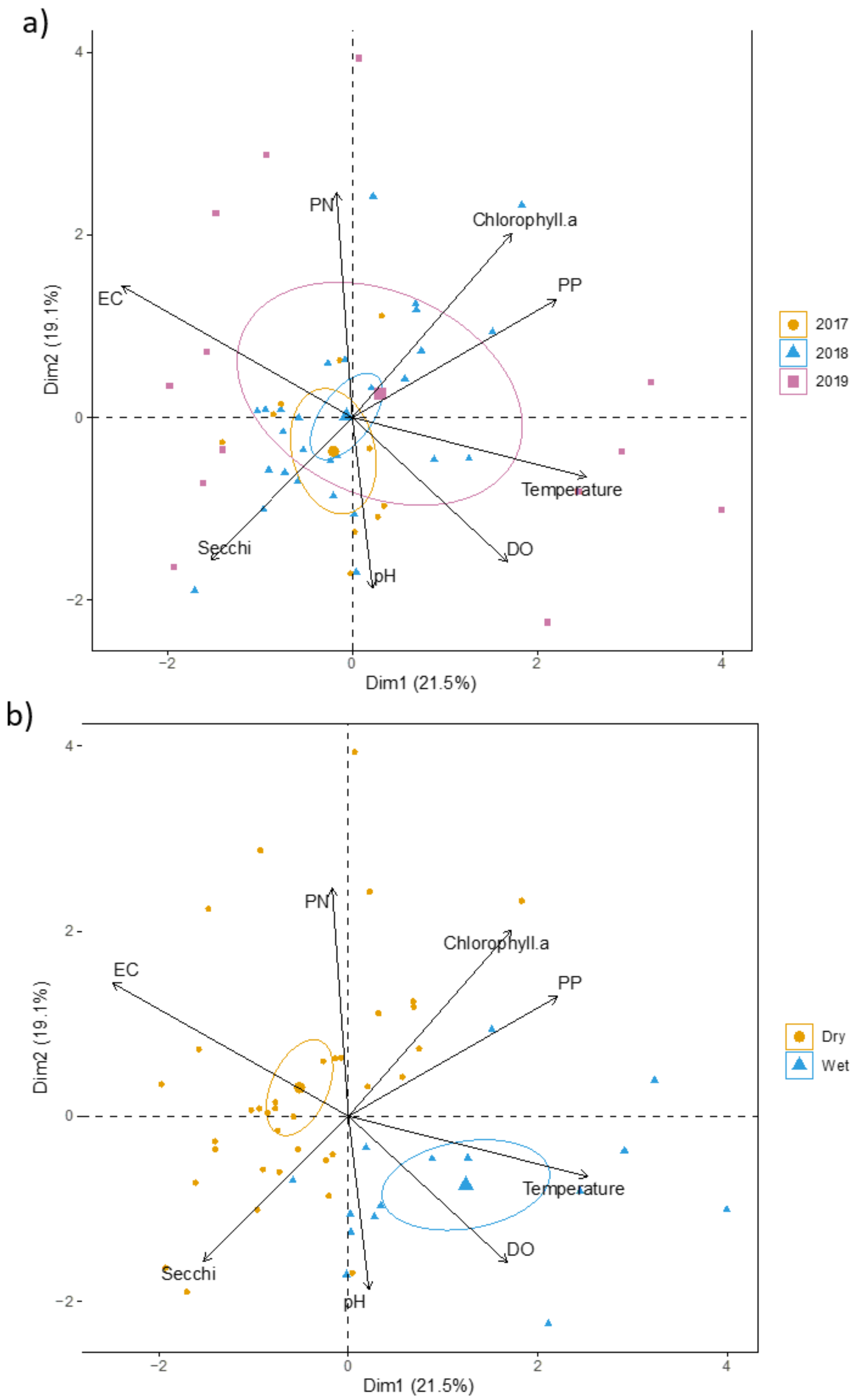

Figure 3.11 Principal components analysis (PCA) exploring relationships between nutrients and physiochemical parameters (black vectors) and monitoring sites. The 95 % confidence interval ellipses show overall differences between: A) sites grouped by month and B) sites grouped by season. Vector labels are abbreviated as follows: PP = Particulate Phosphorus, PN = Particulate Nitrogen, EC = Electrical Conductivity, and DO = Dissolved Oxygen. Total variance explained by Dimension 1 and Dimension 2 = 40.6 %

3.2 Plankton communities

3.2.1 Diversity and abundance

A total of 62 phytoplankton species have been identified, comprising cyanobacteria, diatoms, flagellates and green algae taxa. Several species were recorded at all sites, including Ceratium gibberum, Ceratium trichoceros, Chaectoceros spp, Chlamydomonas spp, Guinardia spp, Hillea spp, Odontella sinesis spp, Phormidium spp, Thalalssionema nitzchioides, and Trichodesmium spp. Trichodesmium spp. were generally the most abundant phytoplankton species recorded across all sites. AMB2 had the highest phytoplankton species richness in November 2017 (28 species), while the lowest diversity was recorded in February 2018 at AMB3 and AMB5 (8 species) (Figure 3.12a). There were large increases in phytoplankton abundance at AMB1, AMB4, AMB5 in November 2018, February 2018, and March 2019, respectively (Figure 3.12b).

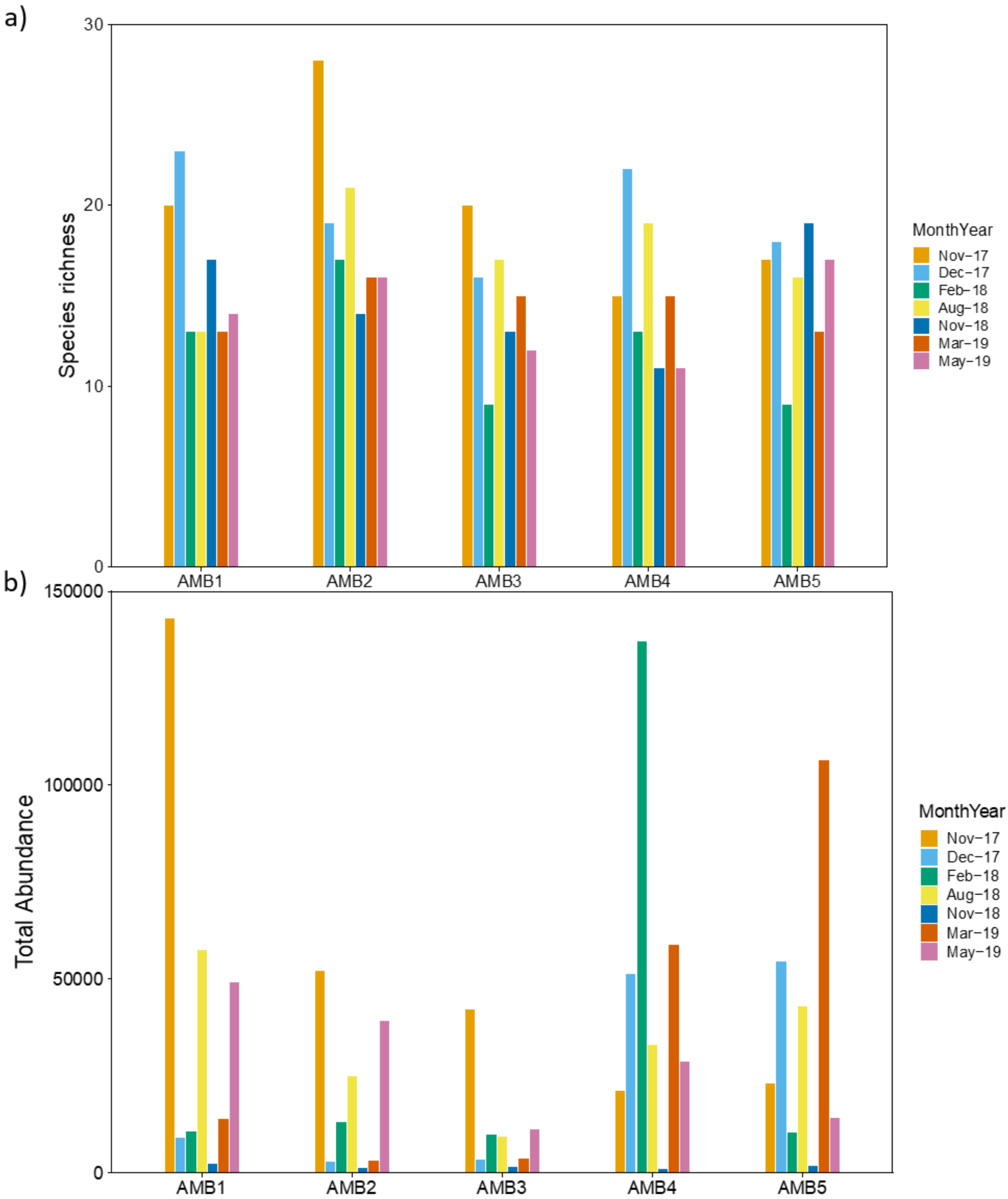

Figure 3.12 a) Species richness of phytoplankton; and b) total abundance of phytoplankton at each site during each survey period.

A total of 30 different species of zooplankton were recorded during all surveys. Several species were recorded at all sites, including *Acartia pacifica, Calanopia elliptica, Dictocysta spp, Echinoidea spp, Gastropoda, Penaeus spp, Portunidae, Flaccisagitta enflata*, *Favella serrata*, and Siphonophorae. AMB1 had the highest diversity of zooplankton species in December 2017 (16 species), while no zooplankton were detected at this site in November 2018 (Figure 3.13a). The highest abundance of zooplankton was recorded in November 2017 at AMB4, mainly due to high numbers of *Acanthometra* spp, *Calanopia elliptica*, and *Echiniodea* (Figure 3.13b). There were additional peaks in zooplankton abundance in August 2018 at AMB1 and AMB3 (Figure 3.13b).

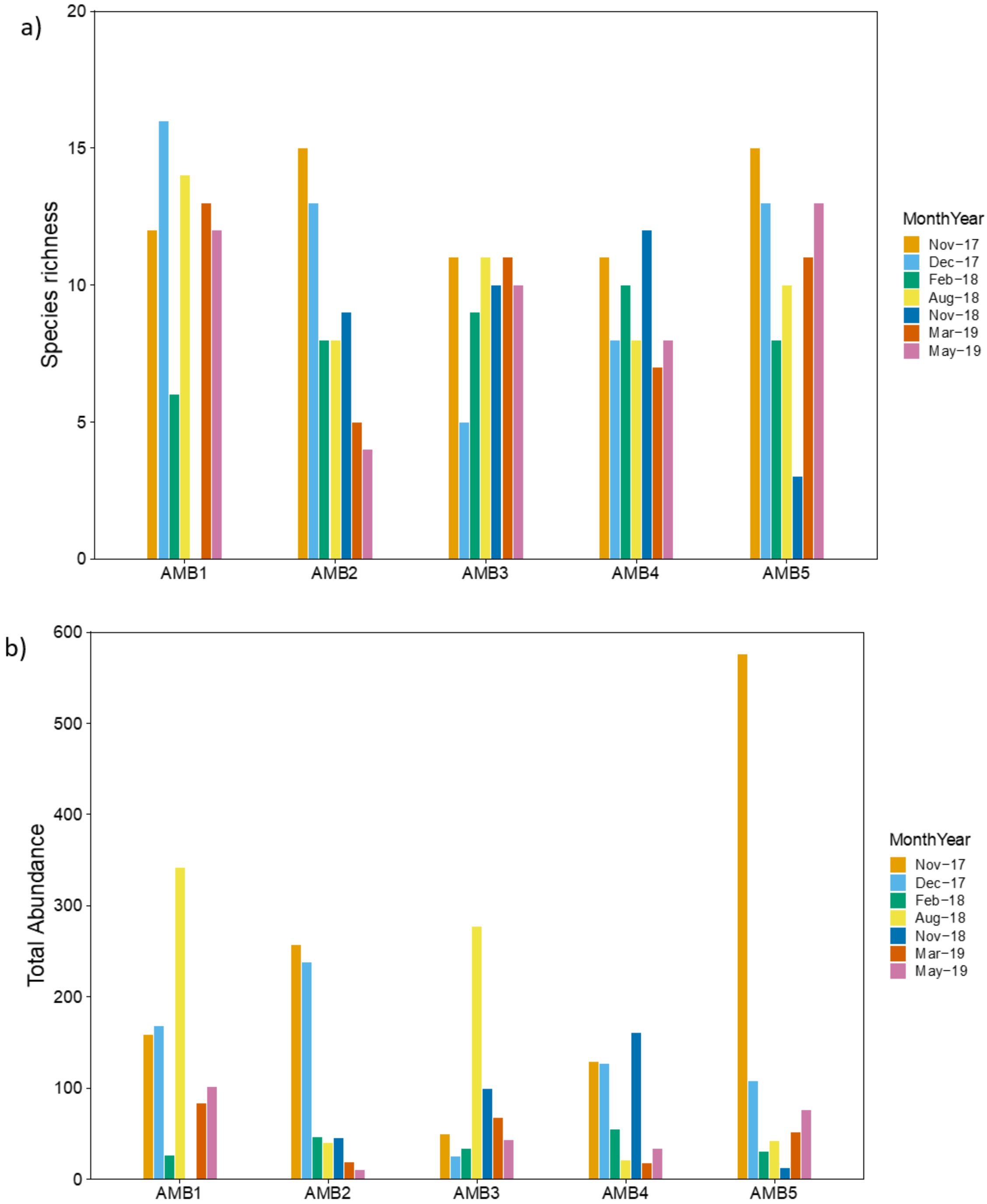

Figure 3.13 a) Species richness of zooplankton, and b) total abundance of zooplankton at each site during each survey period.

3.2.2 Plankton ordinations

Exploratory statistical analysis of the plankton using non-dimensional scaling (nMDS) revealed differences in species composition of phytoplankton (Figure 3.14) and zooplankton communities (Figure 3.15) between survey periods. Overall, phytoplankton communities showed higher separation among survey periods in comparison to zooplankton communities. In particular, phytoplankton communities in November 2018, February 2018, and March 2019 showed little similarity in species composition to other survey periods (Figure 3.14). Continued monitoring will determine whether seasonality also plays a role in shaping these communities.

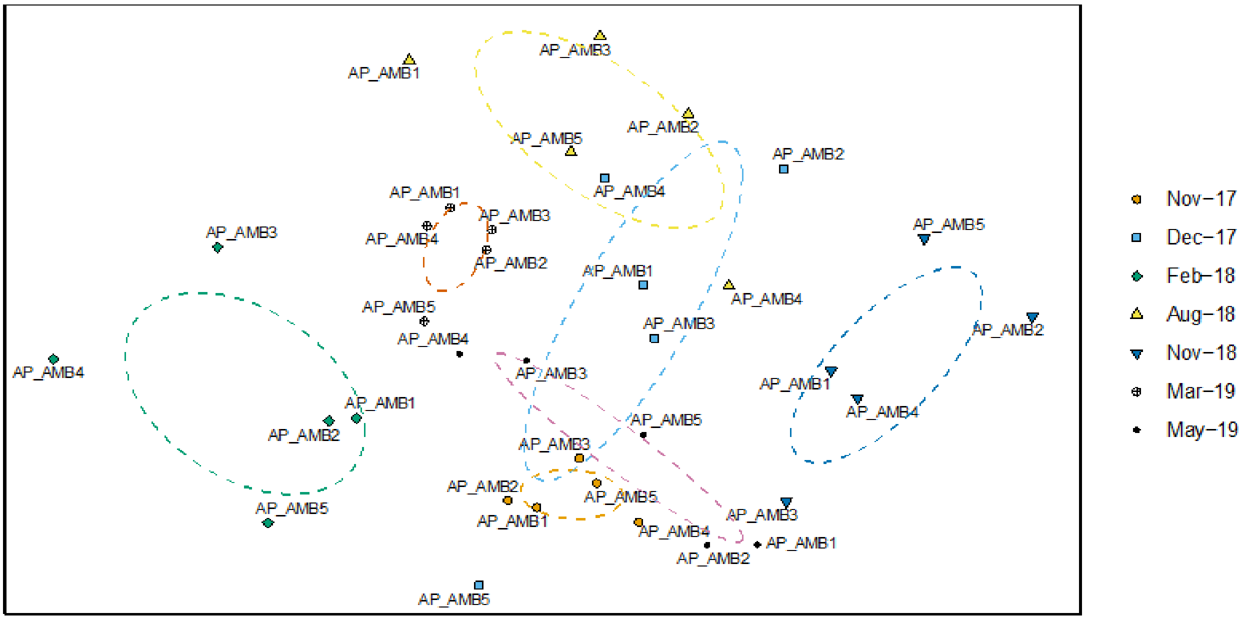

Figure 3.14 Non-dimensional ordination plot for phytoplankton collected during three surveys throughout 2017-2019. Dashed lines represent 95 % confidence interval ellipses for each survey period and colours correspond to survey periods as follows: light orange = November 2017, light blue = December 2017, green = February 2018, yellow = August 2018, dark blue = November 2018, dark orange = March 2019, and pink = May 2019. Data has been squared root transformed on the Bray Curtis distance matrix (stress = 0.22).

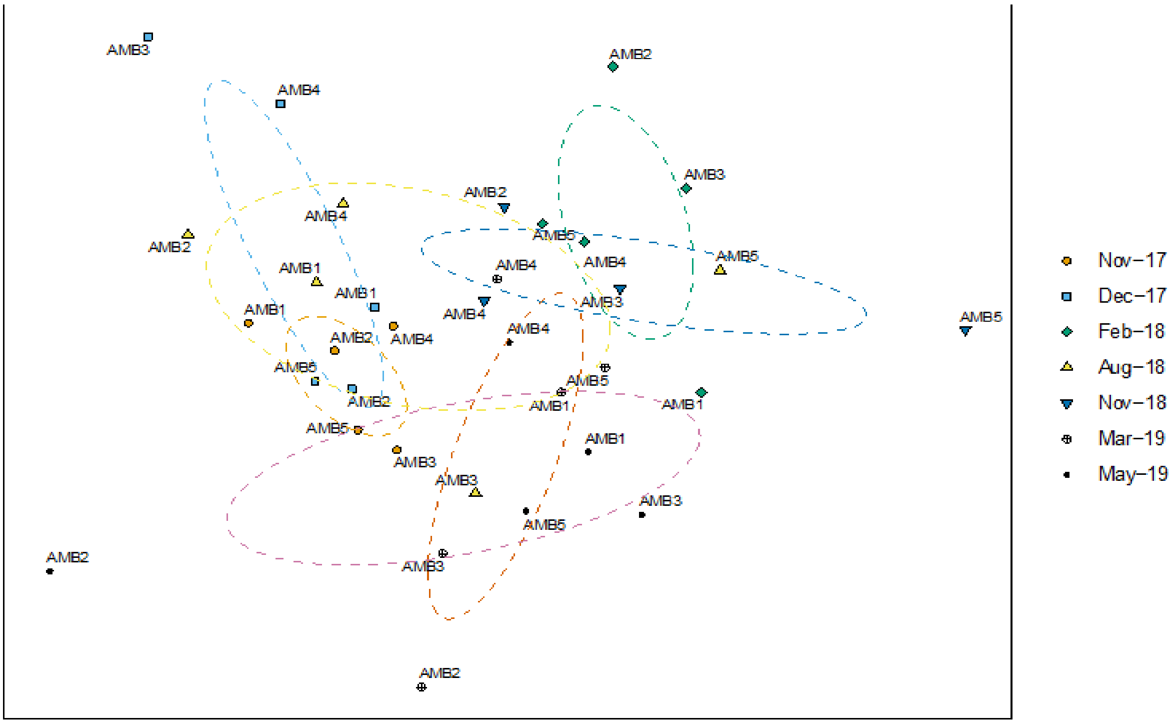

Figure 3.15 Non-dimensional ordination plot for zooplankton collected during three surveys throughout 2017-2019. Dashed lines represent 95 % confidence interval ellipses for each survey period and colours correspond to survey periods as follows: light orange = November 2017, light blue = December 2017, green = February 2018, yellow = August 2018, dark blue = November 2018, dark orange = March 2019, and pink = May 2019. Data has been squared root transformed on the Bray Curtis distance matrix (stress = 0.22).

3.3 Multiparameter water quality logger

Instruments were deployed at five sites, AMB 1 to 5, from July 2018 to July 2019 (see Table 1.1). Using standard statistics, we describe observed trends and differences between sites and discuss the driving forces in these environments. In addition to data loss due to fouling, two deployments were not recovered due to lost or failed instruments: at AMB5 from October to November 2018 and at AMB3 from May to July 2019. Data is presented as an annual statistical summary of root mean square water height (RMS; m), suspended sediment concentration (SSC; mg l^{-1}), sediment deposition rate (mg cm^{-2} day^{-1}), water temperature (°C), and photosynthetically available radiation (PAR; mol m^{-2} d^{-1}) for each site. The summary is depicted using box plots, whereby the central diamonds represent the mean value, the central line represents the median value, and the central box represents the range of the 25 and 75% quartiles. The vertical bars represent the range of the 90th and 10th percentiles. Time series and monthly summaries are included in the appendices.

3.3.1 RMS water height

Root mean square water height (RMS) is mostly driven by weather events that increase RMS simultaneously at all sites. Variation in RMS during and in-between peak events differs among sites due to differences in water depth and exposure to wave energy. All sites had similar RMS values, with median values ranging from 0.014 m to 0.025 m (

Figure **3.16**, Table 3.2). AMB5 had the lowest median RMS (0.014) while AMB3 had the highest median RMS (0.025). Peaks in RMS occurred throughout the deployment period at all sites (Appendix A1.2, Appendix A1.3).

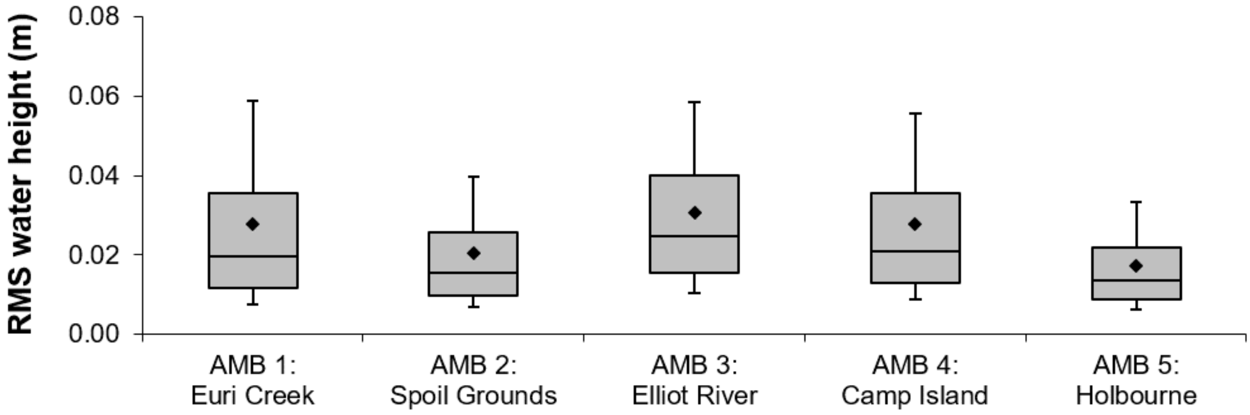

Figure 3.16 Box plot of RMS water height (m) at the five sites for the monitoring period from July 2018 to July 2019. The lower whisker, lower edge of the box, central line, upper edge of the box and upper whisker represent the 10th, 25th, 50th, 75th and 90th percentiles, respectively. The diamonds represent the mean values.

Table 3.3 Summary of RMS water height (m) statistics at the five sites from July 2018 to July 2019.

Site	AMB 1: Euri Creek	AMB 2: Spoil Grounds	AMB 3: Elliot River	AMB 4: Camp Island	AMB 5: Holbourne
Mean	0.028	0.020	0.031	0.028	0.017
Median	0.020	0.016	0.025	0.021	0.014
Minimum	0.000	0.000	0.000	0.000	0.000
Lower quartile	0.012	0.010	0.015	0.013	0.009
Upper quartile	0.035	0.026	0.040	0.035	0.022
Maximum	0.341	0.212	0.240	0.299	0.448
90th percentile	0.059	0.040	0.058	0.056	0.033
10th percentile	0.008	0.007	0.010	0.009	0.006
n	52810	52832	45986	52894	42845
St. Dev	0.025	0.016	0.022	0.022	0.013
St. Error	<0.001	<0.001	<0.001	<0.001	<0.001

3.3.2 NTUe/SSC

Median suspended sediment concentrations (SSC) were ≤2.6 mg/l at all sites (Figure 3.17, Table 3.4). Higher mean SSC at AMB2 and AMB4 indicate that these sites experienced more extreme turbidity events during the monitoring period. AMB4 had the highest variance in (54.0 sd) but similar median SSC as the other sites. AMB3 had the lowest median SSC compared to the other sites.

The NTUe/SSC time series data follows a typical pattern of low background values with recurring peak events (Appendix A1.2). Most sites exhibited SSC extremes in October-December (Appendix A1.2). These events typically occurred simultaneously at all sites and coincide with increases in RMS. This is a pattern observed in coastal locations in north Queensland by the James Cook University Marine Geophysics group (Ridd et al., 2001). Differences in NTUe/SSC among sites result from differences in RMS water height, water depth, benthic geology, hydrodynamics, and proximity to river mouths.

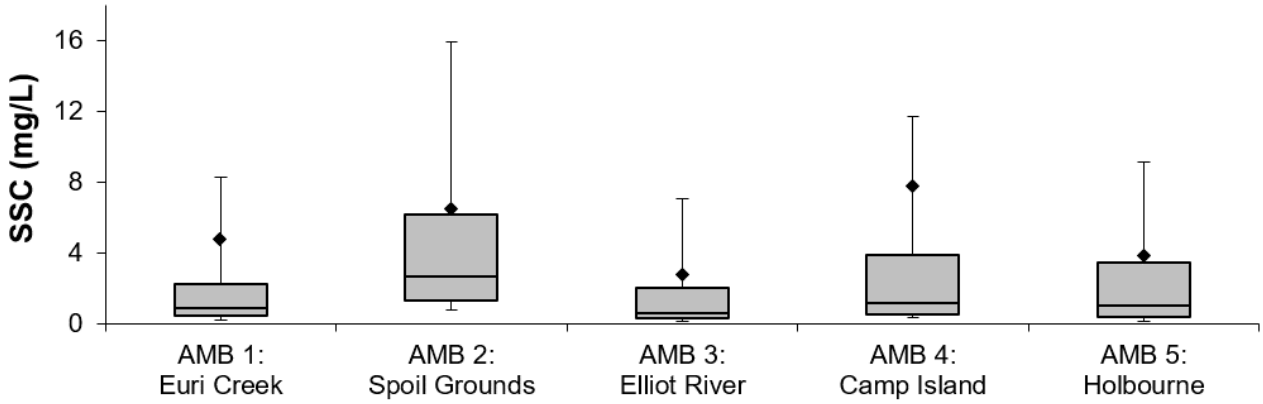

Figure 3.17 Box plot of SSC (mg L^{-1}) from July 2018 to July 2019. The lower whisker, lower edge of the box, central line, upper edge of the box and upper whisker represent the 10^{th}, 25^{th}, 50^{th}, 75^{th} and 90^{th} percentiles, respectively. The diamond represents the mean value.

Table 3.4 Summary of SSC (mg L^{-1}) statistics at the five sites from July 2018 to July 2019.

Site	AMB 1: Euri Creek	AMB 2: Spoil Grounds	AMB 3: Elliot River	AMB 4: Camp Island	AMB 5: Holbourne
Mean	4.79	6.50	2.78	7.79	3.81
Median	0.85	2.64	0.60	1.12	1.00
Minimum	0.00	0.00	0.00	0.00	0.00
Lower quartile	0.41	1.32	0.29	0.54	0.34
Upper quartile	2.21	6.14	2.02	3.89	3.44
Maximum	868.91	307.84	251.19	1904.59	546.13
90th percentile	8.31	15.98	7.08	11.73	9.16
10th percentile	0.18	0.73	0.15	0.32	0.13
n	36408	44181	30488	43154	37430
St. Dev	19.76	11.62	7.62	53.96	12.18
St. Error	0.10	0.06	0.04	0.26	0.06

3.3.3 Deposition

Deposition of sediment is a natural process in all coastal marine waters. Suspended sediment is transported by currents and deposits in environments where wave energy is not sufficient to retain sediment suspended in the water column. The time series of deposition rates indicate that deposition peaks following RMS events but with a lag so that peak deposition occurs when RMS has decreased to near background levels (Appendix A1.2). An explanation for this lag is that, as waves resuspend sediment, little deposition occurs because the energy in the system keeps sediment in suspension. However, when waves decrease and there is no longer enough energy in the system to keep sediment in suspension and deposition occurs.

Management of marine habitats requires that sediment deposition be monitored for changes from ambient values. The Water Quality Guidelines for the Great Barrier Reef Marine Park (GBRMPA 2010) set a sediment deposition trigger value at a mean annual value of 3 mg cm^{-2} day^{-1} and a daily maximum of 15 mg cm^{-2} day^{-1}. However, the Guidelines suggest that 10 mg cm^{-2} day^{-1} sedimentation is valid in areas of coarse sediment, large grainsize, or low organic content.

All coastal sites (AMB1-4), as well as AMB5, exceeded the mean sediment deposition trigger value (Figure 3.18, Table 3.5). However, as these deposition rates are not normally distributed, we focus our interpretation on median values, which ranged from 1.77 (AMB5) - 13.08 (AMB2) mg cm^{-2} day^{-1}.

Differences in deposition rates may be more easily visualised by estimating the thickness of the sediment deposited. For example, using the relationship between density, mass and volume: median deposition value of 5 mg cm^{-2} day^{-1} (e.g, AMB1) is equivalent to a layer of sediment of thickness less than 35 µm, assuming a sediment density of 1.5 g cm^{-3}.

At most sites, the highest deposition rates were observed between November and February (Appendix A1.3).

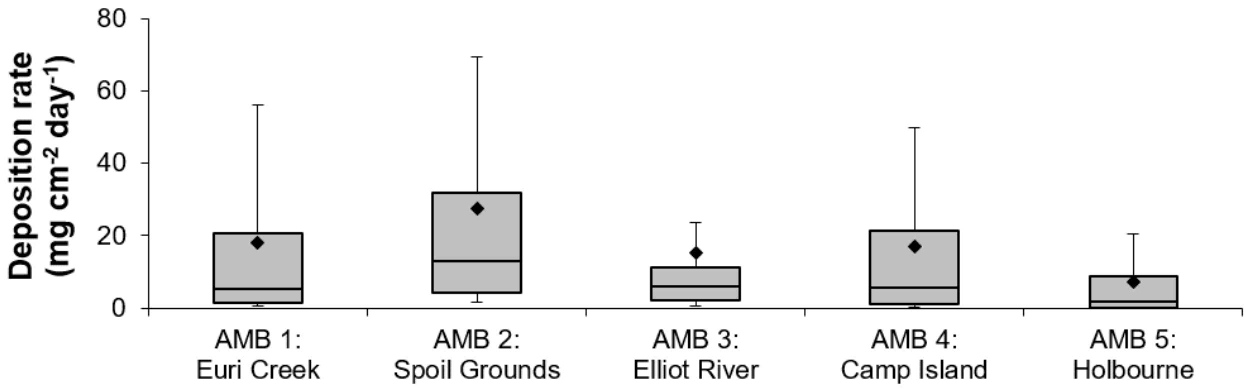

Figure 3.18 Box plot of deposition rates (mg cm-2 day-1) from July 2018 to July 2019. The lower whisker, lower edge of the box, central line, upper edge of the box and upper whisker represent the 10th, 25th, 50th, 75th and 90th percentiles, respectively. The diamond represents the mean value.

Table 3.5 Summary of the mean daily deposition rate (mg cm^{-2} day^{-1}) statistics from July 2018 to July 2019.

Site	AMB 1: Euri Creek	AMB 2: Spoil Grounds	AMB 3: Elliot River	AMB 4: Camp Island	AMB 5: Holbourne
Mean	18.02	27.42	15.17	17.06	7.23
Median	5.12	13.08	5.88	5.63	1.77
Minimum	0.01	0.31	0.04	0.00	0.00
Lower quartile	1.40	4.30	2.01	0.96	0.09
Upper quartile	20.64	31.75	11.22	21.24	8.84
Maximum	166.70	290.20	454.79	465.13	116.12
90th percentile	56.22	69.62	23.67	49.93	20.58
10th percentile	0.41	1.53	0.36	0.15	0.01
n	318	363	257	341	230
St. Dev	28.59	40.96	39.39	33.10	13.39
St. Error	1.60	2.15	2.46	1.79	0.88

3.3.4 Water temperature

Water temperatures were similar among all sites with medians of 26-27 °C and similar ranges of temperatures (Figure 3.19, Table 3.6). Water temperature at all sites approached 30 °C from December until March (Appendix

A.2). Water temperature is not a compliance condition for approval operations, however, the temperature data presented here holds importance in future interpretation of ecological processes in the region, and across the GBR (e.g. Johanson et al., 2015).

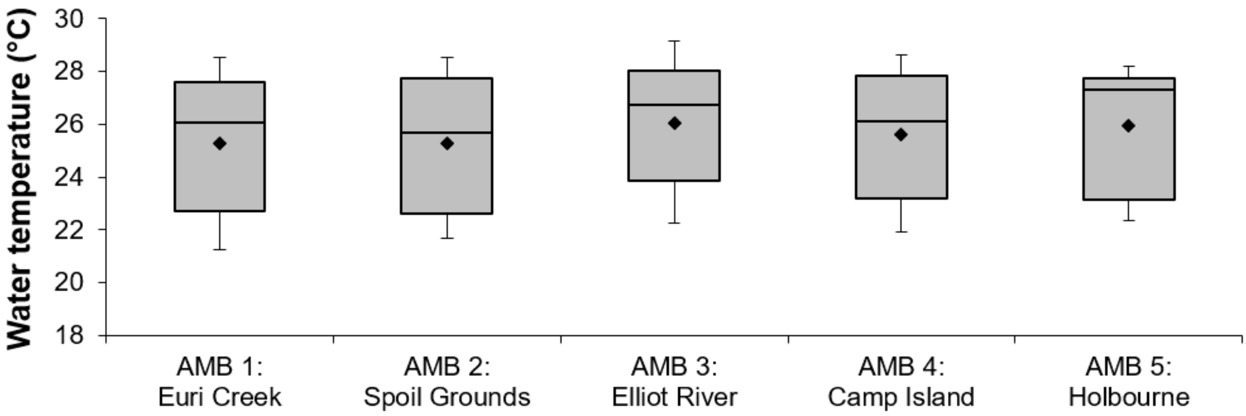

Figure 3.19 Box plot of the water temperature (°C) from July 2018 to July 2019. The lower whisker, lower edge of the box, central line, upper edge of the box and upper whisker represent the 10th, 25th, 50th, 75th and 90th percentiles, respectively. The diamond represents the mean value.

Table 3.6 Summary of water temperature (°C) from July 2018 to July 2019.

Site	AMB 1: Euri Creek	AMB 2: Spoil Grounds	AMB 3: Elliot River	AMB 4: Camp Island	AMB 5: Holbourne
Mean	25.29	25.26	26.04	25.58	25.96
Median	26.04	25.67	26.73	26.09	27.29
Minimum	19.73	20.69	20.33	20.43	20.38
Lower quartile	22.73	22.61	23.86	23.20	23.16
Upper quartile	27.58	27.72	28.02	27.82	27.74
Maximum	30.21	30.02	31.20	30.69	31.25
90th percentile	28.54	28.55	29.17	28.64	28.20
10th percentile	21.25	21.68	22.27	21.90	22.37
n	52792	46470	45975	52860	35593
St. Dev	2.73	2.67	2.58	2.60	2.35
St. Error	0.01	0.01	0.01	0.01	0.01

3.3.5 PAR

Mean levels of benthic photosynthetically available radiation (PAR) ranged from 0.84 to 6.26 mol m^{-2} day^{-1} (Figure 3.20, Table 3.7). AMB3 and AMB5 had the highest mean and variance in PAR, and are proximal to coral sensitive receptor habitats. AMB2 had the lowest mean and lowest variance in PAR, likely due to its deeper location.

Benthic PAR was highly variable within sites throughout the year, but PAR was generally highest in July-August and lowest in December-January (Figure 3.21, Figure 3.22). Semi-regular oscillations between low and high PAR were overridden by larger episodic events caused by storm or rainfall.

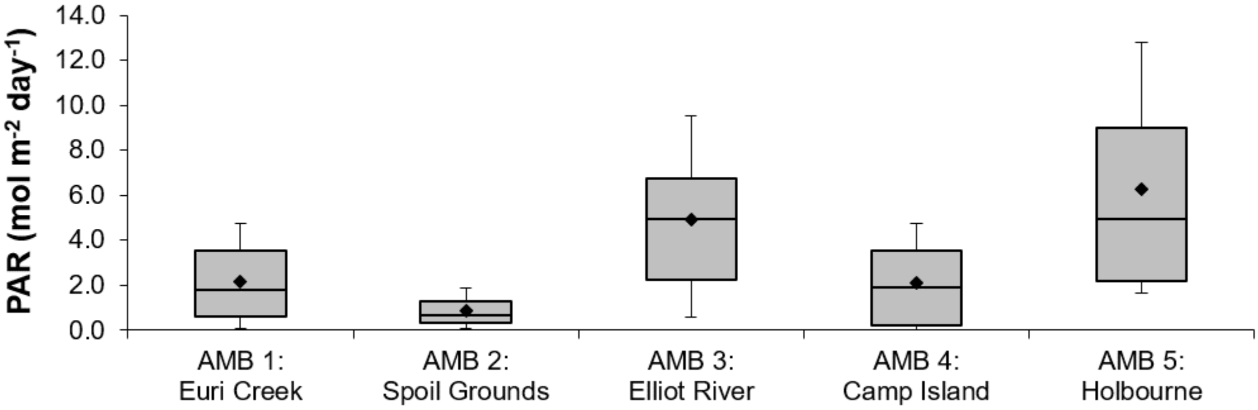

Figure 3.20 Box plot of daily PAR (mol m^{-2} day^{-1}) from July 2018 to July 2019. The lower whisker, lower edge of the box, central line, upper edge of the box and upper whisker represent the 10th, 25th, 50th, 75th and 90th percentiles, respectively. The diamond represents the mean value.

Table 3.7 Summary of daily PAR (mol m^{-2} day^{-1}) from July 2018 to July 2019.

Site	AMB 1: Euri Creek	AMB 2: Spoil Grounds	AMB 3: Elliot River	AMB 4: Camp Island	AMB 5: Holbourne
Mean	2.13	0.84	4.91	2.09	6.26
Median	1.84	0.68	4.96	1.88	4.95
Minimum	0.00	0.00	0.00	0.00	0.33
Lower quartile	0.70	0.32	2.26	0.22	2.16
Upper quartile	3.40	1.28	6.73	3.53	8.97
Maximum	6.30	3.19	13.90	7.24	21.50
90th percentile	4.64	1.85	9.53	4.77	12.81
10th percentile	0.08	0.06	0.55	0.00	1.66
n	364	365	312	364	294
St. Dev	1.66	0.68	3.21	1.83	4.87
St. Error	0.09	0.04	0.18	0.10	0.28

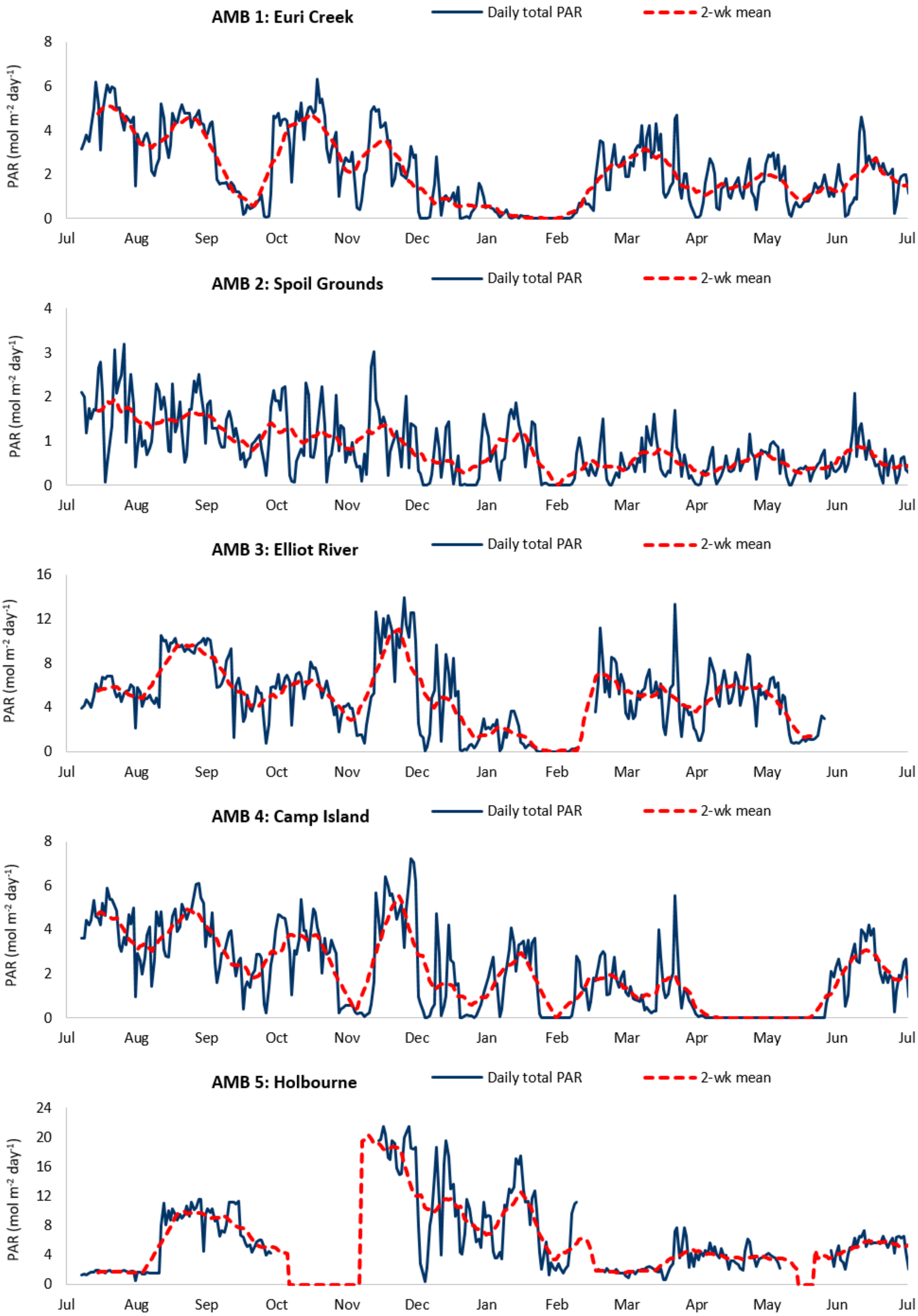

Figure 3.21 Time series of total daily PAR (mol m^{-2} day^{-1}) from July 2018 to July 2019. Daily mean PAR is plotted in blue and a 2 week moving average of daily mean PAR is plotted in red.

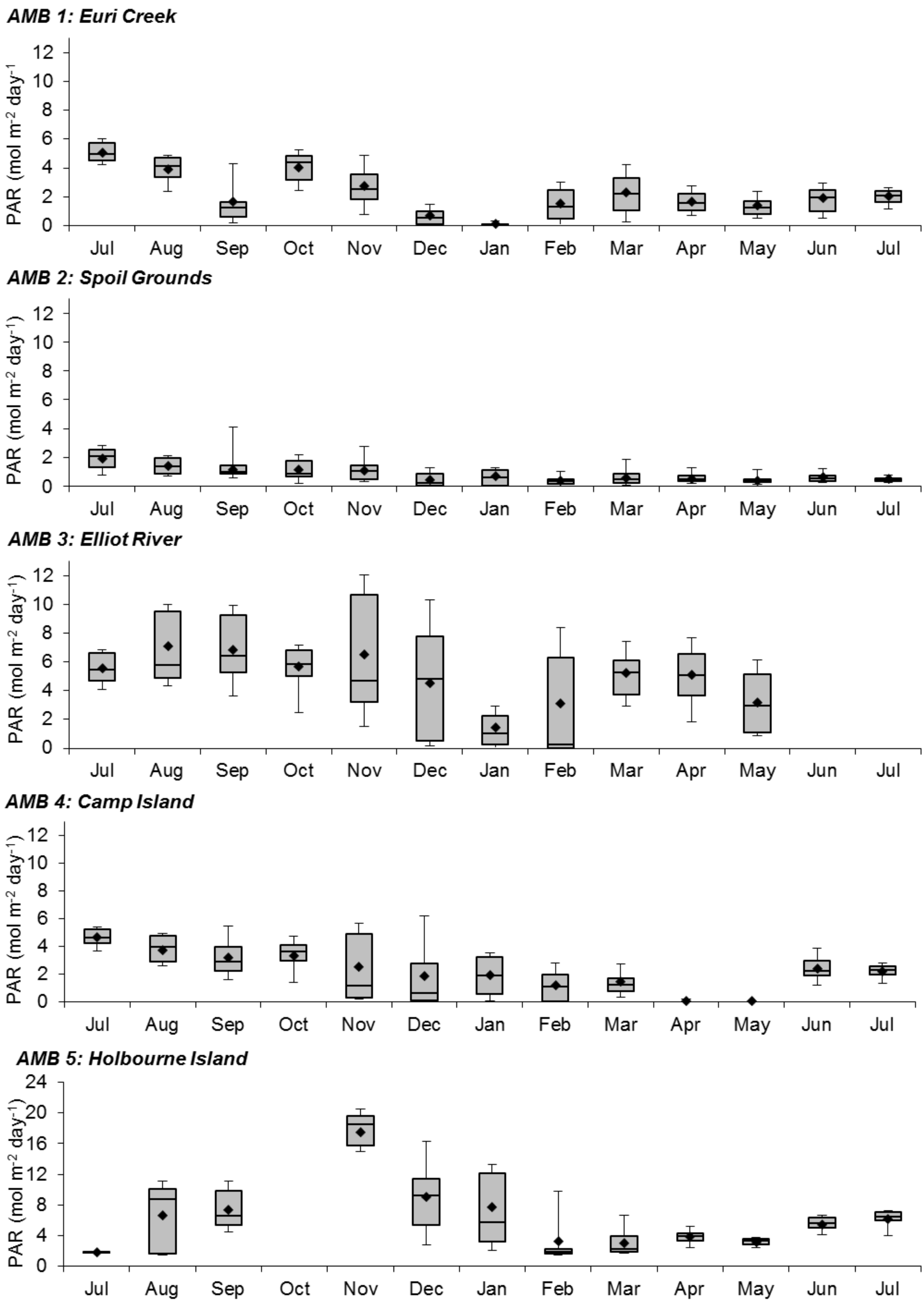

Figure 3.22 Monthly boxplots illustrating the variation in total daily PAR (mol m^{-2} day^{-1}) from July 2018 to July 2019. The lower whisker, lower edge of the box, central line, upper edge of the box and upper whisker represent the 10th, 25th, 50th, 75th and 90th percentiles, respectively. The diamond represents the mean value.

Similarities in patterns of PAR among sites

Direct comparisons of PAR among sites are confounded by the different water depths at each location. However, there are some weak relationships between the benthic PAR at different locations (Figure 3.23). Less than 46% of the variation in PAR at a given site could be explained by the PAR at any other site, highlighting the influence of location conditions (depth, turbidity, etc.) on benthic irradiance. AMB1 and AMB2 have the strongest association (R^2 = 0.45) while AMB3 and AMB4 have the second strongest association (R^2 = 0.41). These three coastal sites are relatively close together, supporting the strong association between respective PAR measurements. These analyses assist in understanding site redundancy opportunities, without missing important detail in characterising water quality in the region.

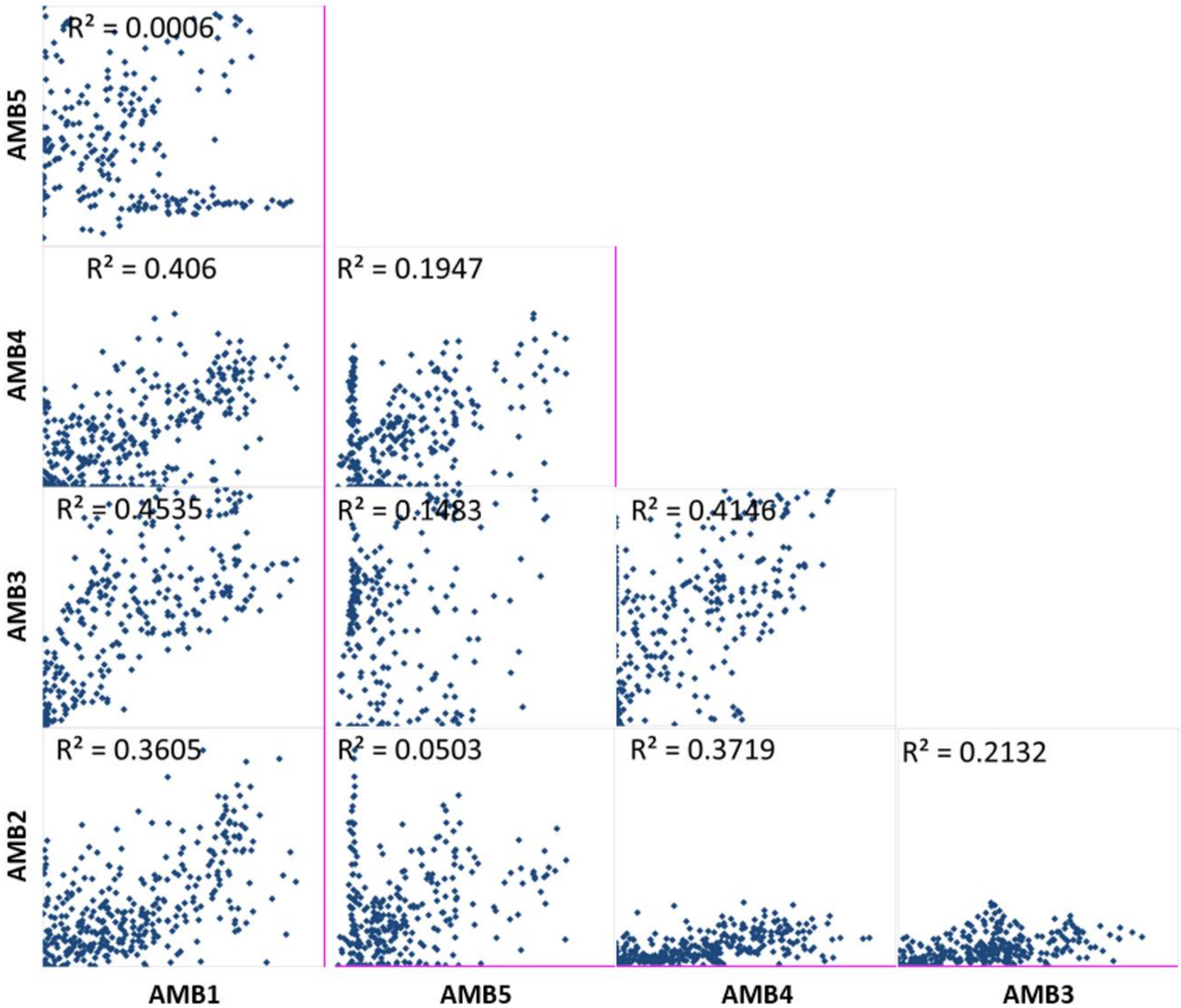

Figure 3.23 Scatterplots of PAR between sites indicating the strength of the relationships between patterns of daily PAR. R^2 values are presented for each comparison.

Relationship between light attenuation and suspended solid concentrations

In sediment-rich coastal waters, the dominant physical process that reduces PAR light intensity is scattering, which if turbidity levels are high enough, can cause underwater light to become isotropic. While the PAR reduction is dominated by scattering, light can also be absorbed before it reaches the seafloor. Investigations into the light attenuation coefficient can provide insight into the dynamic relationship between suspended solid concentrations and PAR intensity.

The amount of PAR attenuation is summarised by the diffuse attenuation coefficient (k_d) using Beer-Lambert's law (Gordon 1989; Dennison et al. 1993; Kirk 1994),

$$\boldsymbol{I_z = I_{z0} e^{-k_d(z-z_0)}}$$

where I_{z0} and I_z are the downward directed irradiances at an upper depth (z_0) and a lower depth (z) respectively (Jerlov 1976; Kirk 1977).

Here, the relationship between light attenuation and suspended sediment concentration (SSC) is examined. In general, when SSC increases, light levels decrease exponentially. An example of this relationship can be seen in Figure 3.24 where during periods of high SSC, light is attenuated and when SSC exceeds approximately 10 mg/L, light extinction occurs.

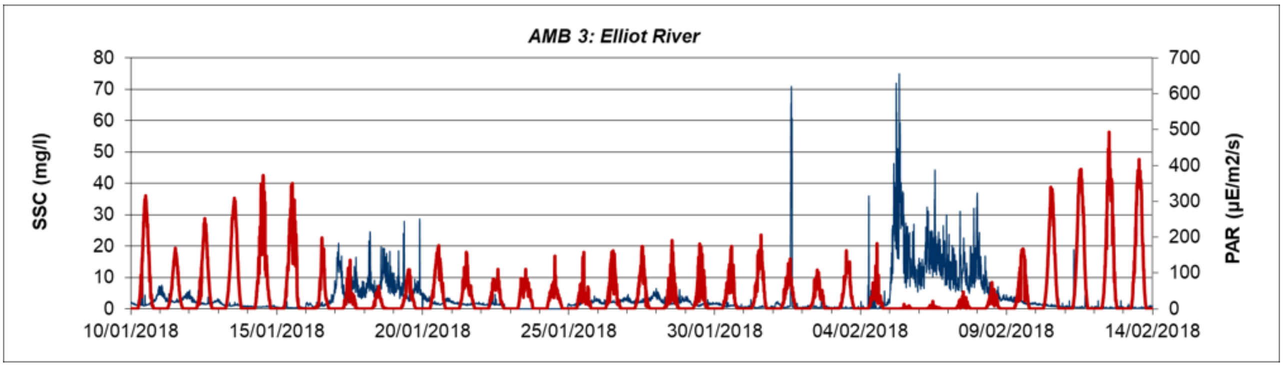

Figure 3.24 A typical example of the relationship between SSC and PAR light, showing light levels decreasing as SSC increases during Jan-Feb 2018 at Elliot River.

3.3.6 Comparison between wet and dry seasons

RMS water height

For RMS, mean values and 90th percentiles were slightly higher during wet seasons, but median values were similar (Figure 3.25). This suggests that the typical RMS was similar between seasons, but periods of elevated RMS were larger in magnitude during the wet season. There wasn't a large difference in RMS between the 2018-2019 wet season and the data available from combined wet seasons.

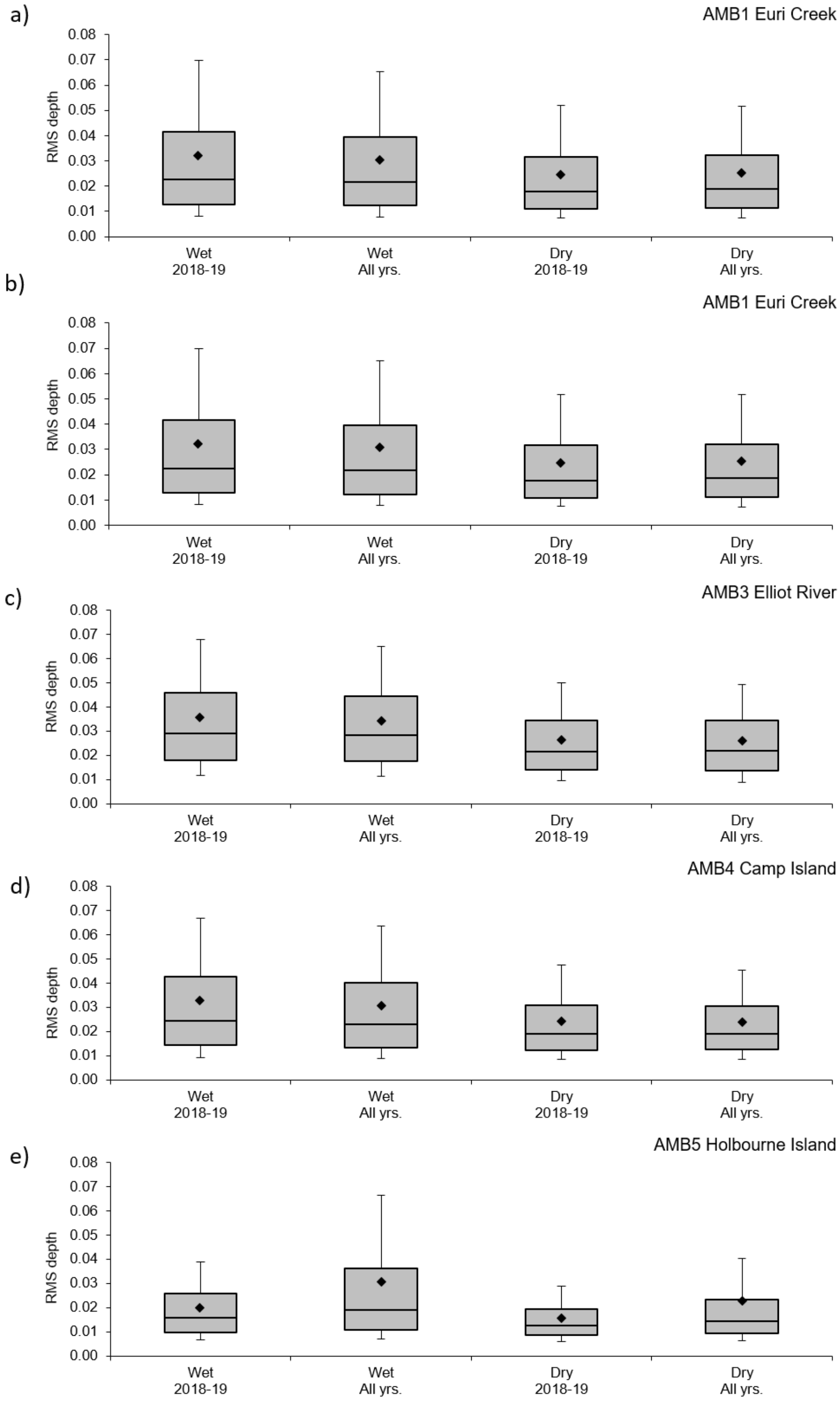

Figure 3.25 RMS box plots for AMB1-AMB5 (a-e). Boxes represent the wet (1 November-31 March) and dry seasons (1 April-31 October) using either one wet season (2018-2019) or two wet seasons (2017-2019).

SSC

Differences in SSC between seasons are less straightforward than for RMS. While median SSC was often similar between wet and dry seasons, the upper quartiles typically increased during the wet season, indicated more extreme turbidity events (Figure 3.26). For the coastal sites AMB1-4, the 90th percentile of SSC was approximately double that of dry seasons. However, at AMB2-AMB4 (not AMB1) the median and mean SSC were largely similar between seasons, suggesting that these events didn't influence the typical turbidity at these sites. For AMB1, higher turbidity was observed during the wet seasons as the median value doubled from 0.7 to 1.5 mg L^{-1} for the dry and wet seasons of 2018-2019.

Notably, AMB5 exhibited an opposite trend from the coastal sites, AMB1-4, whereby median SSC was 2.4 mg L^{-1} in the dry season and 0.6 mg L^{-1} in the wet season.

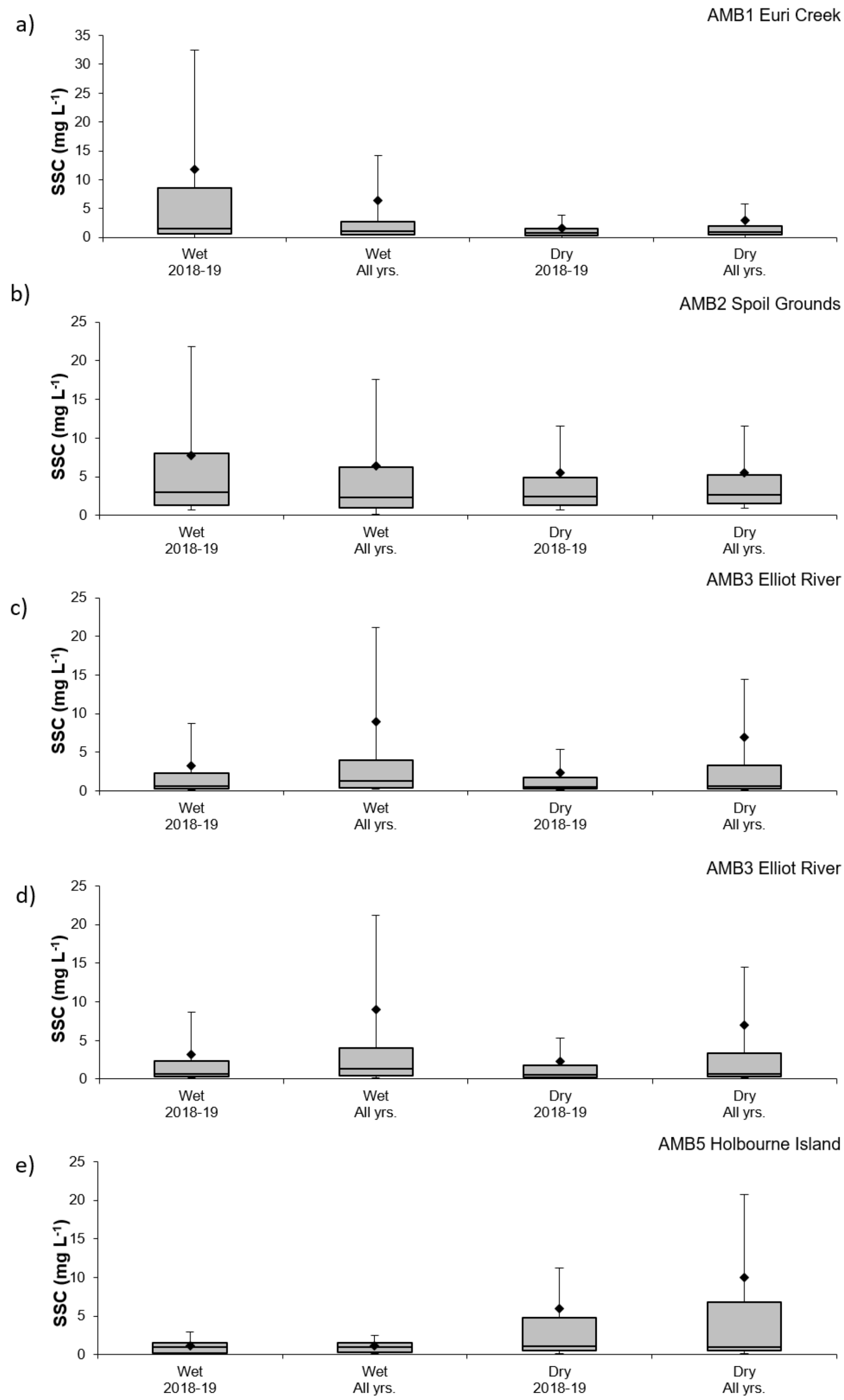

Figure 3.26 SSC box plots for AMB1-AMB5 (a-e). Boxes represent the wet (1 November-31 March) and dry seasons (1 April-31 October) using either one wet season (2018-2019) or two wet seasons (2017-2019).

Deposition rate

In general, deposition rates were higher during wet seasons (Figure 3.27), particularly so for AMB1, AMB4, and AMB5. At AMB3, median deposition rates were similar between seasons (wet: 0.7 mg cm^{-2} d^{-1}, dry: 0.5 mg cm^{-2} d^{-1}), but the largest deposition rates (i.e., 90th percentile) were larger when compared to the dry season (wet: 8.7 mg cm^{-2} d^{-1}, dry: 5.3 mg cm^{-2} d^{-1}).

In contrast, deposition rates at AMB2 were relatively similar between seasons (median 3.0 mg cm^{-2} d^{-1} wet, 2.4 mg cm^{-2} d^{-1} dry). Ongoing investigation will provide more data to verify whether these differences represent real seasonal trends or instead reflect a series of episodic climate conditions in the region (see Figures 1.2 and 1.3).

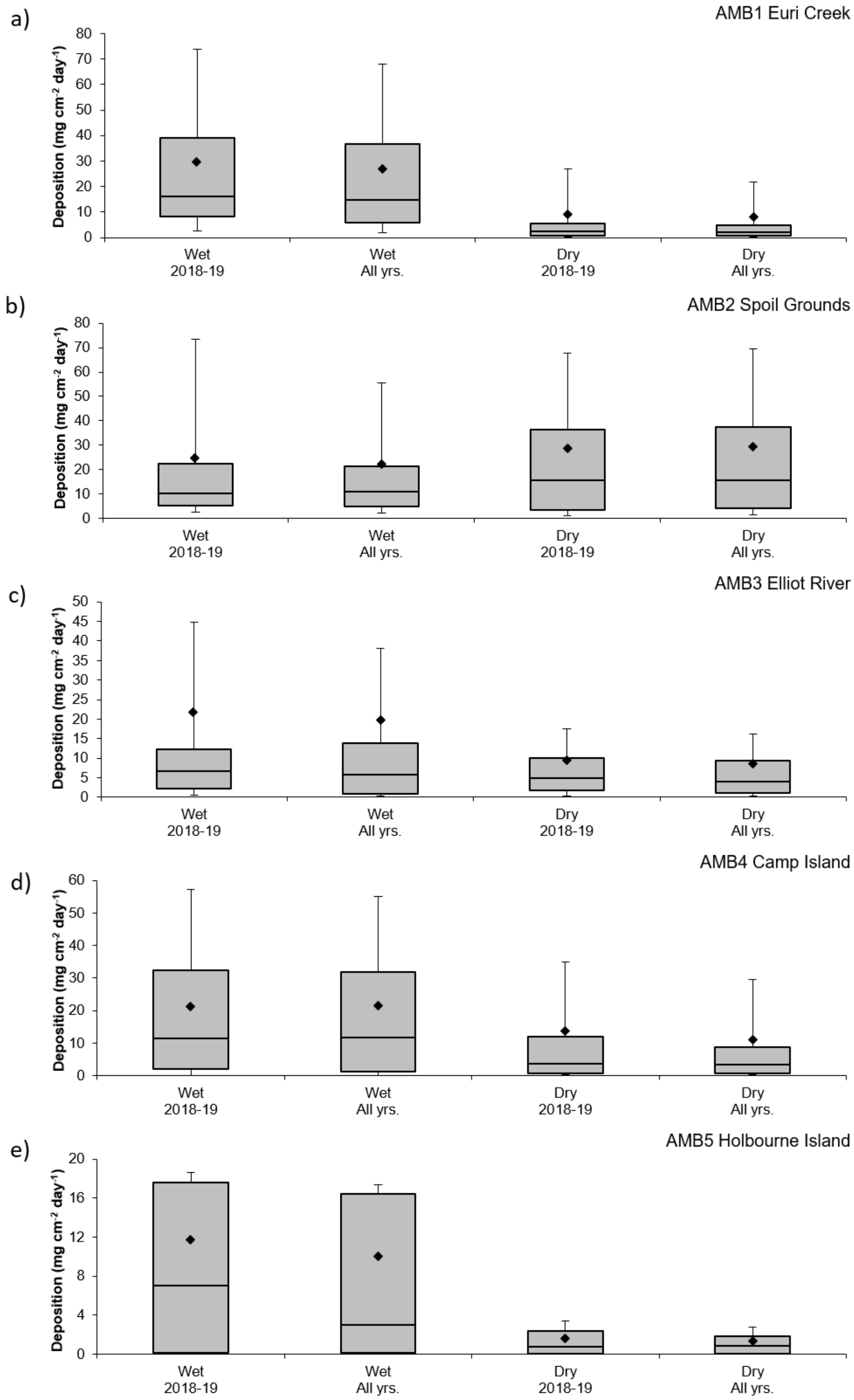

Figure 3.27 Deposition box plots for AMB1-AMB5 (a-e). Boxes represent the wet (1 November-31 March) and dry seasons (1 April-31 October) using either one wet season (2018-2019) or two wet seasons (2017-2019).

Total daily PAR

Photosynthetically available radiation (PAR) could differ between seasons due to longer day length or increased cloud cover during the wet season. However, daily PAR for AMB3 and AMB4 increased 76 and 93 % (using medians), respectively, during the dry season (Figure 3.28). Daily PAR totals for AMB1 and AMB2 were generally similar between wet and dry seasons. In contrast to the other sites, daily PAR at AMB5 decreased by 50 % (using medians) during the dry season and showed the largest variance over the wet seasons. These sites suggest that there isn't a general pattern in PAR between seasons, especially at sites close to shore. Differences in depth, distance from the coast, and distance from river mouths may influence how PAR differs between seasons at a given location.

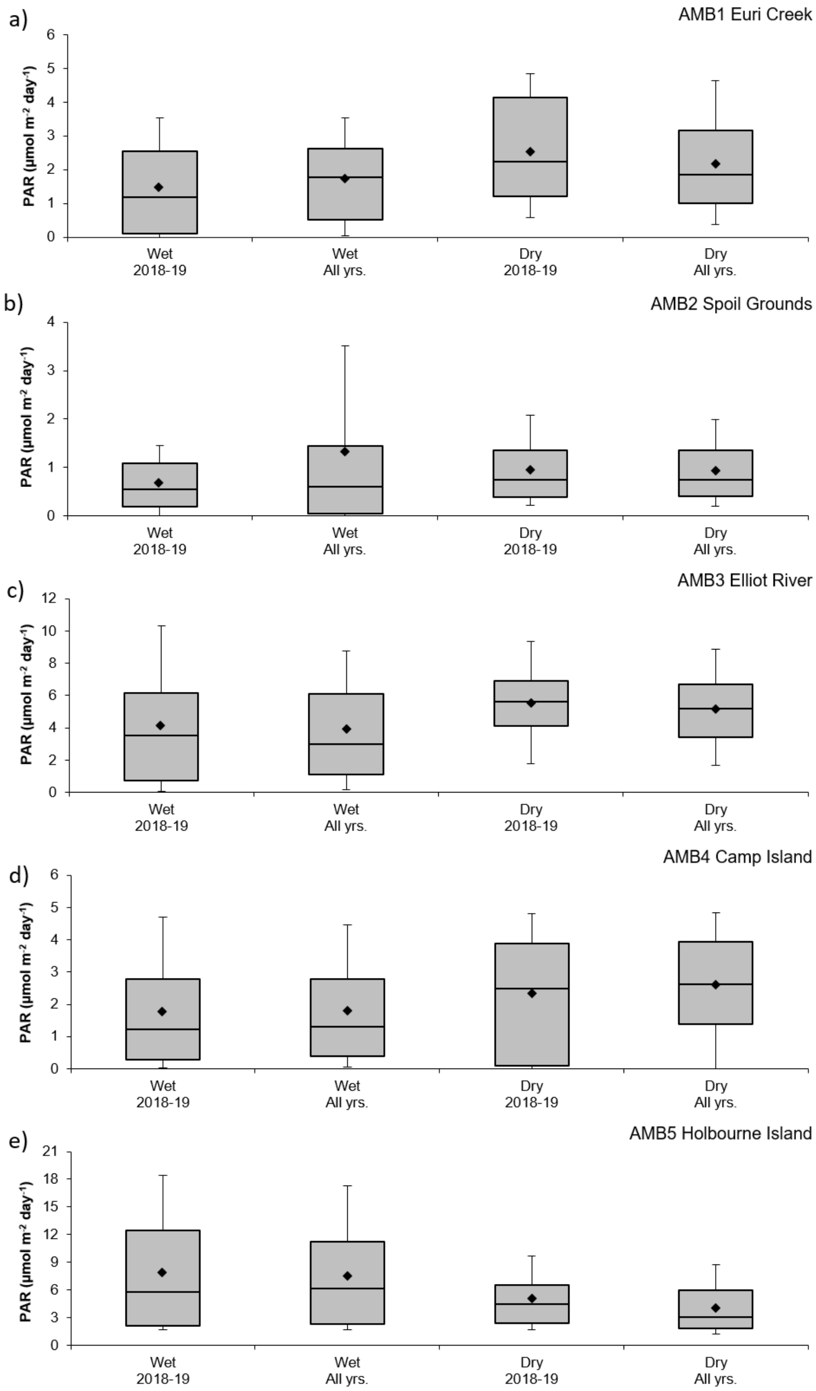

Figure 3.28 PAR box plots for AMB1-AMB5 (a-e). Boxes represent the wet (1 November-31 March) and dry seasons (1 April-31 October) using either one wet season (2018-2019) or two wet seasons (2017-2019).

Water temperature

There is a clear difference in water temperature between the wet and dry seasons (Figure 3.29). Temperatures are higher during the wet season, with median temperatures between 28 and 29 °C at all sites, with much less variation than in the dry season. Median dry season temperatures ranged from 22 to 24 °C with more variation than in the wet season.

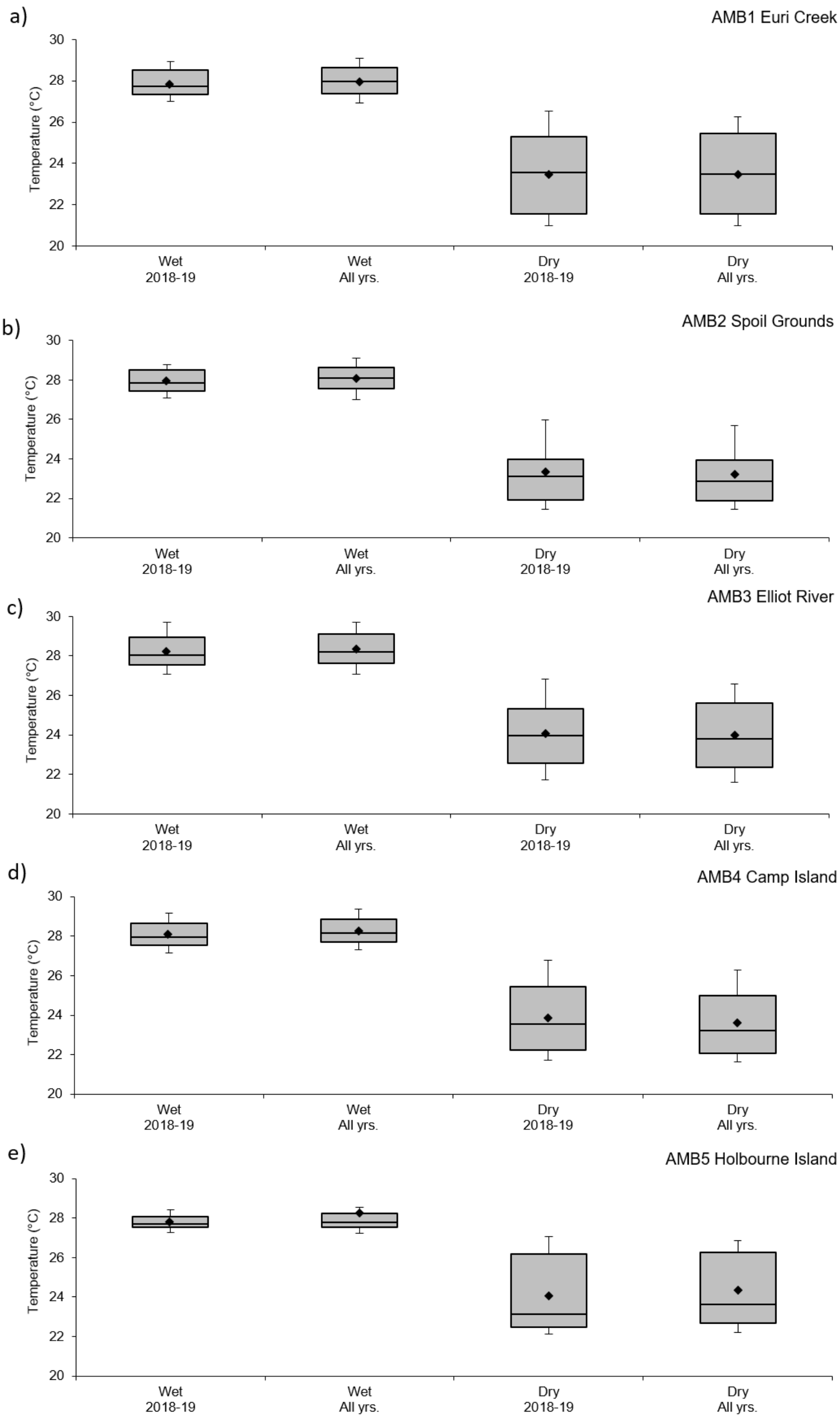

Figure 3.29 2014-2018 water temperature box plots for: a) wet seasons (1 November-31 March); and b) dry seasons (1 April-31 October).

3.4 Current meter

Current meter data was collected at all five sites. Marotte HS current meter instruments were deployed for the full monitoring period from July 2018 to July 2019 for AMB 1-5. The current meter data indicates the prominent current direction and velocity at each site. Data shows that coastal current, tidal current or a combination of both influence current direction and magnitude. The figures below display the current meter data in current rose and average current speed rose diagrams. The current rose diagrams provide a visual representation of relative prominence of current velocity and direction. The average current speed rose diagrams displays the average current speed in every direction. Presented together these diagrams highlight the prominent direction of current and the average velocity of the current in this direction. A short and long animation illustrating how the current speed and direction changes over time at each site are accessible to view via sharepoint (Figure 3.30). Links to the videos are provided in Appendix A1.4.

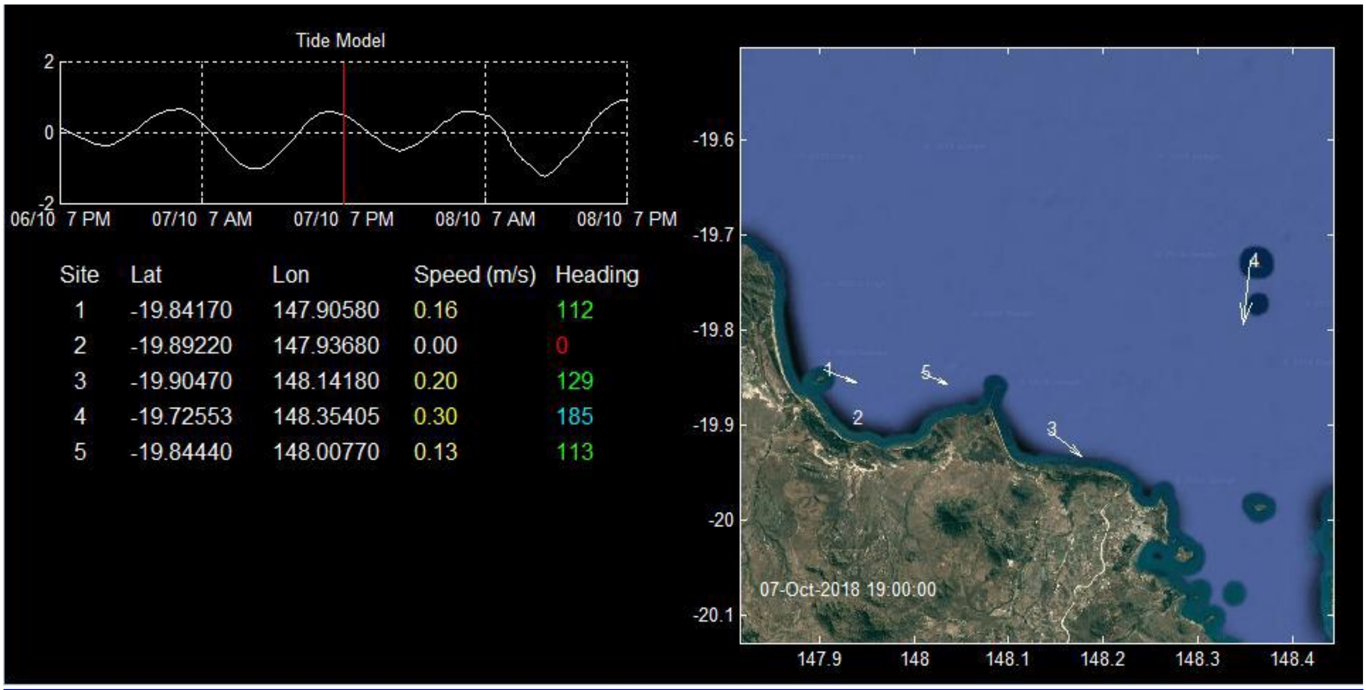

Figure 3.30 Example screengrab from current speed and direction animations

3.4.1 AMB 1: Euri Creek

The current at Euri Creek ranges from SE to NW with peaks at SSE and SW and average velocities are between 0.06 m s^{-1} and 0.12 m s^{-1} (as shown in

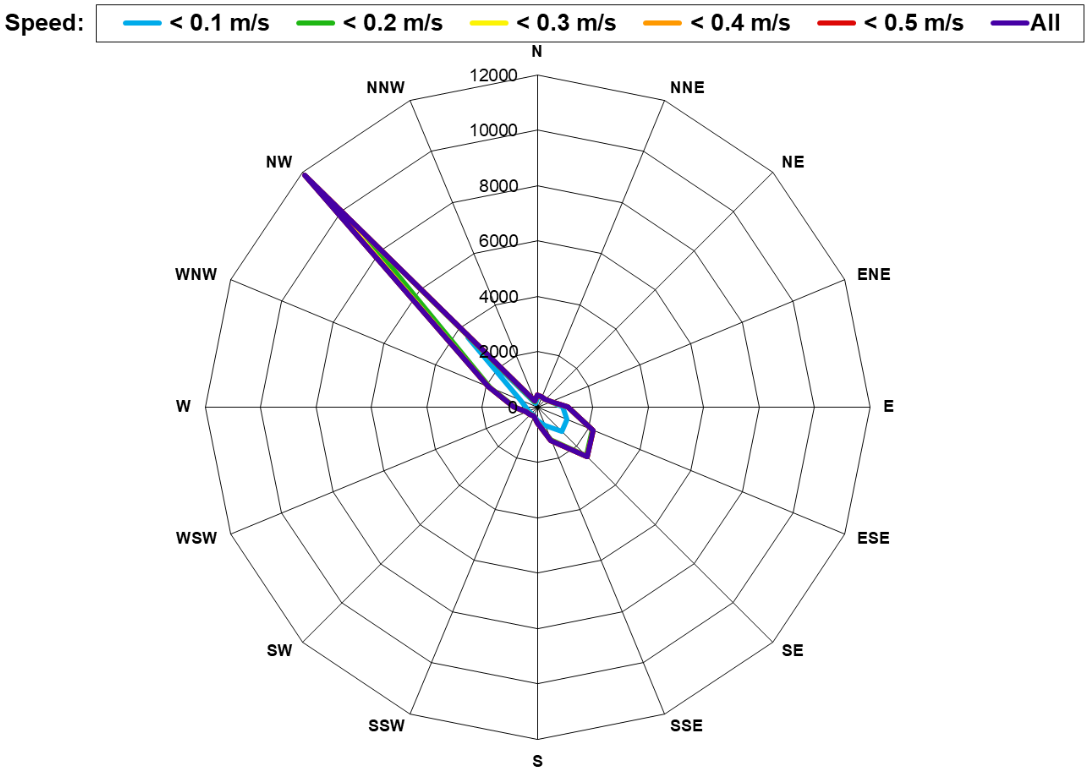

Figure **3.31** and Figure 3.32). This shows that the current is flowing along the coast. Changes in current velocity are likely the result of tidal current influence.

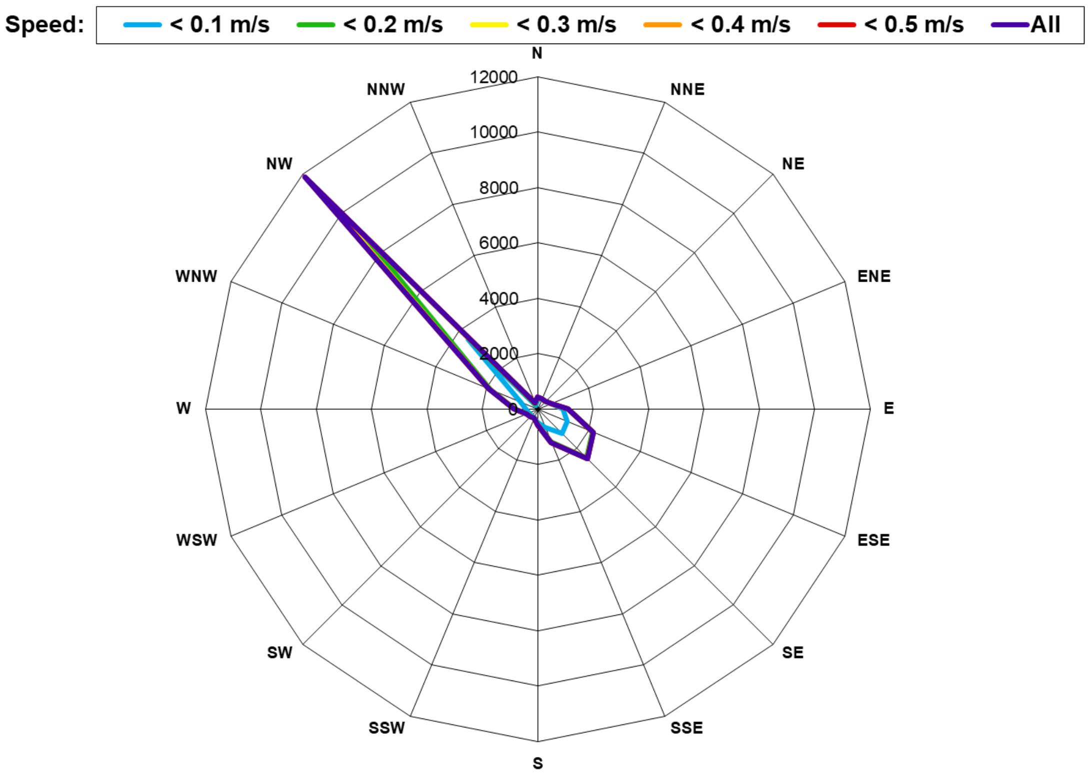

Figure 3.31 Current rose at Euri Creek (AMB 1) for the monitoring period from July 2018 to July 2019. The current rose plots the number of currents recorded in each direction within the ranges of different current speeds indicated in the legend.

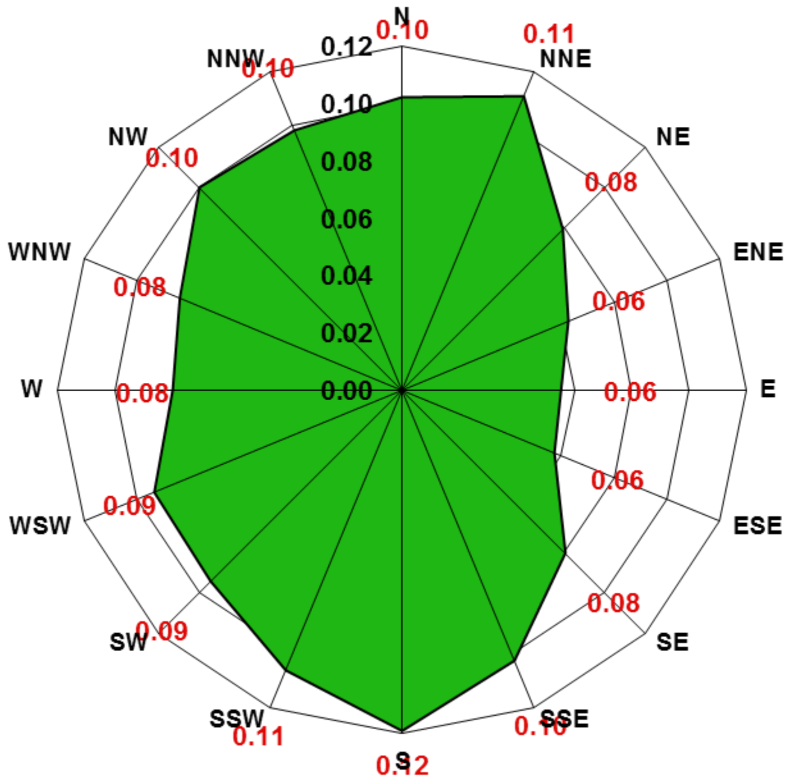

Figure 3.32 Average current speed rose at Euri Creek (AMB 1) for the monitoring period from July 2018 to July 2019. The average current speed is coloured in green while the red values indicate the average current value at each direction.

3.4.2 AMB 2: Spoil Grounds

The most frequent current directions at the Spoil Grounds are ENE and SSW, but other directions are also commonly observed (Figure 3.33), corresponding with the sites position away from the coast where current direction rotates with tidal shifts. Average velocities range between 0.08 m s^{-1} and 0.16 m s^{-1} (Figure 3.34).

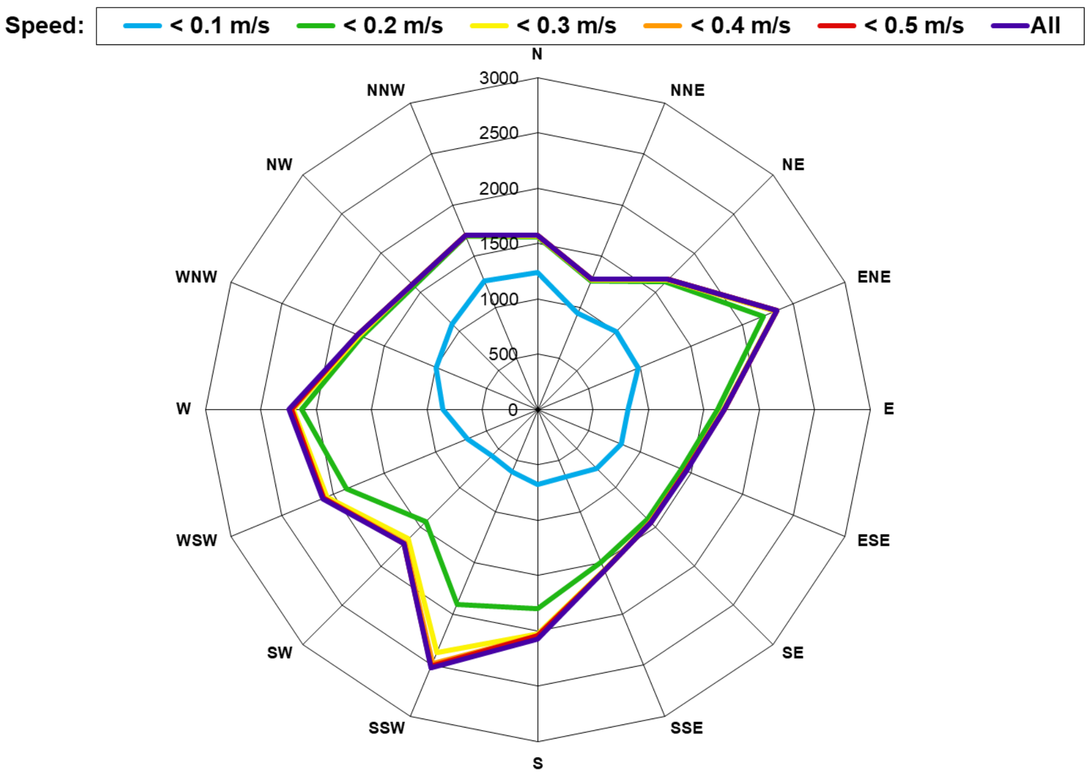

Figure 3.33 Current rose at Spoil Grounds (AMB 2) for the monitoring period from July 2018 to July 2019. The current rose plots the number of currents recorded in each direction within the ranges of different current speeds indicated in the legend.

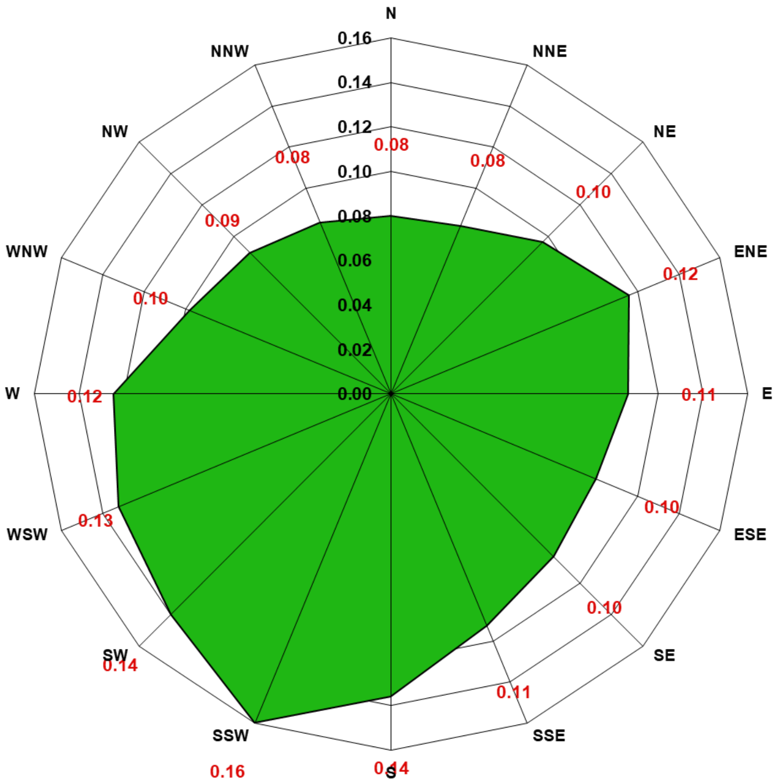

Figure 3.34 Average current speed rose at Spoil Grounds (AMB 2) for the monitoring period from July 2018 to July 2019. The average current speed is rose is coloured in green, while the red values indicate the average current value at each specific direction.

3.4.3 AMB 3: Elliot River

The current at Elliot River ranges from SE to NW (Figure 3.35), reflecting currents flowing along the coast. Average velocities are between 0.05 m s^{-1} and 0.09 m s^{-1} (Figure 3.36). Changes in current velocity are likely the result of tidal influence.

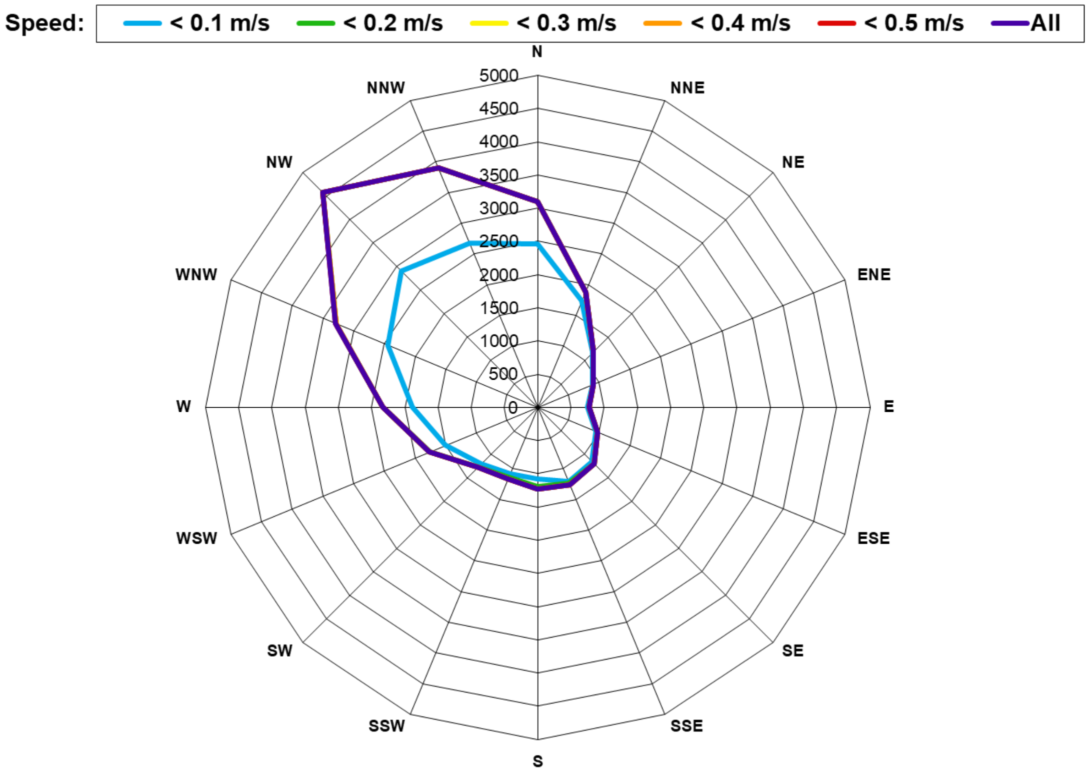

Figure 3.35 Current rose at Camp Island Elliot River (AMB 43) for the monitoring period from July 2018 to July 2019. The current rose plots the number of currents recorded in each direction within the ranges of different current speeds indicated in the legend.

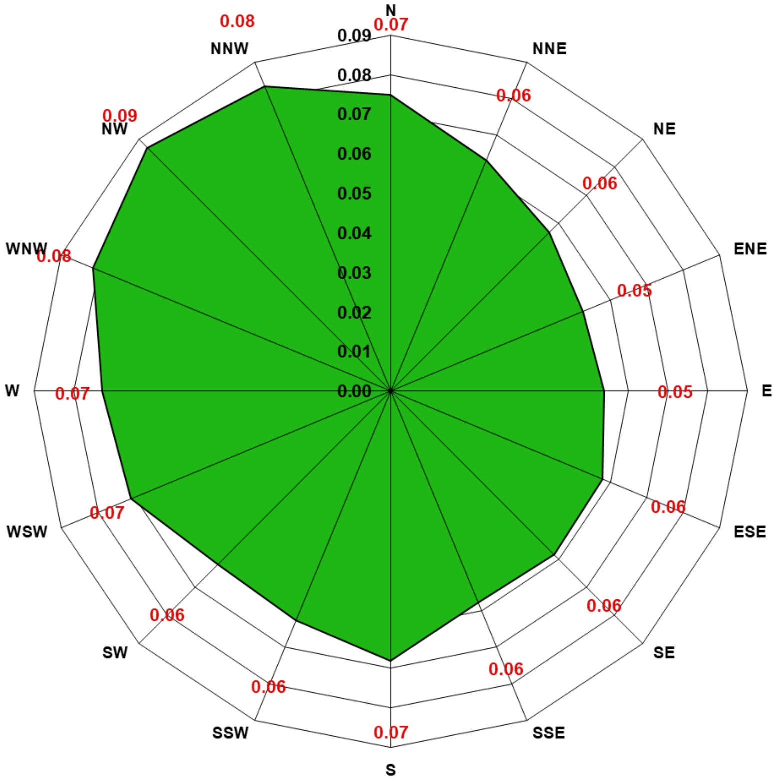

Figure 3.36 Average current speed rose at Elliot River (AMB 3) for the monitoring period from July 2018 to July 2019. The average current speed is rose is coloured in green, while the red values indicate the average current value at each specific direction.

3.4.4 AMB 4: Camp Island

The current at Camp Island predominately flowed to the NNW and ESE, flowing along the coast (Figure 3.37). Average current velocities ranged from 0.06 to 0.15 m s^{-1} (Figure 3.38). This shows that the current is flowing along the coast. Changes in current velocity are likely the result of tidal current influence.

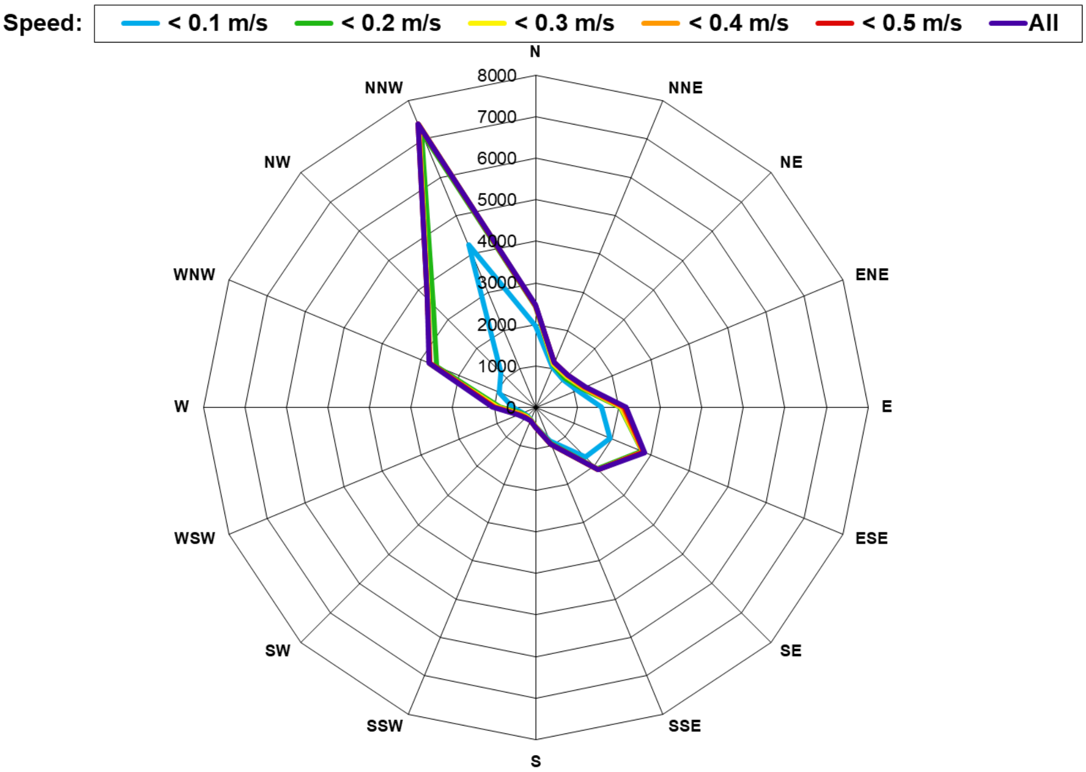

Figure 3.37 Current rose at Camp Island (AMB 4) for the monitoring period from July 2018 to July 2019. The current rose plots the number of currents recorded in each direction within the ranges of different current speeds indicated in the legend.

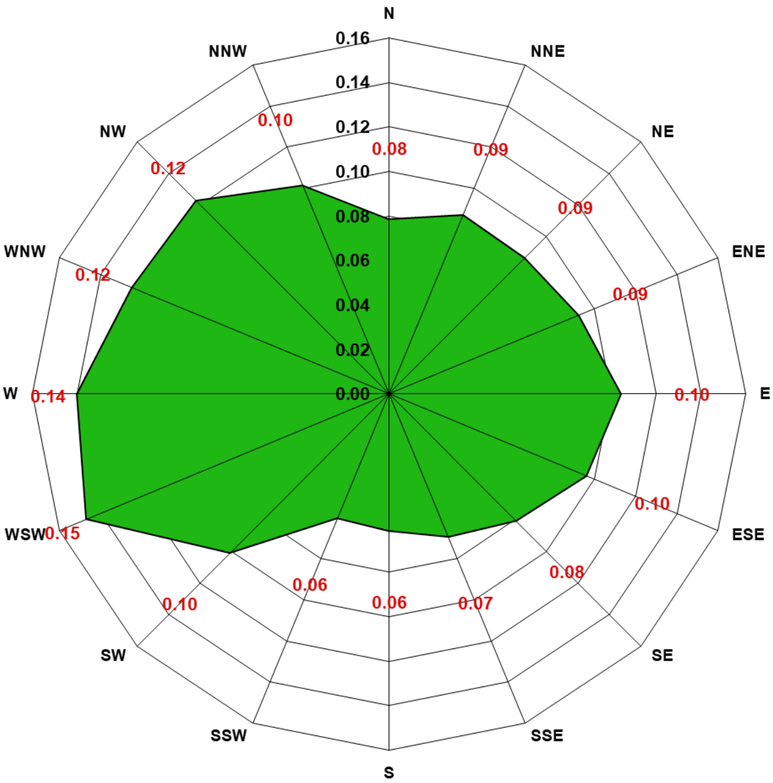

Figure 3.38 Average current speed rose at Camp Island (AMB 4) for the monitoring period from July 2018 to July 2019. The average current speed is coloured in green and the red values indicate the average current value at each specific direction.

3.4.5 AMB 5: Holbourne Island

The current at Holbourne Island ranges from S to NNE due to the fact that the site is on the NW side of the island (Figure 3.39). Average velocities ranged from 0.06 to 0.11 m s^{-1} (Figure 3.40). Changes in current velocity are likely the result of tidal current influence.

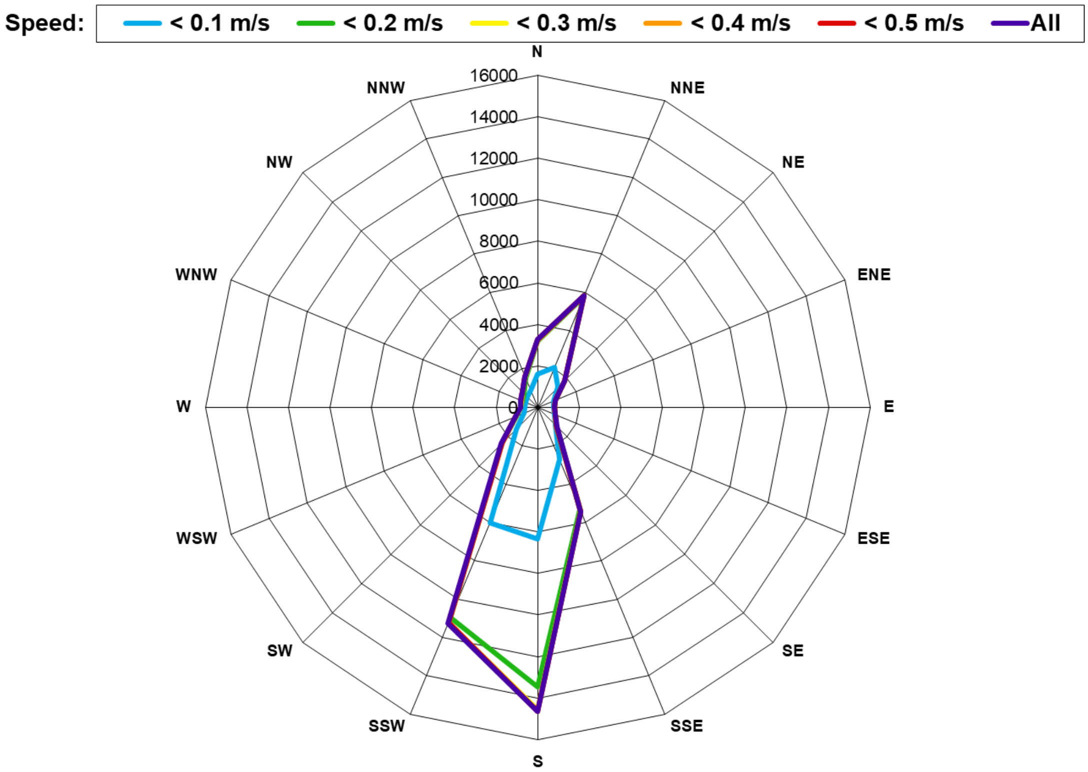

Figure 3.39 Current rose at Holbourne Island (AMB 5) for the monitoring period from July 2018 to July 2019. The current rose plots the number of currents recorded in each direction within the ranges of different current speeds indicated in the legend.

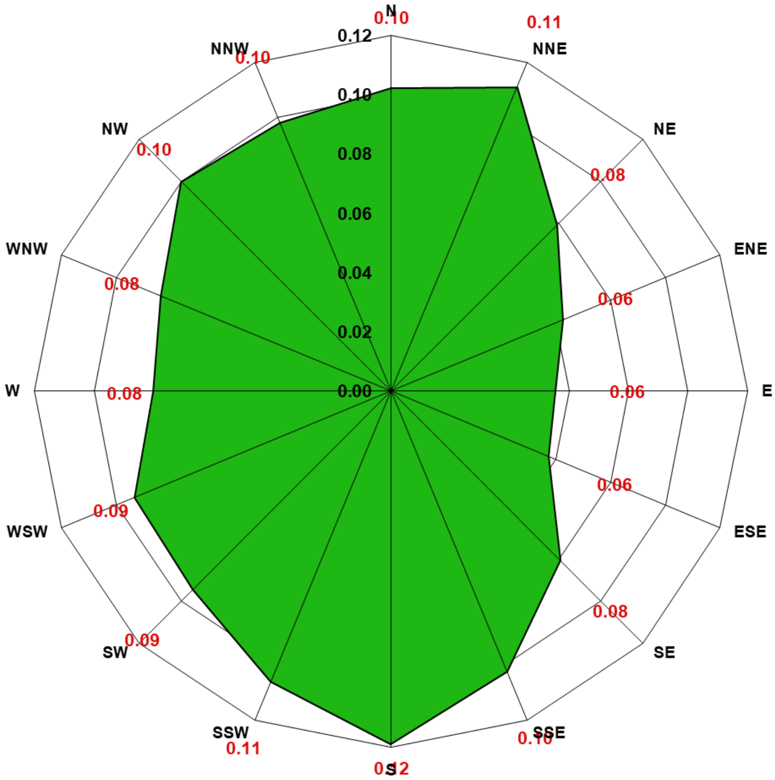

Figure 3.40 Average current speed rose at Holbourne Island (AMB 5) for the monitoring period from July 2018 to July 2019. The average current speed is rose is coloured in green, while the red values indicate the average current value at each specific direction.

3.5 River Plumes

3.5.1 Site specific outputs

AMB1 (Euri Creek)

A stepwise regression analysis was run against the AMB1 data (Euri Creek) to identify the appropriate variable selection, excluding autocorrelation and outliers, for the multiple regression analysis. RMS of water depth, the NESW and NWSE wind components explained 30% of the SSC variability (Table 3.8). The relative importance analysis suggested that RMS of water depth is the most influential parameter on SSC (73% of overall R^2), followed by the NWSE wind component (15% of the overall R^2) and the NESW wind component (12% of the overall R^2) (Figure 3.41). The relationship between the RMS water depth and SSC followed the expected trend, with SSC increasing with RMS water depth (Figure 3.42).

Table 3.8 Statistical summary of the stepwise regression analysis to AMB1 data

	AMB1		
Predictors	*Estimates*	*CI*	*p*
(Intercept)	7.20	5.54 – 8.85	**<0.001**
log(RMS)	1.68	1.31 – 2.05	**<0.001**
wind NESW	0.05	0.02 – 0.07	**0.002**
wind NWSE	0.04	0.02 – 0.07	**<0.001**
Observations	259		
R^2 / adjusted R^2	0.302 / 0.293		

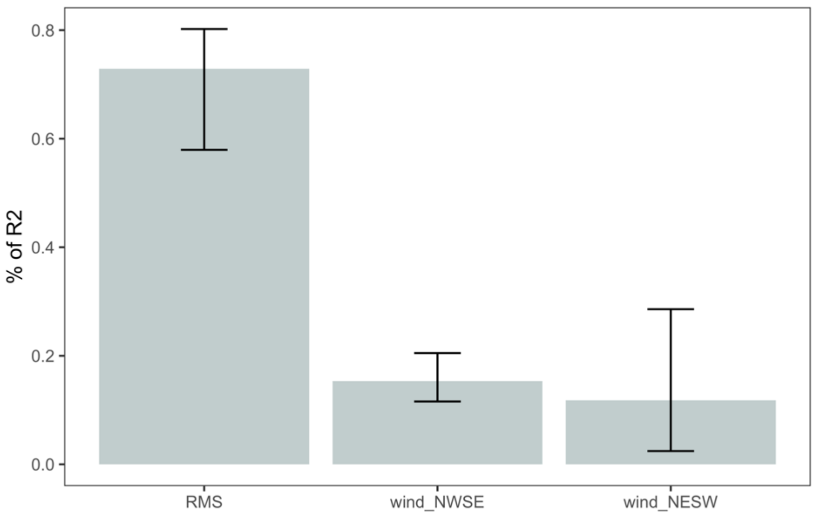

Figure 3.41 Bootstrapping relative importance analysis following a stepwise multiple regression analysis. Bars represent 95% bootstrap confidence intervals, and % of r squared values are normalized to sum 100%

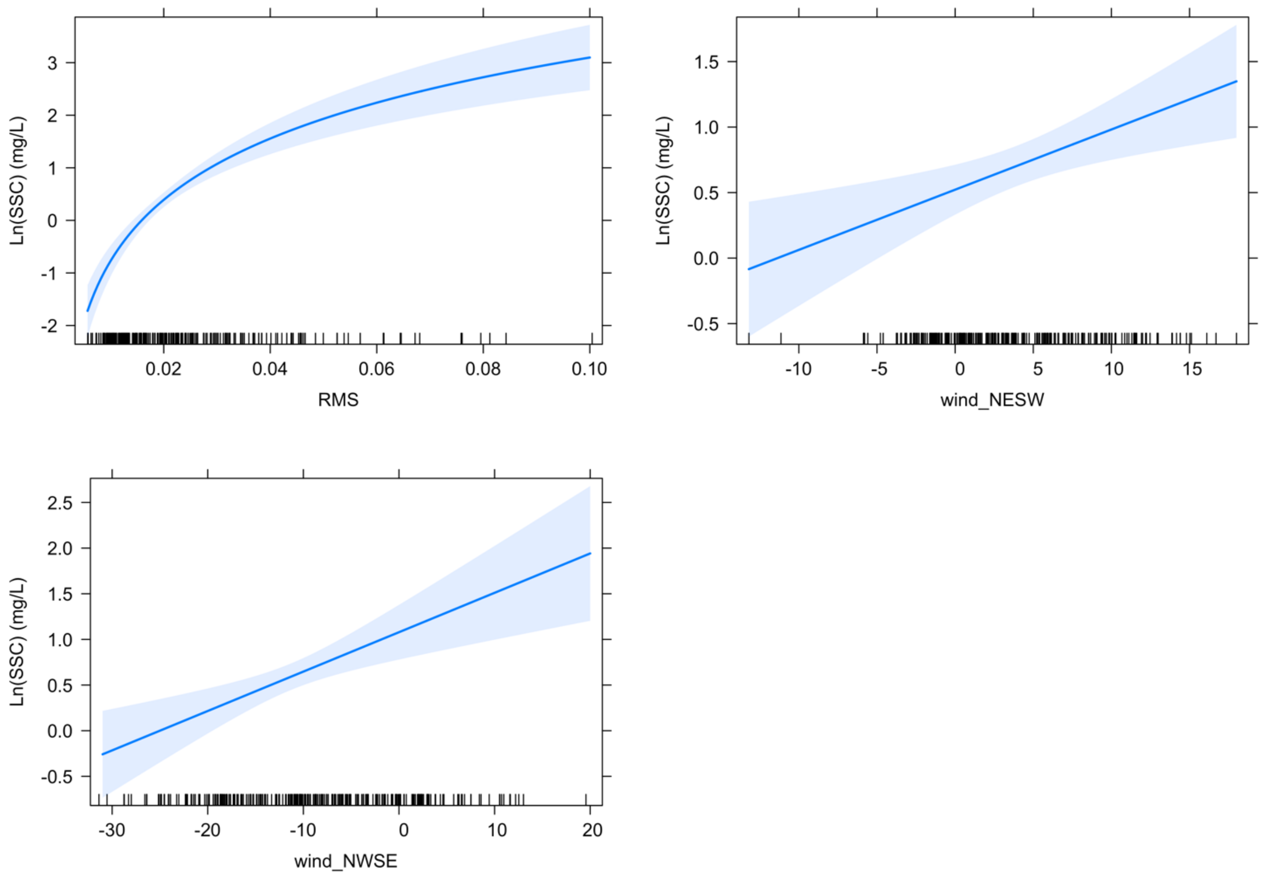

Figure 3.42 Partial effect plots for AMB1 parameters affecting the concentration of suspended solids in the water column. Grey area indicates 95% CI and rug on x-axis stand for data density

AMB2 (Bowen Spoil Grounds)

A stepwise regression analysis was run against the AMB2 data to identify the appropriate variable selection, excluding autocorrelation and outliers, for the multiple regression analysis. RMS of water depth, Don River discharge, and the NESW and NWSE wind components explained 15% of the SSC variability (Table 3.9). The relative importance analysis suggested that RMS of water depth is the most influential parameter on SSC (44% of overall R^2), followed by Don River discharge (34% of overall R^2), the NESW wind component (14% of the overall R^2) and the NWSE wind component (8% of the overall R^2) (Figure 3.43). The partial effects plot shows that SSC was positively related to each of the influential environmental parameters (Figure 3.44).

Table 3.9 Statistical summary of the stepwise regression analysis to AMB2 data

	AMB2		
Predictors	*Estimates*	*CI*	*p*
(Intercept)	3.75	2.46 – 5.04	**<0.001**
log(RMS)	0.62	0.35 – 0.90	**<0.001**
log(Don + 1)	0.09	0.05 – 0.13	**<0.001**
wind NESW	0.02	0.00 – 0.05	**0.020**
wind NWSE	0.02	0.00 – 0.03	**0.047**
Observations	319		
R^2 / adjusted R^2	0.159 / 0.148		

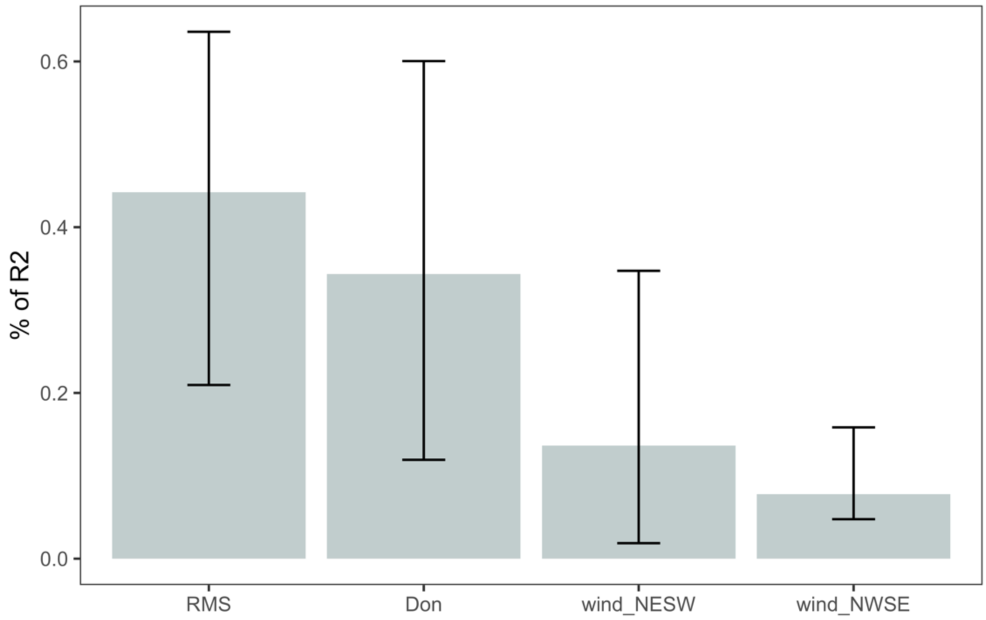

Figure 3.43 Bootstrapping relative importance analysis following a stepwise multiple regression analysis. Bars represent 95% bootstrap confidence intervals, and % of r squared values are normalized to sum 100%. Overall R^2 = 0.35

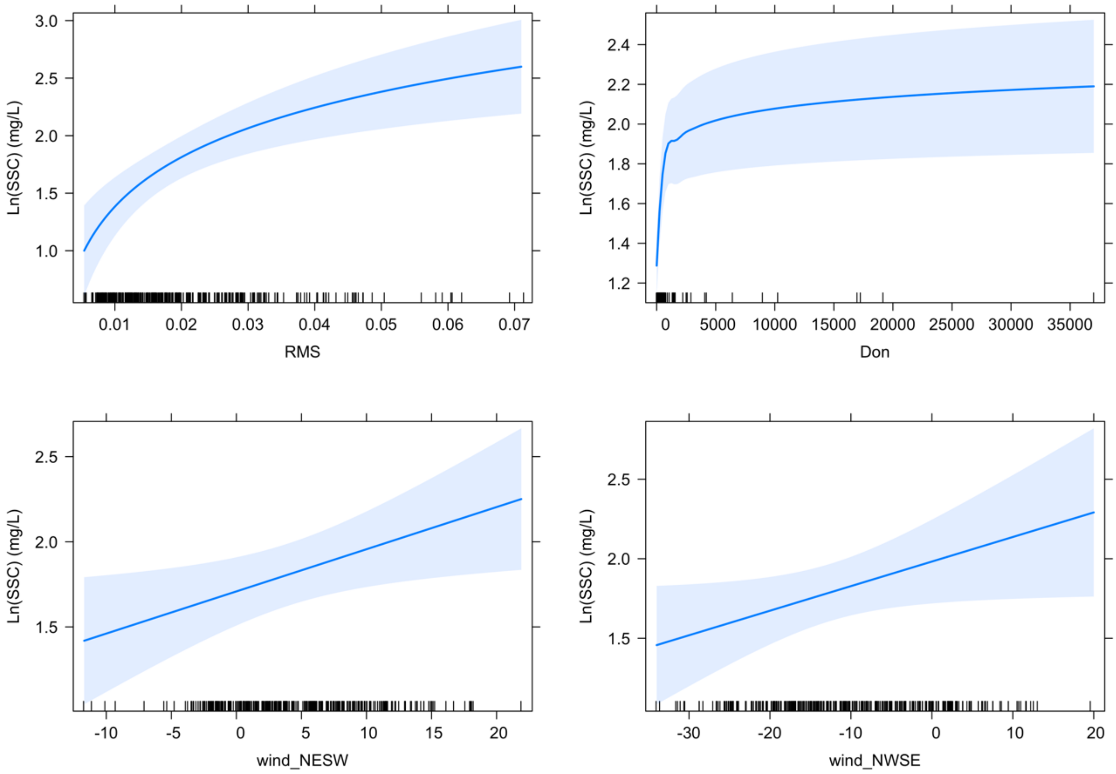

Figure 3.44 Partial effect plots for AMB2 parameters affecting the concentration of suspended solids in the water column. Grey area indicates 95% CI and rug on x-axis stand for data density

AMB3 (Elliot River)

A stepwise regression analysis was run against the AMB3 data to identify the appropriate variable selection, excluding autocorrelation and outliers, for the multiple regression analysis. RMS of water depth and Euri River discharge explained 31% of the SSC variability (Table 3.10). The relative importance analysis suggested that RMS of water depth was the most influential parameter on SSC (92% of overall R^2), followed by Euri River discharge (8% of overall R^2) (Figure 3.45). Partial effects plots (Figure 3.46) show that SSC increases with RMS of water depth, but decrease in relation to Euri River discharge.

Table 3.10 Statistical summary of the stepwise regression analysis to AMB3 data

	AMB3		
Predictors	*Estimates*	*CI*	*p*
(Intercept)	5.74	4.62 – 6.85	**<0.001**
log(RMS)	1.42	1.13 – 1.71	**<0.001**
log(Euri + 1)	-0.10	-0.16 – -0.04	**0.001**
Observations	215		
R^2 / adjusted R^2	0.309 / 0.302		

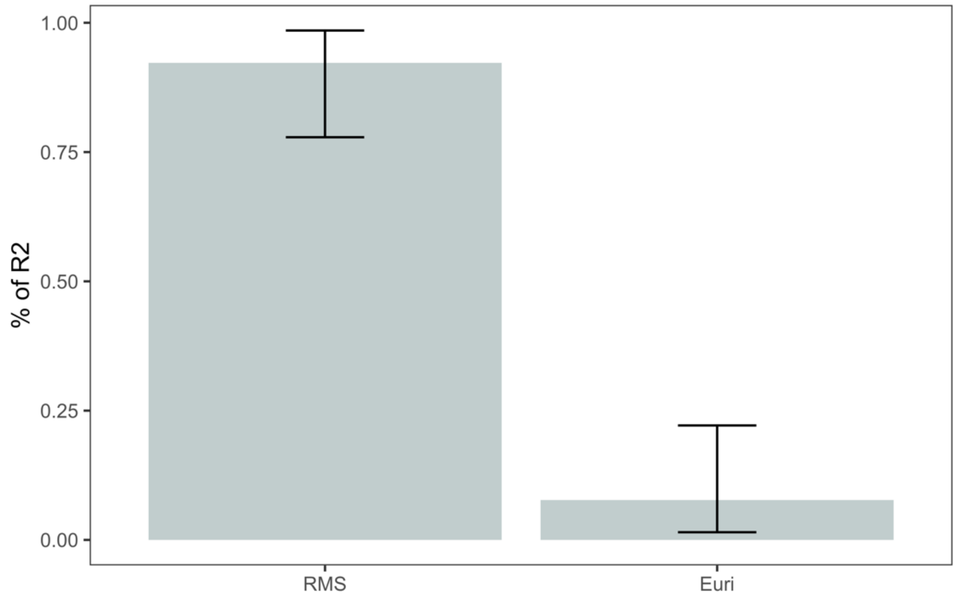

Figure 3.45 Bootstrapping relative importance analysis following a stepwise multiple regression analysis. Bars represent 95% bootstrap confidence intervals, and % of r squared values are normalized to sum 100%

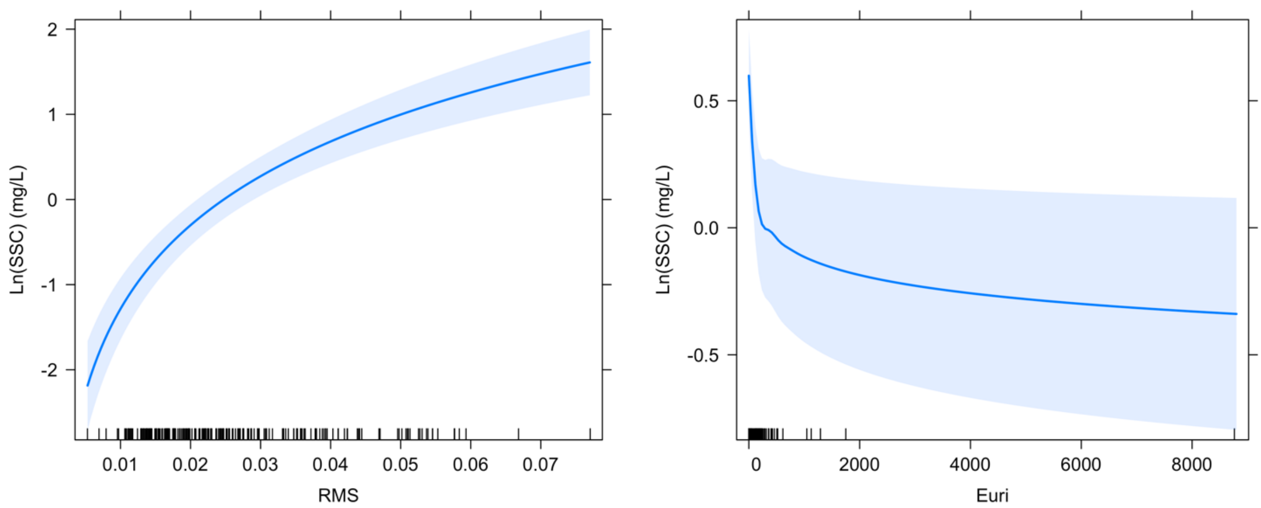

Figure 3.46 Partial effect plots for AMB3 parameters affecting the concentration of suspended solids in the water column. Grey area indicates 95% CI and rug on x-axis stand for data density

AMB4 (Camp Island)

A stepwise regression analysis was run against the AMB4 data to identify the appropriate variable selection, excluding autocorrelation and outliers, for the multiple regression analysis. RMS of water depth and the NESW wind component explained 17% of the SSC variability (Table 3.12). The relative importance analysis suggested that RMS of water depth was the most influential parameter on SSC (92% of overall R^2) followed by the NESW wind component (8% of overall R^2) (Figure 3.47). Partial effects plots (Figure 3.48) show that SSC increases in relation to both influential environmental parameters.

Table 3.11 Statistical summary of the stepwise regression analysis to AMB4 data

	AMB4		
Predictors	*Estimates*	*CI*	*p*
(Intercept)	4.44	3.67 – 5.22	**<0.001**
log(RMS)	0.81	0.61 – 1.02	**<0.001**
wind NESW	0.03	0.01 – 0.05	**0.006**
Observations	303		
R^2 / adjusted R^2	0.178 / 0.172		

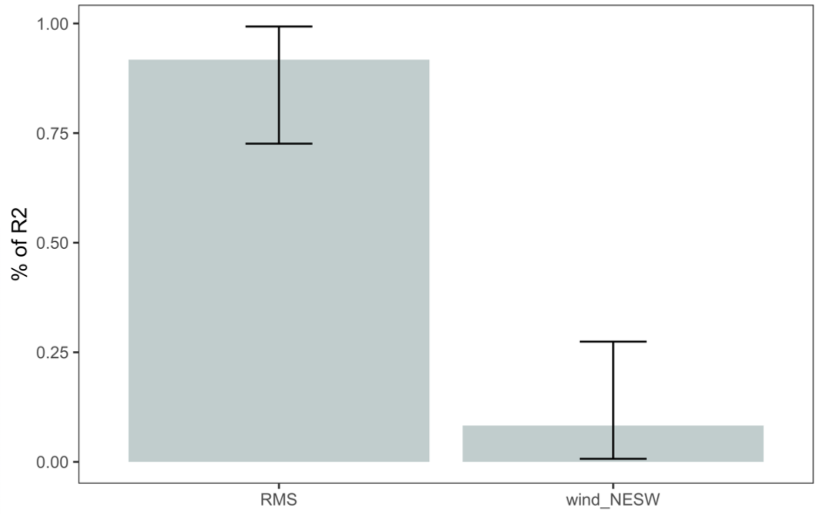

Figure 3.47 Bootstrapping relative importance analysis following a stepwise multiple regression analysis. Bars represent 95% bootstrap confidence intervals, and % of r squared values are normalized to sum 100%. Overall R^2 = 0.41

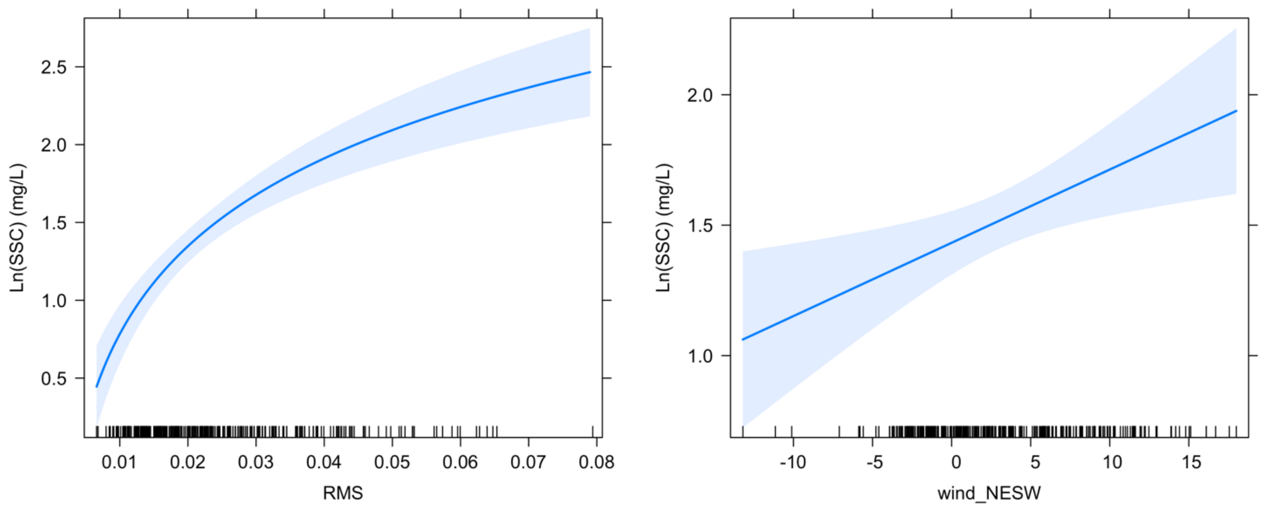

Figure 3.48 Partial effect plots for AMB4 parameters affecting the concentration of suspended solids in the water column. Grey area indicates 95% CI and rug on x-axis stand for data density

AMB5 (Holbourne Island)

A stepwise regression analysis was run against the AMB5 data to identify the appropriate variable selection, excluding autocorrelation and outliers, for the multiple regression analysis. RMS of water depth, Don River discharge, the NESW and NWSE wind components, and tidal amplitude together explained 36% of the SSC variability (Table 3.13). Relative importance analysis suggested that the NESW and NWSE wind components were the most influential parameters on SSC, together explaining 74% of the overall R^2 (Figure 3.49). Don river discharge explained 14% of the overall R^2, while tidal amplitude and RMS of water depth each explained 5% of the overall R^2. Partial effects plots show that SSC increases in relation to increased Don River discharge and tidal amplitude, although wide confidence intervals indicate that these are weak relationships (Figure 3.50).

Table 3.12 Statistical summary of the stepwise regression analysis to AMB5 data

	AMB5		
Predictors	*Estimates*	*CI*	*p*
(Intercept)	-4.21	-5.99 – -2.42	**<0.001**
log(RMS)	-0.69	-1.04 – -0.33	**<0.001**
log(Don + 1)	0.13	0.08 – 0.18	**<0.001**
wind NESW	-0.10	-0.12 – -0.07	**<0.001**
wind NWSE	-0.06	-0.07 – -0.04	**<0.001**
Amplitude	0.43	0.20 – 0.67	**<0.001**
Observations	265		
R^2 / adjusted R^2	0.355 / 0.342		

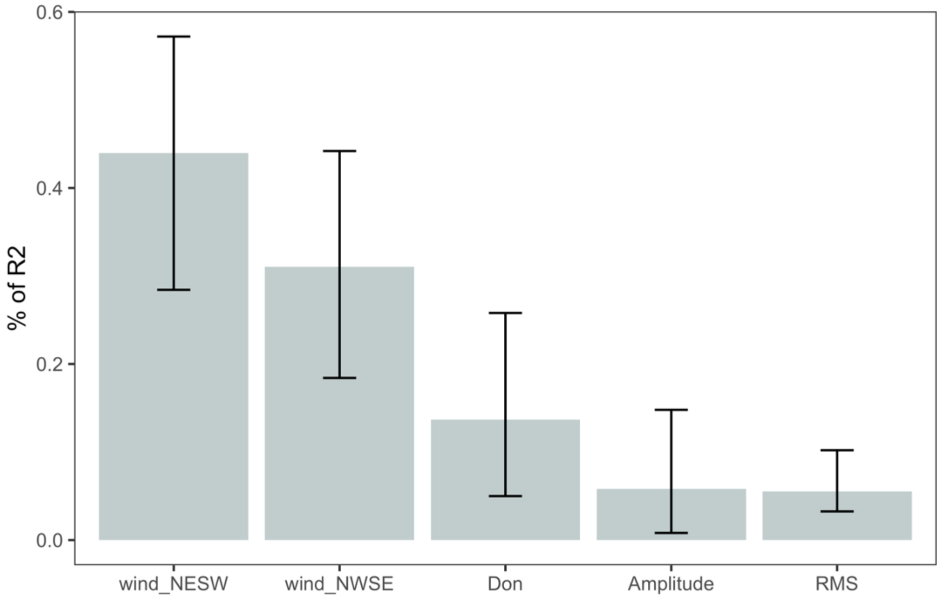

Figure 3.49 Bootstrapping relative importance analysis following a stepwise multiple regression analysis. Bars represent 95% bootstrap confidence intervals, and % of r squared values are normalized to sum 100%.

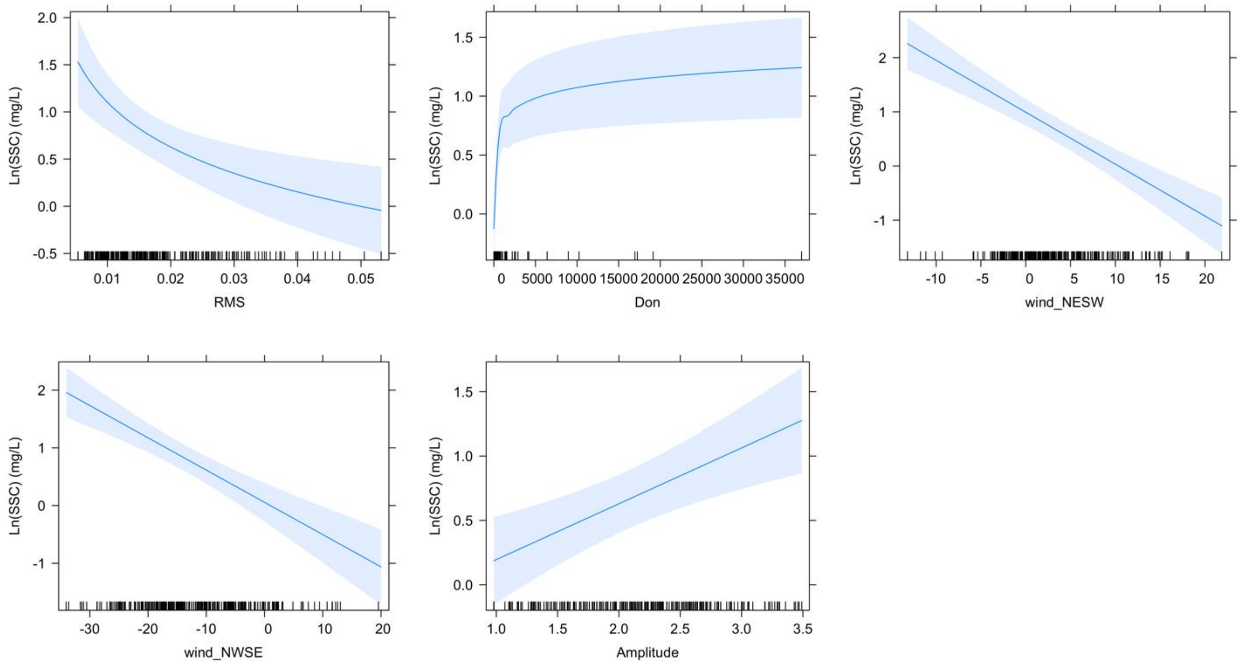

Figure 3.50 Partial effect plots for AMB5 parameters affecting the concentration of suspended solids in the water column. Grey area indicates 95% CI and rug on x-axis stand for data density

4 CONCLUSIONS AND RECOMMENDATIONS

4.1 Conclusions

4.1.1 Climatic conditions

- It is important to note when interpreting the 2018-2019 results that overall rainfall was low in the Abbot Point region but in February 2019 there was a particularly high river discharge event associated with a monsoonal tropical low.
- Comparison of these data with future years will be important to characterise ambient water quality conditions, particularly after the region experiences above average rainfall in the future.
- The wind speed and direction recorded at Abbot Point has been a useful inclusion in this assessment. The daily average wind speed and direction recorded for the reporting period was predominantly from the south east, with 30% of days having wind speeds greater than 24km h^{-1}.

4.1.2 Ambient water quality

- Seasonal differences in water quality were minor, except for temperature which was highest during the summer months.
- The water column is well mixed with profiles for dissolved oxygen, temperature, electrical conductivity, pH and turbidity showing no abrupt changes. Although turbidity was generally highest in the bottom horizon. This is an important consideration for when examining receptor habitats, such as corals and seagrass that are sensitive to water clarity changes. Measuring bottom horizon turbidity is a very relevant component of this program; surface measurements for turbidity, or indeed suspended solid concentrations, might not be an entirely relevant measure when the objective is to protect and enhance benthic habitats.
- Particulate nitrogen concentrations exceeded the guidelines throughout most of the 2018-2019 monitoring period.
- Chlorophyll-*a* concentrations exceeded the GBRMPA (2010) Water Quality Guideline in most months and all sites surveyed during the 2018-2019 monitoring period.
- Copper, nickel, and arsenic were detected in water samples collected in August 2018, although the concentrations were below relevant guideline values. No other metals were detected throughout the reporting period.
- Atrazine, Diuron, Hexazinone, and Tebutryn were detected during all survey in the 2018/2019 period although their concentrations did not exceed relevant guideline values. All other pesticides and herbicides tested for during ambient monitoring surveys were below the analytical limit of detection.
- An assessment of the plankton community (both phytoplankton and zooplankton) was completed during this reporting period. Phytoplankton abundance was high over the 2018/19 wet season, while diversity was lowest in February 2018. As the dataset grows, relationships between the plankton community and other physiochemical/nutrient parameters will be evaluated.

4.1.3 Sediment deposition and turbidity

- Continuous sediment deposition and turbidity logging data supports the pattern found more broadly in North Queensland coastal marine environments, that during dry periods with minimal rainfall, elevated turbidity along the coastline is driven by the re-suspension of sediment (Orpin and Ridd 2012), and this has been most notable here given the links drawn between RMS water depth and NTUe/SSC. Large peaks in NTUe/SSC and RMS water depth were recorded over periods longer than a week.
- The NTUe/SSC time series data at each site followed a typical pattern of low background values with recurring peak events. These peak events occurred at the same times at each site and coincided with peaks in RMS water height. This is a typical pattern which is similar to data collected in coastal locations in north Queensland
- RMS water height values were mostly driven by weather events and this is clearly evident in the data as peaks in RMS water heights were observed at the same times at all sites over the survey year. Variation in the magnitude of RMS water height values during peak events and during non-event periods differs among sites due to differences in water depth and site exposure to wave energy.

- Time series deposition data shows that deposition tends to peak following high RMS water height events but with a lag so that peak deposition occurs at a time when RMS water height has decreased to near background levels. An explanation for this lag is that as waves resuspend sediment, little deposition is expected because the energy in the system will keep the sediment in suspension. It is only when waves decrease and there is no longer enough energy in the system to keep the same quantity of sediment in suspension that deposition begins to occur.
- Current meter data indicates the prominent current direction and velocity at each site and shows that coastal current, tidal current or a combination of both influence current direction and magnitude.

4.1.4 Photosynthetically active radiation (PAR)

- Fine-scale patterns of PAR are primarily driven by tidal cycles with fortnightly increases in PAR coinciding with neap tides and lower tidal flows. Larger episodic events which lead to extended periods of low light conditions are driven by a combination of strong winds leading to increases in wave height and resuspension of particles (Orpin and Ridd 2012), and rainfall events resulting from storms leading to increased catchment flows and an input of suspended solids (Fabricius et al., 2013).
- Benthic PAR was highly variable within sites throughout the year, with peaks and troughs occurring both regularly and intermittently over time. Semi-regular oscillations between low and high PAR levels were overridden by larger episodic events caused by storm or rainfall events. It is important to note that a full year of PAR data has not yet been collected. As the data set increases, this will enable a greater insight into any trends that occur, whether these be tidally influenced or dependent on seasonality and cloud cover. Benthic PAR is also important to assess and validate NTUe sensor data.
- While turbidity is the main indicator of water quality used in monitoring of dredge activity and benthic light is significantly correlated with suspended solid concentrations (Erftemeijer and Lewis 2006; Erftemeijer et al., 2012), the relationship between these two parameters is not always strong (Sofonia and Unsworth 2010). At many of the sites where both turbidity and benthic light were measured, the concentration of suspended solids in the water column explained less than half of the variation in PAR. As PAR is more biologically relevant to the health of photosynthetic benthic habitats such as seagrass, algae and corals it is becoming more useful as a management response tool when used in conjunction with known thresholds for healthy growth for these habitats (e.g., Chartrand et al., 2012). For this reason, it is important to include photosynthetically active radiation (PAR) in the suite of water quality variables when capturing local baseline conditions of ambient water quality.

4.2 Recommendations

4.2.1 Consolidation of the water quality loggers

- It is recommended that the ambient monitoring program remain into the 2019/20 period. It will be important to ensure that the site network is ready to capture a range of wet season conditions, in order to characterise the variability in conditions for the region.

4.2.2 Data base repository

- An electronic version of the ambient marine water quality database has been prepared as an annexure to this report. It currently comprises MS-Excel Workbooks containing raw data files including results for water chemistry (in-situ field measurements, nutrients, filterable metals, pesticides/herbicides) collected as during the quarterly sampling, and all the continuous high frequency logger data files for sediment deposition, PAR, turbidity, water temperature, and RMS recorded during the period July 2018 and July 2019. This data base continues to be maintained by TropWATER personal, with back up copy archived on the James Cook University network with restricted access.

5 REFERENCES

ANZECC and ARMCANZ (2000) Australian Water Quality Guidelines for Fresh and Marine Waters. Australia and New Zealand Environment Conservation Council and Agriculture and Resource Management Council of Australia and New Zealand, Canberra.

ANZECC and ARMCANZ (2000b) Australian Guidelines for Water Quality Monitoring and Reporting. Australia and New Zealand Environment Conservation Council and Agriculture and Resource Management Council of Australia and New Zealand, Canberra. ISBN 09578245 1 3. ISSN 1038 7072.

APHA (1998) Standard Methods for the Examination of Water and Wastewater. 20th Edition. American Public Health Association, American Water Works Association and Water Environment Foundation. Washington, U.S.A.

Brodie, J. E., Kroon, F. J., Schaffelke, B., Wolanski, E. C., Lewis, S. E., Devlin, M. J., Bohnet, I. C, Bainbridge, Z. T., Waterhouse, J., Davis, A. M. (2012) Terrestrial pollutant runoff to the Great Barrier Reef: an update of issues, priorities and management responses. Marine Pollution Bulletin, 65, 81-100.

Bunt, J., Larcombe, P., Jago, C. F. (1999) Quantifiying the response of optical backscatter devices and transmissiometers to variations in suspended particulate matter (SPM). Continental Shelf Research 19: 1199-1220

Capone, D. G., Zehr, J. P., Paerl, H. W., Bergman, B., Carpenter, E. J. (1997). Trichodesmium, a globally significant marine cyanobacterium. Science, 276, 1221-1229.

Chartrand, K. M., Ralph, P. J., Petrou, K., Rasheed, M. A. (2012) Development of a light-based seagrass management approach for the Gladstone Western Basin dredging program. DEEDI Publication, Fisheries Queensland, Cairns.

Conner, C. S., De Visser, A. M. (1992) A laboratory investigation of particle size effects on an optical backscatterance sensor. Marine Geology 108:151-159

Cook, R. D., Weisberg, S. (1982) Residuals and Influence in Regression. Chapman and Hall.

Crawley, M.J. (2007) The R Book. John Wiley and Sons, Ltd.

DEHP (2010) Monitoring and Sampling Manual 2009. Environmental Protection (Water) Policy 2009. Version 1 September 2009. Queensland, Department of Environment and Resource Management.

Devlin, M. J., McKinna, L. W., Alvarez-Romero, J. G., Petus, C., Abott, B., Harkness, P., Brodie, J. (2012) Mapping the pollutants in surface riverine flood plume waters in the Great Barrier Reef, Australia. Marine Pollution Bulletin, 65, 224-235. doi: 10.1016/j.marpolbul.2012.03.001

Erftemeijer, P. L. A., B. Riegl, B. W. Hoeksema, Todd, P. A. (2012) Environmental impacts of dredging and other sediment disturbances on corals: A review. Marine Pollution Bulletin 64, 1737-1765.

Erftemeijer, P. L. A., Lewis, R. R. R. (2006) Environmental impacts of dredging on seagrasses: a review. Marine Pollution Bulletin 52, 1553-1572.

Fabricius, K. E., G. De'ath, C. Humphrey, I. Zagorskis, Schaffelke, B. (2013) Intra-annual variation in turbidity in response to terrestrial runoff on near-shore coral reefs of the Great Barrier Reef. Estuarine, Coastal and Shelf Science 116, 57-65.

Fox, J., Monette, G. (1992) Generalized collinearity diagnostics. JASA, 87, 178–183.

GBRMPA (2010) Water quality guidelines for the Great Barrier Reef Marine Park 2010 current edition. Great Barrier Reef Marine Park Authority.

GBRMPA (2013) Great Barrier Reef Region Strategic Assessment Report. Australian Government, Great Barrier Reef Marine Park Authority. pp. 636.

Grömping, G. (2006) Relative Importance for Linear Regression in R: The Package relaimpo. Journal of Statistical Software, 17, 1-27.

Johansen, J. L., Pratchett, M. S., Messmer, V., Coker, D. J., Tobin, A. J., Hoey, A. S. (2015) Large predatory coral trout species unlikely to meet increasing energetic demands in a warming ocean. Scientific Reports, 5.

Kirk, J. T. O. (1985) Effects of suspendiods (turbidity) on penetration of solar rediation in aquatic ecosystems. Hydrobiologia, 125, 195-208.

Kroon, F. J., Kuhnert, P. M., Henderson, B. L., Wilkinson, S. N., Kinsey-Henderson, A., Abbott, B., Brodie. J. E., Turner, R. D. (2012) River loads of suspended solids, nitrogen, phosphorus and herbicides delivered to the Great Barrier Reef lagoon. Marine Pollution Bulletin, 65, 167-181.

Lahet, F., Stramski, D. (2010). MODIS imagery of turbid plumes in San Diego coastal waters during rainstorm events. Remote Sensing of Environment, 114, 332-344.

Larcombe P, Ridd PV, Prytz A, Wilson, B. (1995) Factors controlling suspended sediment ion inner-shelf coral reefs, Townsville, Australia. Coral Reefs 14:163-171

Logan, M., Fabricius, K., Weeks, S., Rodriguez, A., Lewis, S., Brodie, J. (2014) Tracking GBR water clarity over time and demonstrating the effects of river discharge events. Progress Report: Southern and Northern NRM Regions. Report to the National Environmental Research Program. Reef and Rainforest Research Centre Limited, Cairns (53pp.).

Ludwig, K. A., Hanes, D. M. (1990) A laboratory explanation of optical backscatterance suspended solids sensors exposed to sand-mud mixtures. Mar Geol 94:173-179

Orpin, A. R., Ridd, P. V. (2012) Exposure of inshore corals to suspended sediments due to wave-resuspension and river plumes in the central Great Barrier Reef: A reappraisal. Continental Shelf Research 47, 55-67.

R Core Team (2015) R: A language and environment for statistical computing. R Foundation for Statistical Computing, Vienna, Austria. URL http://www.R-project.org/.

Ridd, P.V., Day, G., Thomas, S., Harradence, J., Renagi, O., Fox, D., Bunt, J., Renagi, O., Jago, C. (2001) Measurement of sediment deposition rates using an Optical Backscatter Sensor. Estuarine Coastal and Shelf Science, 52, 155-163.

Schaffelke, B., Carleton, J., Skuza, M., Zagorskis, I., Furnas, M. J. (2012) Water quality in the inshore Great Barrier Reef lagoon: Implications for long-term monitoring and management. Marine Pollution Bulletin, 65(4), 249-260.

Sofonia, J. J., Unsworth, R. K. F. (2010) Development of water quality thresholds during dredging for the protection of benthic primary producer habitats. Journal of Environmental Monitoring 12:159-163.

Standards Australia (1998) Water Quality – Sampling. Part 1: Guidance on the design of sampling programs, sampling techniques and the preservation and handling of samples. AS/NZS 5667.1:1998. Standards Australia, Homebush.

Thomas, S., Ridd, P. V., Renagi, O. (2003) Laboratory investigation on the effect of particle size, water flow and bottom surface roughness upon the response of an upward- pointing optical backscatter sensor to sediment accumulation. Continental Shelf Research. 23, 1545-1557.

TropWATER (2015) Assessment of the contamination risk posed by sampling consumables to the detection and monitoring of filterable metals in water samples. Internal report. Centre for Tropical Water and Aquatic Ecosystem Research, James Cook University.

Wolanski, E., Delesalle, B., Gibbs, R. (1994) Carbonate mud in Mataiva Atoll, French Polynesia: Suspension and export. Marine Pollution Bulletin 29:36-41.

A1 APPENDIX

A1.1 Calibration procedures

Turbidity/Deposition Calibration

The turbidity and deposition sensors on each instrument are calibrated to a set of plastic optical standards that give consistent NTU return values. This enables the calculation of raw data values into NTU values. The NTU values can then be converted into SSC and ASSD values through the SSC calibration process. Deposition sensors are calibrated to give measurements in units of mg/cm2 using the methodology outlined in Ridd et al (2000) and Thomas et al (2003). Instruments are calibrated every six months or after every deployment. Sediment samples are taken at each deployment site and used to determine sediment calibration coefficients used to account for variations in grain size and shape that can alter the implied SSC value.

SSC Calibration

An instrument is placed in a large container (50 l) with black sides and the output is read on a computer attached to the logger. Saltwater is used to fill the container. Sediment from the study site is added to a small container of salt water and agitated. The water-sediment slurry is then added to the large container which is stirred with a small submerged pump. A water sample is taken and analysed for total suspended sediment (TSS) using standard laboratory techniques in the ACTFR laboratory at JCU which is accredited for these measurements. Approximately 6 different concentrations of sediment are used for each site. TSS is then plotted against the NTU reading from the logger for each of the different sediment concentrations. A linear correlation between NTU and SSC is then calculated. The correlations typically have an r2 value equal to or greater than 0.9.

Light Calibration

The light sensors on each logger are calibrated every six months or after every deployment. The light sensor is calibrated against a LICOR U250A submersible sensor that was calibrated in the factory within the last 12 months. The results of the logger light sensor and LICOR U250A are compared and a calibration coefficient is used to ensure accurate reporting of PAR data. An in field comparison between the logger light sensor and LICOR U250A is made on deployment of the instruments to ensure accurate reporting of the data. In field calibration of the nephelometer light sensor against the LICOR U250A at varying depth has been carried out to account for changes in sensitivity changes at depth.

Pressure Sensor Calibration

All pressure sensors are calibrated against a pressure gauge and the pressure is converted into depth in metres.

A1.2 Time series data

A1.2.1 AMB 1: Euri Creek

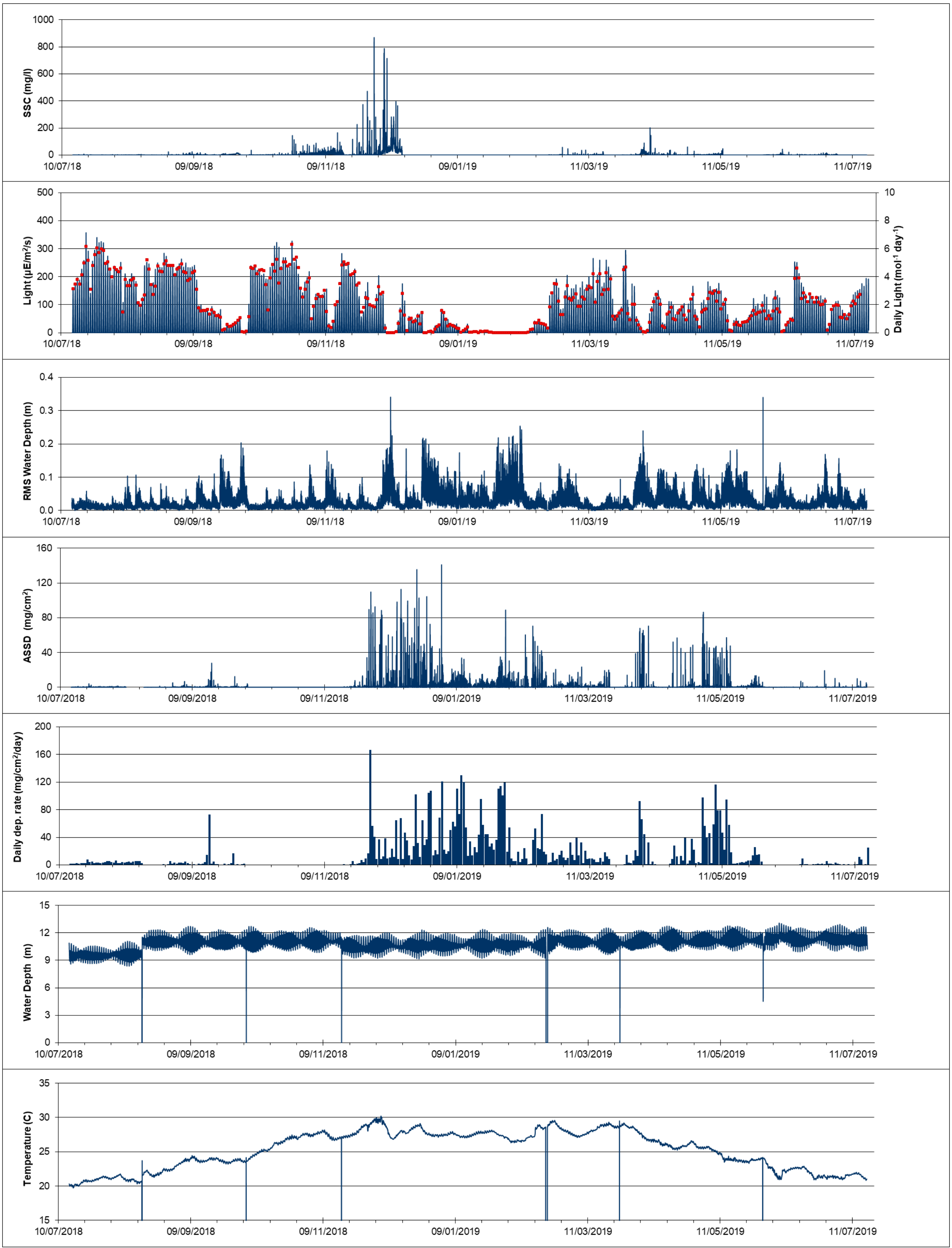

A1.2.2 AMB 2: Spoil Grounds

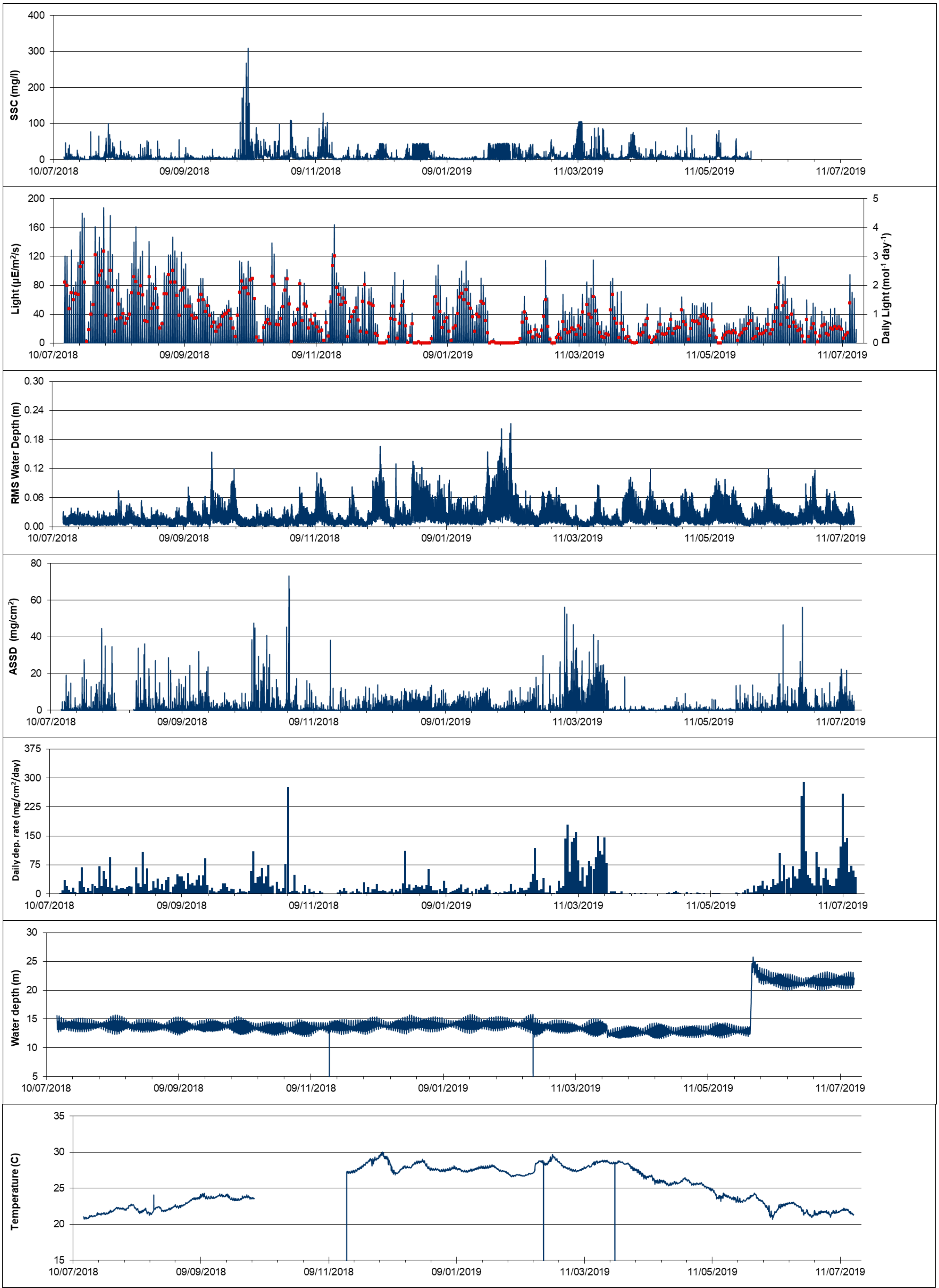

A1.2.3 AMB 3: Elliot River

A1.2.4 AMB 4: Camp Island

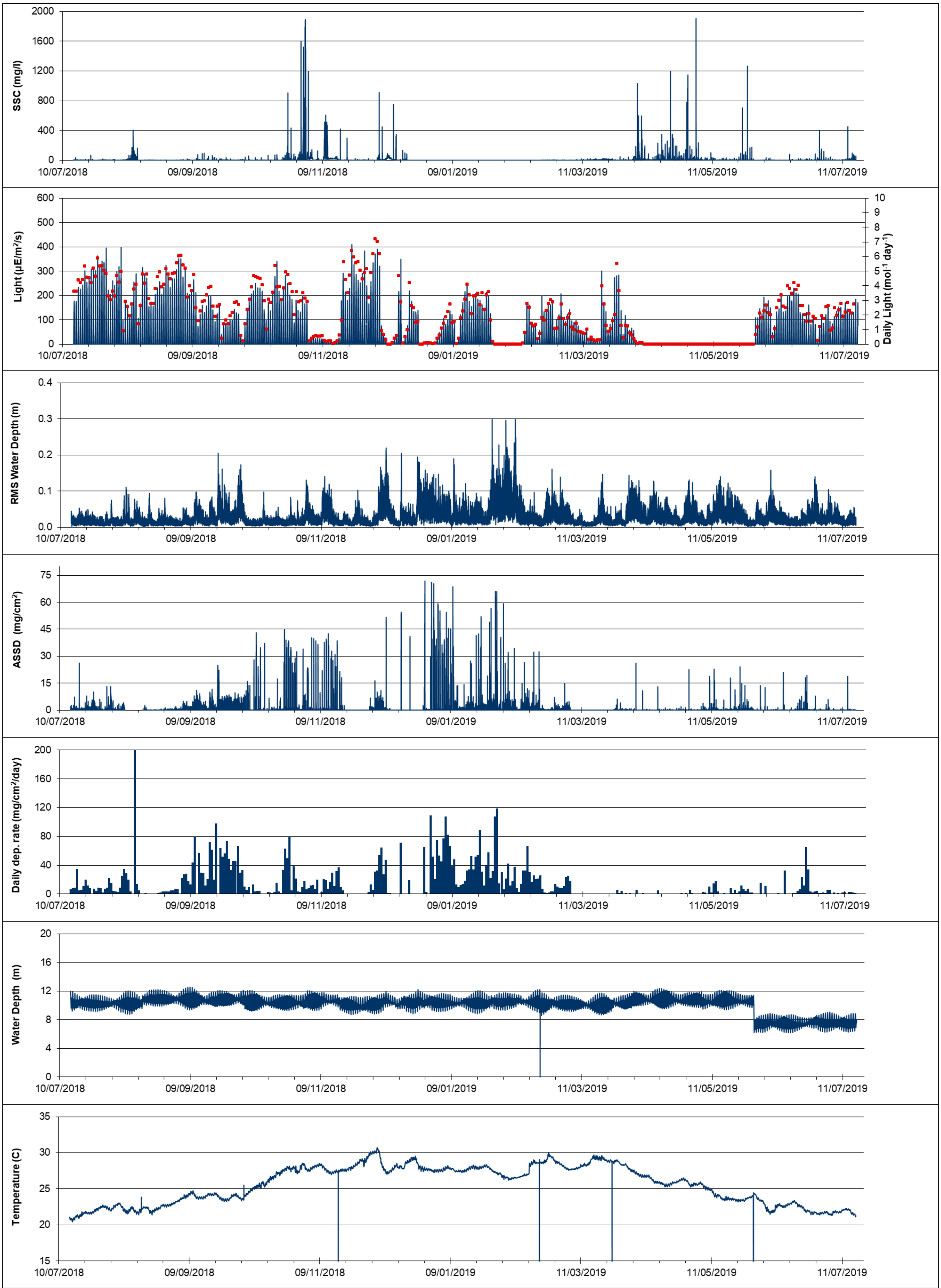

A1.2.5 AMB 5: Holbourne

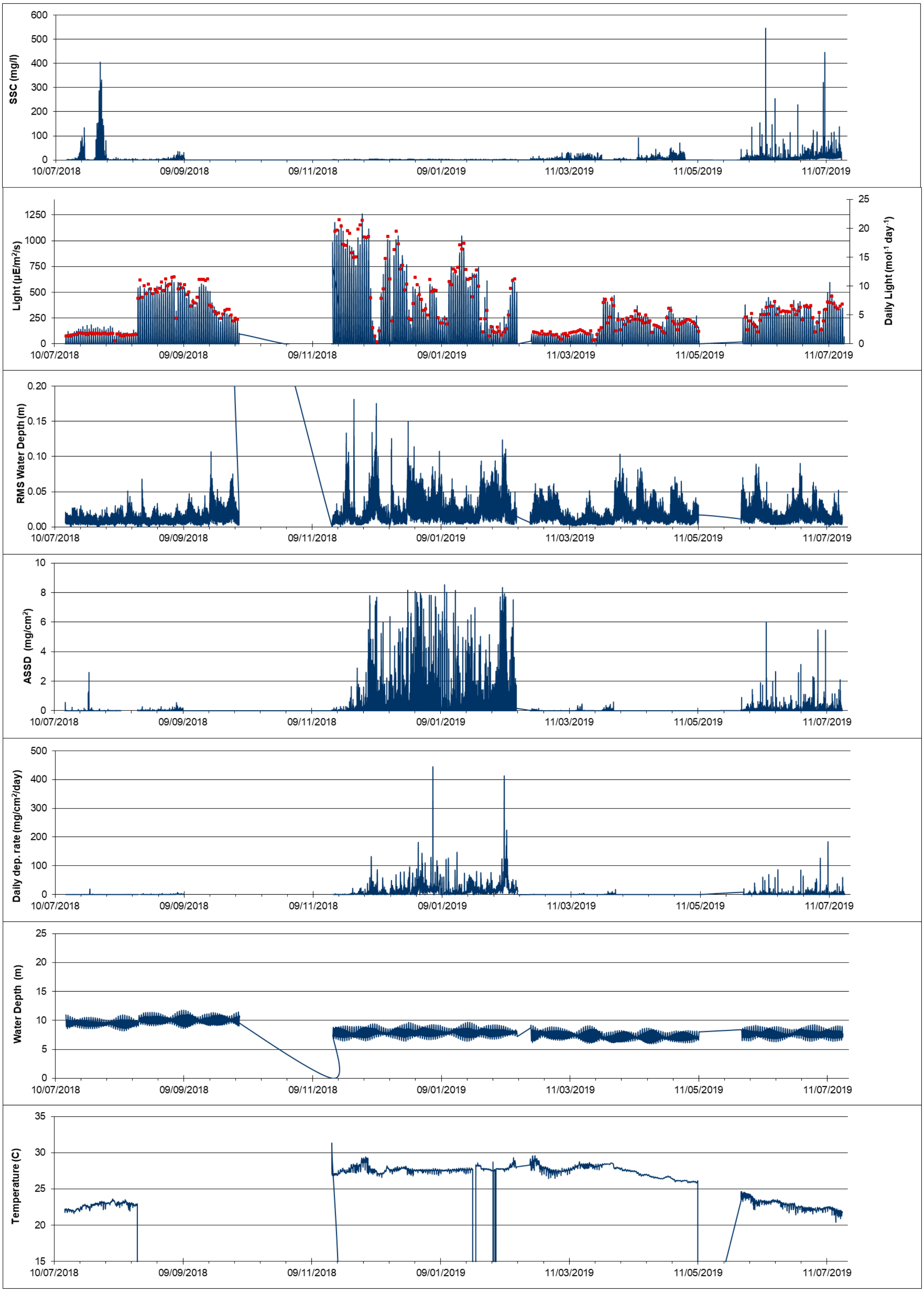

A1.3 Summary of monthly statistics

A1.3.1 AMB 1: Euri Creek

SCC (mg L^{-1})	07/2018	08/2018	09/2018	10/2018	11/2018	12/2018	01/2019	02/2019	03/2019	04/2019	05/2019	06/2019	07/2019
Mean	0.32	0.44	2.18	1.70	7.63	47.07		1.01	1.08	3.63	2.63	1.45	1.29
median	0.24	0.32	0.65	0.76	3.50	31.85		0.74	0.57	1.42	1.59	0.83	0.60
min	0.00	0.00	0.00	0.00	0.03	0.25		0.00	0.00	0.08	0.27	0.00	0.00
lower	0.11	0.17	0.28	0.55	1.00	9.61		0.44	0.25	0.92	0.99	0.57	0.41
upper	0.42	0.54	3.25	1.39	9.39	54.90		1.26	1.11	2.72	2.72	1.37	1.81
max	7.53	23.97	24.58	144.27	471.37	868.91		57.38	46.88	201.63	47.10	42.92	10.04
90th percentile	0.65	0.94	5.79	3.13	17.58	105.96		2.02	2.10	8.86	4.85	3.16	3.12
10th percentile	0.06	0.09	0.10	0.39	0.56	2.13		0.24	0.09	0.63	0.70	0.34	0.33
n	2133	4442	4243	3930	4214	1940		1229	3354	4320	1584	4320	432
St. Dev	0.37	0.64	3.10	5.17	16.11	67.21		1.79	2.27	7.84	4.04	2.12	1.38
St. Error	0.01	0.01	0.05	0.08	0.25	1.53		0.05	0.04	0.12	0.10	0.03	0.07

Daily dep. (mg cm^{-2} day^{-1})	07/2018	08/2018	09/2018	10/2018	11/2018	12/2018	01/2019	02/2019	03/2019	04/2019	05/2019	06/2019	07/2019
Mean	4.02	2.53	5.37		19.08	39.07	53.92	17.94	15.24	22.93	14.81	1.47	6.05
median	3.67	2.69	1.28		6.40	27.63	44.68	13.98	8.41	6.12	4.01	1.14	1.10
min	2.22	0.06	0.25		0.25	7.93	5.63	0.82	0.48	0.23	0.07	0.01	0.55
lower	2.94	0.27	0.77		1.20	13.48	20.47	7.15	3.49	1.43	0.54	0.49	0.78
upper	4.71	4.30	2.24		13.16	57.66	84.67	23.21	17.35	38.90	15.61	1.53	8.64
max	7.65	5.68	72.67		166.70	120.57	129.90	73.82	92.73	116.31	94.56	9.36	25.14

90th percentile	5.84	5.23	9.93		42.25	102.21	114.37	37.24	33.69	60.79	48.93	2.27	15.45
10th percentile	2.57	0.11	0.53		0.65	8.99	13.40	3.81	0.92	0.38	0.15	0.11	0.56
n	17	30	26	0	20	31	31	28	30	30	29	30	8
St. Dev	1.49	2.00	14.31		38.03	33.04	39.40	16.55	20.72	31.42	24.42	1.89	8.71
St. Error	0.36	0.37	2.81		8.50	5.93	7.08	3.13	3.78	5.74	4.53	0.34	3.08

RMS depth	07/2018	08/2018	09/2018	10/2018	11/2018	12/2018	01/2019	02/2019	03/2019	04/2019	05/2019	06/2019	07/2019
Mean	0.01	0.02	0.02	0.02	0.02	0.04	0.04	0.04	0.02	0.04	0.04	0.03	0.03
median	0.01	0.01	0.02	0.01	0.02	0.03	0.03	0.03	0.01	0.03	0.03	0.02	0.02
min	0.00	0.00	0.00	0.00	0.00	0.00	0.00	0.00	0.00	0.00	0.00	0.00	0.00
lower	0.01	0.01	0.01	0.01	0.01	0.01	0.02	0.02	0.01	0.02	0.02	0.01	0.01
upper	0.01	0.02	0.03	0.02	0.03	0.06	0.05	0.05	0.02	0.05	0.05	0.03	0.03
max	0.06	0.11	0.16	0.20	0.18	0.34	0.22	0.25	0.12	0.24	0.18	0.17	0.16
90th percentile	0.02	0.03	0.05	0.03	0.05	0.10	0.07	0.09	0.04	0.07	0.07	0.05	0.05
10th percentile	0.01	0.01	0.01	0.01	0.01	0.01	0.02	0.01	0.01	0.01	0.01	0.01	0.01
n	2448	4444	4320	4463	4243	4464	4462	3924	4463	4320	4033	4320	2016
St. Dev	0.01	0.01	0.02	0.02	0.02	0.04	0.02	0.04	0.01	0.03	0.02	0.02	0.02
St. Error	0.00	0.00	0.00	0.00	0.00	0.00	0.00	0.00	0.00	0.00	0.00	0.00	0.00

Temp. (°C)	07/2018	08/2018	09/2018	10/2018	11/2018	12/2018	01/2019	02/2019	03/2019	04/2019	05/2019	06/2019	07/2019
Mean	20.67	21.48	23.66	25.66	27.61	28.21	27.55	27.74	28.26	26.41	24.37	22.03	21.49
median	20.73	21.47	23.69	25.65	27.52	28.01	27.52	27.37	28.50	26.20	23.92	22.17	21.56
min	19.73	20.32	22.50	23.43	26.65	26.82	26.98	26.32	27.09	25.23	23.31	20.91	20.92
lower	20.24	21.00	23.51	24.58	27.20	27.51	27.34	26.67	27.67	25.83	23.75	21.39	21.26
upper	21.00	21.99	23.89	26.90	27.87	28.84	27.77	28.62	28.79	26.75	25.20	22.61	21.73
max	21.48	23.62	24.45	27.71	29.04	30.21	28.16	29.57	29.48	28.61	25.80	23.68	22.00
90th percentile	21.28	22.35	24.06	27.20	28.63	29.46	27.94	29.12	28.96	27.67	25.60	22.75	21.84
10th percentile	20.07	20.70	23.25	23.74	26.93	27.24	27.19	26.52	27.37	25.55	23.60	21.16	21.12

n	2448	4444	4320	4463	4237	4464	4462	3918	4463	4320	4033	4320	2016
St. Dev	0.44	0.58	0.34	1.28	0.58	0.84	0.28	1.02	0.61	0.78	0.79	0.65	0.27
St. Error	0.01	0.01	0.01	0.02	0.01	0.01	0.00	0.02	0.01	0.01	0.01	0.01	0.01

Light (mol quanta m^{-2} day^{-1})	07/2018	08/2018	09/2018	10/2018	11/2018	12/2018	01/2019	02/2019	03/2019	04/2019	05/2019	06/2019	07/2019
Mean	5.01	3.87	1.59	3.95	2.72	0.66	0.09	1.48	2.26	1.62	1.34	1.87	1.98
median	4.95	4.15	1.23	4.41	2.56	0.55	0.04	1.28	2.20	1.59	1.22	1.98	2.07
min	3.11	1.49	0.06	0.99	0.32	0.00	0.00	0.00	0.04	0.39	0.12	0.09	0.99
lower	4.55	3.36	0.59	3.14	1.86	0.06	0.00	0.50	1.08	1.05	0.78	0.99	1.60
upper	5.71	4.70	1.65	4.82	3.53	1.00	0.10	2.46	3.27	2.18	1.72	2.50	2.41
max	6.17	5.19	4.65	6.30	5.06	2.81	0.46	3.53	4.70	2.89	2.99	4.62	2.75
90^{th} percentile	6.02	4.90	4.31	5.23	4.85	1.45	0.29	3.01	4.22	2.73	2.40	2.96	2.63
10^{th} percentile	4.21	2.38	0.18	2.44	0.79	0.00	0.00	0.04	0.28	0.72	0.54	0.54	1.16
n	17	31	30	31	30	31	31	28	31	30	29	30	7
St. Dev	0.83	1.00	1.42	1.24	1.38	0.66	0.13	1.17	1.44	0.73	0.76	1.12	0.64
St. Error	0.20	0.18	0.26	0.22	0.25	0.12	0.02	0.22	0.26	0.13	0.14	0.20	0.24

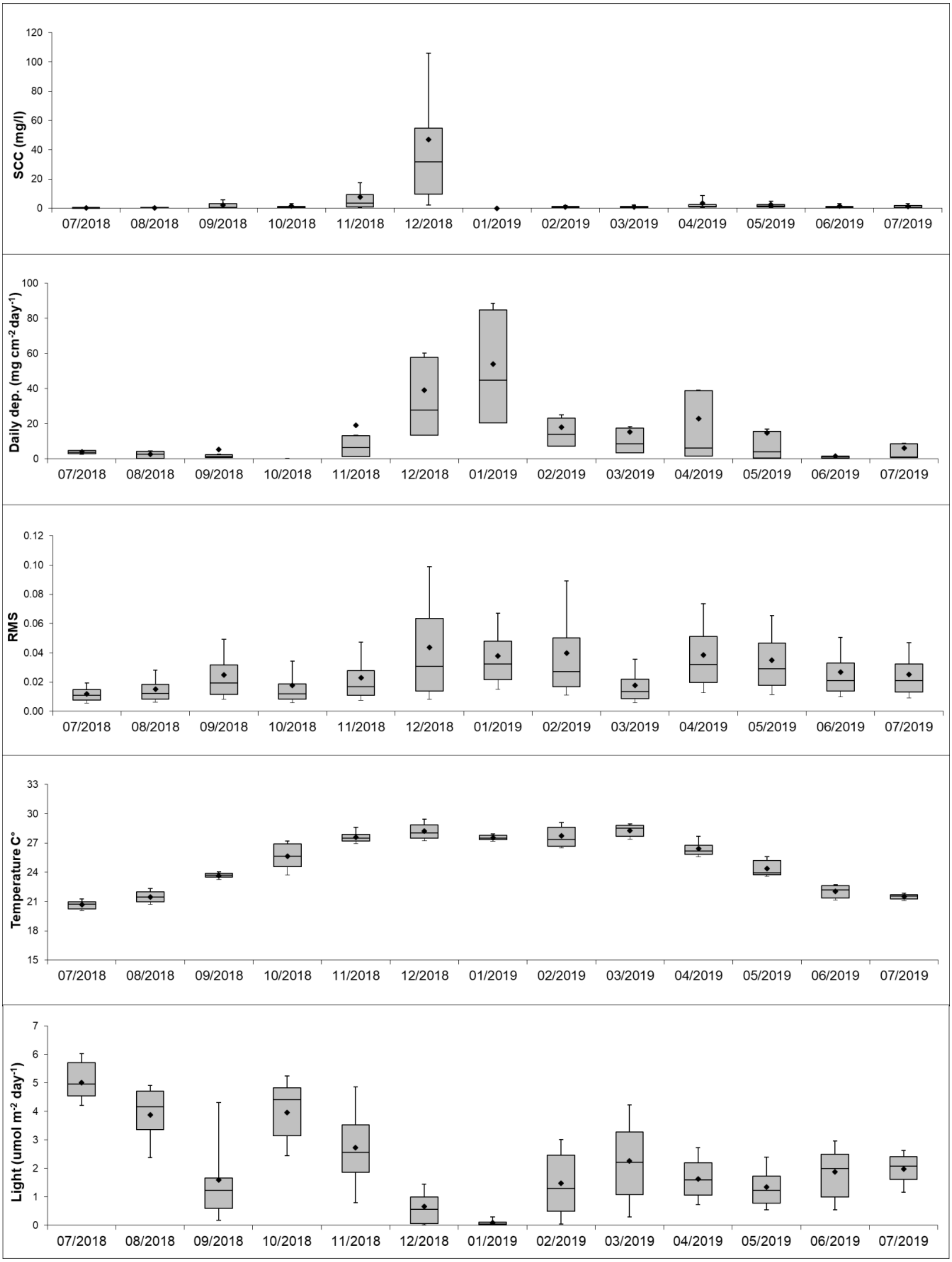

SCC (mg/l)
Daily dep. (mg cm⁻² day⁻¹)
RMS
Temperature C°
Light (umol m⁻² day⁻¹)
07/2018
08/2018
09/2018
10/2018
11/2018
12/2018
01/2019
02/2019
03/2019
04/2019
05/2019
06/2019
07/2019

A1.3.2 AMB 2: Spoil Grounds

SCC (mg L^{-1})	07/2018	08/2018	09/2018	10/2018	11/2018	12/2018	01/2019	02/2019	03/2019	04/2019	05/2019	06/2019	07/2019
Mean	3.49	4.79	2.13	11.05	7.34	9.78	3.43	11.05	8.00	6.03	4.28		
median	2.23	2.47	1.54	4.35	2.96	4.24	1.33	6.25	3.28	3.35	2.16		
min	0.00	0.00	0.02	0.00	0.08	0.00	0.00	0.00	0.00	0.00	0.00		
lower	1.09	1.28	0.99	1.88	1.51	1.46	0.78	3.14	1.56	1.82	1.23		
upper	4.07	5.32	2.47	11.81	6.95	14.19	2.93	15.22	6.55	6.22	3.68		
max	77.18	100.14	55.45	307.84	127.30	44.69	44.80	55.46	106.52	87.76	81.39		
90th percentile	7.22	9.88	3.82	24.43	15.62	29.77	7.86	30.21	15.47	13.14	7.33		
10th percentile	0.52	0.79	0.59	1.02	0.85	0.80	0.46	1.94	0.74	1.08	0.56		
n	2133	4458	4320	4430	4227	3974	4398	3264	4338	4318	4243		
St. Dev	5.21	7.46	2.93	20.57	12.81	11.52	6.12	11.13	15.22	8.41	7.79		
St. Error	0.11	0.11	0.04	0.31	0.20	0.18	0.09	0.19	0.23	0.13	0.12		

Daily dep. rate (mg cm^{-2} day^{-1})	07/2018	08/2018	09/2018	10/2018	11/2018	12/2018	01/2019	02/2019	03/2019	04/2019	05/2019	06/2019	07/2019
Mean	25.72	28.13	25.45	36.45	7.98	18.57	9.66	36.18	48.59	2.01	7.04	61.91	106.75
median	17.93	19.33	21.97	20.42	6.25	13.07	8.43	15.89	18.21	1.37	2.65	39.98	72.96
min	1.81	5.03	2.12	0.95	0.73	3.00	0.57	1.60	0.44	0.37	0.31	16.56	43.94
lower	15.09	14.07	11.86	6.80	3.18	8.22	3.73	8.89	1.94	0.87	1.49	26.90	60.57
upper	32.37	31.82	36.32	45.72	11.54	21.11	14.33	36.48	85.91	2.65	10.43	68.80	132.95
max	71.54	108.11	92.31	276.29	30.04	111.50	25.83	178.70	160.03	8.41	34.04	290.20	259.31
90th percentile	62.46	66.30	48.68	74.00	14.95	27.50	18.92	123.75	145.13	3.92	21.52	108.44	167.80

10th percentile	5.26	8.54	6.73	4.57	1.50	6.87	2.21	3.99	1.12	0.50	0.70	21.19	54.13
n	17	30	30	30	29	31	31	28	31	30	30	30	9
St. Dev	21.56	25.11	20.01	52.91	7.13	20.84	7.22	47.90	54.19	1.72	8.72	63.08	68.02
St. Error	5.23	4.59	3.65	9.66	1.32	3.74	1.30	9.05	9.73	0.31	1.59	11.52	22.67

RMS depth	07/2018	08/2018	09/2018	10/2018	11/2018	12/2018	01/2019	02/2019	03/2019	04/2019	05/2019	06/2019	07/2019
Mean	0.012	0.013	0.018	0.014	0.017	0.028	0.027	0.032	0.014	0.024	0.023	0.022	0.021
median	0.011	0.011	0.015	0.010	0.013	0.022	0.023	0.024	0.011	0.021	0.019	0.018	0.019
min	0.000	0.000	0.000	0.000	0.000	0.000	0.003	0.000	0.000	0.000	0.000	0.004	0.004
lower	0.008	0.008	0.010	0.007	0.009	0.011	0.015	0.015	0.007	0.013	0.012	0.013	0.013
upper	0.014	0.015	0.023	0.015	0.021	0.040	0.034	0.041	0.018	0.031	0.030	0.026	0.026
max	0.038	0.074	0.153	0.119	0.111	0.166	0.154	0.212	0.086	0.118	0.098	0.119	0.076
90^{th} percentile	0.018	0.021	0.033	0.025	0.033	0.058	0.048	0.064	0.027	0.043	0.042	0.038	0.035
10^{th} percentile	0.006	0.006	0.007	0.005	0.007	0.007	0.011	0.010	0.005	0.009	0.008	0.009	0.010
n	2448	4462	4320	4463	4243	4464	4462	4028	4462	4320	4244	4320	2016
St. Dev	0.005	0.007	0.012	0.012	0.012	0.022	0.017	0.025	0.010	0.014	0.014	0.014	0.011
St. Error	0.000	0.000	0.000	0.000	0.000	0.000	0.000	0.000	0.000	0.000	0.000	0.000	0.000

Temp. (°C)	07/2018	08/2018	09/2018	10/2018	11/2018	12/2018	01/2019	02/2019	03/2019	04/2019	05/2019	06/2019	07/2019
Mean	21.45	22.14	23.62	23.68	27.91	28.22	27.64	27.76	28.20	26.39	24.27	22.24	21.73
median	21.42	22.17	23.64	23.66	27.80	28.02	27.62	27.32	28.38	26.12	23.94	22.38	21.70
min	20.71	21.24	22.68	23.49	27.07	26.85	27.20	26.58	27.27	25.33	23.03	20.69	20.97
lower	21.12	21.91	23.44	23.59	27.31	27.62	27.43	26.85	27.77	25.81	23.61	21.54	21.61
upper	21.72	22.39	23.83	23.76	28.50	28.73	27.82	28.65	28.60	26.73	25.13	22.85	21.91
max	22.34	24.03	24.30	23.95	29.13	30.02	28.27	29.69	28.90	28.39	25.79	23.99	22.23
90^{th} percentile	22.15	22.59	23.98	23.86	28.82	29.28	27.95	28.93	28.73	27.66	25.59	23.16	22.01
10^{th} percentile	20.89	21.66	23.29	23.54	27.19	27.36	27.35	26.73	27.49	25.64	23.27	21.22	21.51

n	2448	4462	4320	500	1856	4464	4462	4022	4456	4320	4244	4320	2016
St. Dev	0.42	0.34	0.31	0.12	0.62	0.73	0.23	0.93	0.47	0.76	0.86	0.73	0.22
St. Error	0.01	0.01	0.00	0.01	0.01	0.01	0.00	0.01	0.01	0.01	0.01	0.01	0.00

Light (mol quanta m^{-2} day^{-1})	07/2018	08/2018	09/2018	10/2018	11/2018	12/2018	01/2019	02/2019	03/2019	04/2019	05/2019	06/2019	07/2019
Mean	1.92	1.43	1.12	1.14	1.09	0.46	0.67	0.39	0.58	0.51	0.41	0.63	0.54
median	2.09	1.35	1.02	0.86	1.03	0.23	0.60	0.32	0.47	0.51	0.36	0.55	0.50
min	0.07	0.42	0.22	0.07	0.10	0.00	0.00	0.00	0.01	0.02	0.00	0.04	0.16
lower	1.34	0.86	0.85	0.64	0.47	0.01	0.02	0.15	0.23	0.32	0.27	0.35	0.34
upper	2.51	1.94	1.44	1.77	1.42	0.84	1.12	0.50	0.88	0.72	0.50	0.74	0.57
max	3.19	2.52	2.14	2.31	3.02	1.61	1.86	1.50	1.69	1.15	0.99	2.09	1.39
90^{th} percentile	2.90	2.29	1.84	2.19	1.94	1.31	1.51	0.88	1.15	0.82	0.81	1.23	0.82
10^{th} percentile	0.77	0.69	0.56	0.22	0.32	0.00	0.00	0.01	0.08	0.20	0.15	0.24	0.25
n	17	31	30	31	30	31	31	28	31	30	30	30	8
St. Dev	0.90	0.62	0.49	0.71	0.71	0.53	0.61	0.37	0.46	0.27	0.26	0.43	0.37
St. Error	0.22	0.11	0.09	0.13	0.13	0.09	0.11	0.07	0.08	0.05	0.05	0.08	0.13

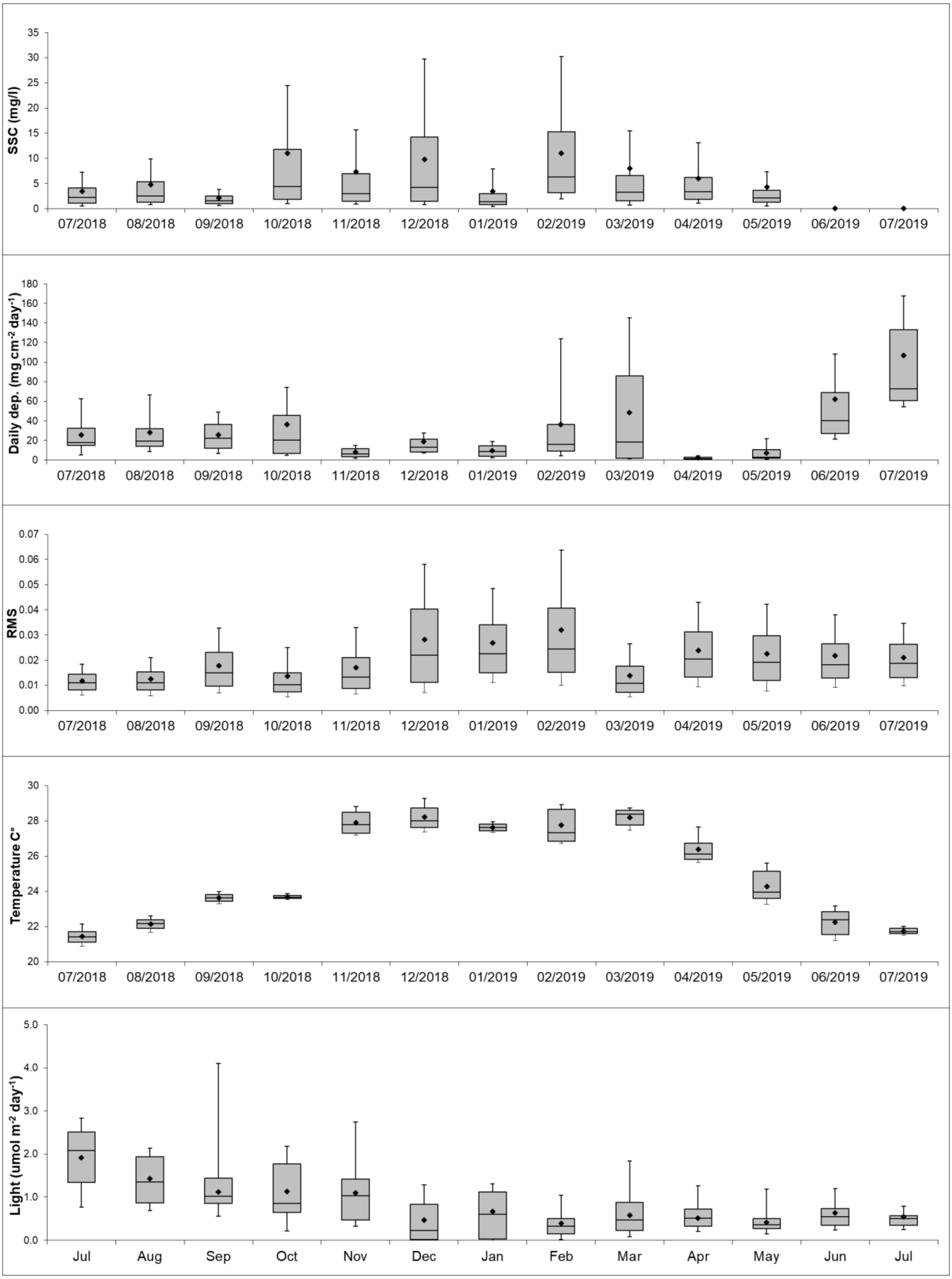

SSC (mg/l)
Daily dep. (mg cm-2 day-1)
RMS
Temperature C°
Light (umol m-2 day-1)
07/2018
08/2018
09/2018
10/2018
11/2018
12/2018
01/2019
02/2019
03/2019
04/2019
05/2019
06/2019
07/2019
Jul
Aug
Sep
Oct
Nov
Dec
Jan
Feb
Mar
Apr
May
Jun
Jul

A1.3.3 AMB 3: Elliot River

SCC (mg L^{-1})	07/2018	08/2018	09/2018	10/2018	11/2018	12/2018	01/2019	02/2019	03/2019	04/2019	05/2019	06/2019	07/2019
Mean	0.62	2.92	1.68	2.08	1.66	7.80	5.44	0.67	0.57	4.72			
median	0.33	0.54	0.79	0.29	0.64	2.67	5.00	0.51	0.36	3.53			
min	0.00	0.00	0.05	0.00	0.02	0.00	2.22	0.00	0.00	0.71			
lower	0.19	0.30	0.42	0.17	0.36	0.86	3.84	0.20	0.19	2.30			
upper	0.54	1.71	1.75	0.51	1.28	10.11	6.59	0.98	0.58	5.70			
max	101.54	125.27	34.31	129.17	129.17	251.19	17.26	4.79	39.07	51.15			
90th percentile	0.79	6.49	4.05	3.09	2.99	17.12	7.98	1.59	1.02	9.36			
10th percentile	0.11	0.20	0.27	0.11	0.24	0.26	3.20	0.05	0.06	1.52			
n	2133	4429	2994	3944	4227	4449	720	1348	4444	1724			
St. Dev	3.33	7.85	2.45	7.60	4.99	14.32	2.13	0.61	1.16	4.12			
St. Error	0.07	0.12	0.04	0.12	0.08	0.21	0.08	0.02	0.02	0.10			

Daily dep. rate (mg cm^{-2} day^{-1})	07/2018	08/2018	09/2018	10/2018	11/2018	12/2018	01/2019	02/2019	03/2019	04/2019	05/2019	06/2019	07/2019
Mean	8.33	5.46	23.24	6.39	4.09	16.64	70.76		1.06	9.01	9.34		
median	6.14	4.76	8.93	5.90	3.14	9.68	17.32		0.57	7.68	10.54		
min	2.96	0.08	0.04	1.31	0.10	0.55	2.44		0.16	2.12	1.64		
lower	4.58	1.01	0.26	3.23	1.55	5.38	8.22		0.31	4.54	4.28		
upper	11.17	8.15	24.53	9.72	5.06	19.95	85.49		1.21	10.98	11.59		
max	19.77	14.69	121.94	11.79	22.37	101.39	454.79		5.48	25.82	18.64		

90th percentile	14.98	13.88	72.63	11.06	8.39	31.48	191.09		2.03	17.66	15.82		
10th percentile	3.63	0.19	0.14	2.08	0.34	1.43	5.06		0.28	2.56	2.70		
n	17	30	30	31	30	31	24	0	23	30	5	0	0
St. Dev	4.93	4.86	33.83	3.50	4.42	19.43	105.66		1.25	6.08	6.67		
St. Error	1.19	0.89	6.18	0.63	0.81	3.49	21.57		0.26	1.11	2.98		

RMS depth	07/2018	08/2018	09/2018	10/2018	11/2018	12/2018	01/2019	02/2019	03/2019	04/2019	05/2019	06/2019	07/2019
Mean	0.019	0.019	0.028	0.022	0.028	0.039	0.043	0.045	0.023	0.035	0.033		
median	0.017	0.016	0.024	0.017	0.023	0.033	0.038	0.036	0.020	0.032	0.030		
min	0.001	0.000	0.003	0.002	0.003	0.003	0.005	0.003	0.002	0.004	0.003		
lower	0.012	0.011	0.015	0.012	0.016	0.020	0.026	0.022	0.012	0.022	0.019		
upper	0.023	0.023	0.037	0.025	0.035	0.053	0.054	0.058	0.031	0.045	0.044		
max	0.097	0.109	0.122	0.163	0.134	0.191	0.240	0.226	0.148	0.169	0.149		
90th percentile	0.031	0.034	0.052	0.043	0.052	0.074	0.075	0.089	0.043	0.060	0.056		
10th percentile	0.008	0.008	0.010	0.009	0.012	0.012	0.018	0.014	0.008	0.015	0.013		
n	2448	4451	4320	4463	4244	4464	4462	4028	4463	4320	4245		
St. Dev	0.010	0.011	0.018	0.017	0.018	0.026	0.025	0.032	0.015	0.018	0.018		
St. Error	0.000	0.000	0.000	0.000	0.000	0.000	0.000	0.000	0.000	0.000	0.000		

Temp. (°C)	07/2018	08/2018	09/2018	10/2018	11/2018	12/2018	01/2019	02/2019	03/2019	04/2019	05/2019	06/2019	07/2019
Mean	21.64	22.13	24.01	26.28	28.04	28.73	27.76	28.02	28.60	25.70	23.53		
median	21.67	22.13	24.00	26.44	27.85	28.45	27.77	28.37	28.38	25.58	23.28		
min	20.33	20.97	22.61	23.29	26.57	26.78	26.90	25.88	27.42	24.21	22.40		
lower	21.04	21.74	23.73	25.48	27.47	27.80	27.48	26.57	27.90	25.12	22.77		
upper	22.14	22.51	24.32	27.42	28.34	29.47	28.05	29.16	29.32	26.18	24.19		
max	22.90	24.87	25.36	28.66	30.35	31.20	28.63	30.81	30.67	27.82	25.25		
90th percentile	22.55	22.76	24.53	27.95	29.57	30.53	28.25	29.96	29.72	26.79	24.89		
10th percentile	20.77	21.50	23.44	23.93	27.09	27.53	27.28	26.24	27.64	24.90	22.61		
n	2448	4451	4320	4463	4243	4464	4462	4018	4463	4320	4245		
St. Dev	0.65	0.48	0.43	1.42	0.86	1.11	0.37	1.41	0.82	0.73	0.86		
St. Error	0.01	0.01	0.01	0.02	0.01	0.02	0.01	0.02	0.01	0.01	0.01		

Light (mol quanta m^{-2} day^{-1})	07/2018	08/2018	09/2018	10/2018	11/2018	12/2018	01/2019	02/2019	03/2019	04/2019	05/2019	06/2019	07/2019
Mean	5.48	7.01	6.82	5.61	6.47	4.44	1.36	3.03	5.20	5.05	3.15		
median	5.49	5.80	6.41	5.87	4.67	4.85	1.06	0.27	5.25	5.09	2.97		
min	3.93	2.14	1.24	0.71	0.76	0.03	0.00	0.00	1.34	0.96	0.72		

lower	4.71	4.87	5.26	5.05	3.19	0.55	0.28	0.00	3.70	3.67	1.07
upper	6.60	9.50	9.24	6.84	10.67	7.75	2.26	6.31	6.14	6.58	5.15
max	6.86	10.50	10.25	8.14	13.90	12.58	3.70	11.23	13.34	8.83	6.72
90th percentile	6.83	9.98	9.91	7.19	12.08	10.32	2.93	8.39	7.45	7.66	6.17
10th percentile	4.10	4.33	3.62	2.49	1.53	0.16	0.00	0.00	2.94	1.87	0.86
n	17	31	30	31	30	31	31	21	31	30	29
St. Dev	1.06	2.53	2.54	1.73	4.17	4.22	1.22	3.79	2.37	2.25	2.18
St. Error	0.26	0.45	0.46	0.31	0.76	0.76	0.22	0.83	0.43	0.41	0.41

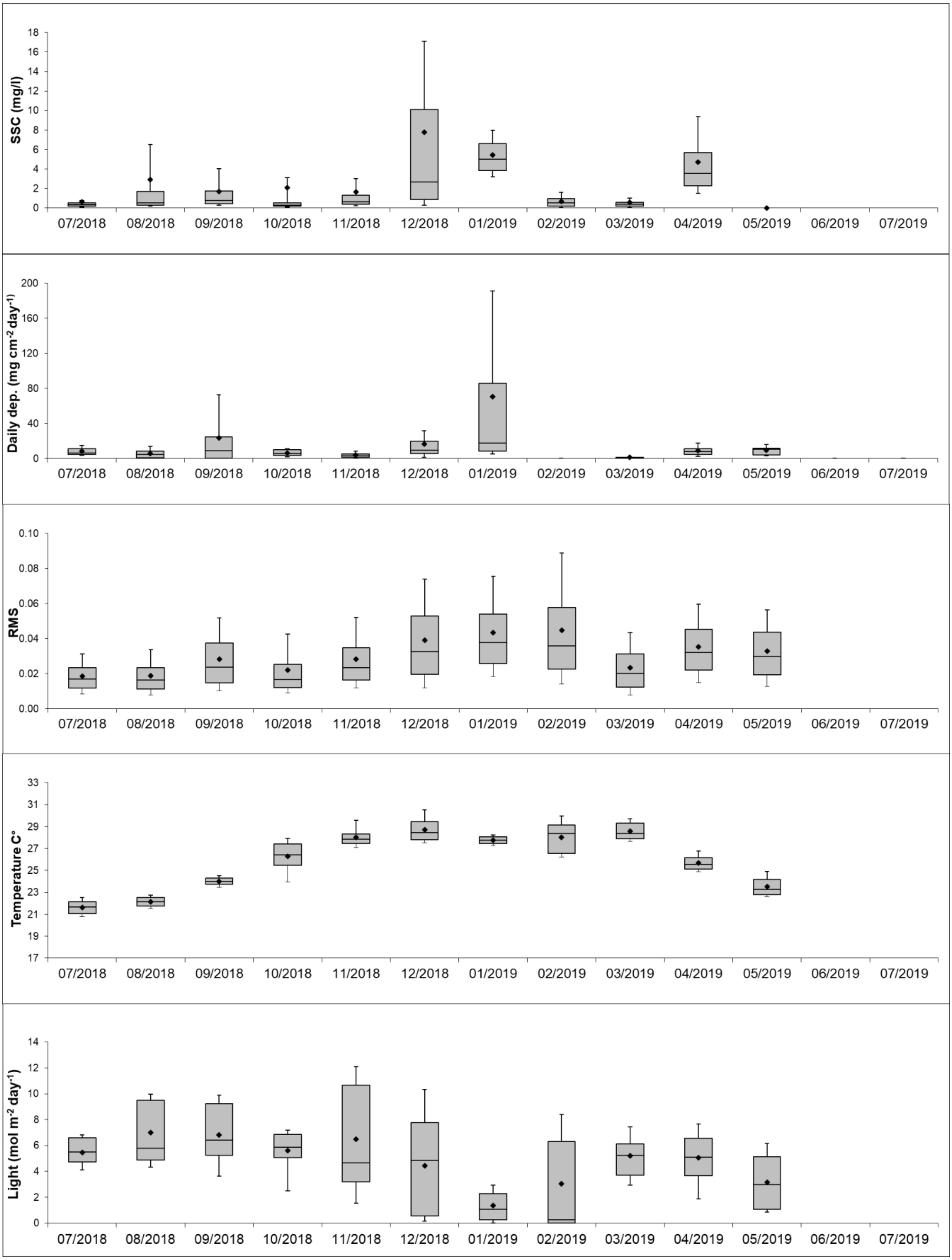
SSC (mg/l)
0 2 4 6 8 10 12 14 16 18
07/2018 08/2018 09/2018 10/2018 11/2018 12/2018 01/2019 02/2019 03/2019 04/2019 05/2019 06/2019 07/2019
Daily dep. (mg cm-2 day-1)
0 40 80 120 160 200
07/2018 08/2018 09/2018 10/2018 11/2018 12/2018 01/2019 02/2019 03/2019 04/2019 05/2019 06/2019 07/2019
RMS
0.00 0.02 0.04 0.06 0.08 0.10
07/2018 08/2018 09/2018 10/2018 11/2018 12/2018 01/2019 02/2019 03/2019 04/2019 05/2019 06/2019 07/2019
Temperature C°
17 19 21 23 25 27 29 31 33
07/2018 08/2018 09/2018 10/2018 11/2018 12/2018 01/2019 02/2019 03/2019 04/2019 05/2019 06/2019 07/2019
Light (mol m-2 day-1)
0 2 4 6 8 10 12 14
07/2018 08/2018 09/2018 10/2018 11/2018 12/2018 01/2019 02/2019 03/2019 04/2019 05/2019 06/2019 07/2019

A1.3.4 AMB 4: Camp Island

SCC (mg/L)	07/2018	08/2018	09/2018	10/2018	11/2018	12/2018	01/2019	02/2019	03/2019	04/2019	05/2019	06/2019	07/2019
Mean	1.64	3.52	1.91	14.87	19.34	11.83		1.37	2.88	16.90	6.93	1.63	3.07
median	0.98	0.79	1.10	0.55	1.31	3.28		1.23	0.97	7.43	1.31	0.66	0.94
min	0.00	0.00	0.03	0.00	0.00	0.00		0.00	0.00	0.61	0.15	0.21	0.44
lower	0.56	0.42	0.52	0.36	0.71	0.58		0.62	0.40	4.93	0.68	0.47	0.72
upper	1.83	1.82	2.11	1.15	18.11	12.20		1.86	3.43	11.49	4.51	1.24	1.68
max	67.13	402.36	93.37	1882.14	1773.72	901.45		7.41	46.73	1196.34	1904.59	393.88	451.27
90th percentile	3.16	4.20	3.73	4.92	31.81	28.49		2.47	8.95	20.90	10.90	2.90	3.95
10th percentile	0.31	0.17	0.28	0.23	0.46	0.18		0.26	0.20	2.98	0.43	0.38	0.62
n	2118	4374	4290	4329	4231	2539	0	1360	4380	4316	4239	4320	2016
St. Dev	2.90	14.91	3.85	119.16	83.82	34.78		1.01	4.13	63.69	48.52	8.12	17.02
St. Error	0.06	0.23	0.06	1.81	1.29	0.69		0.03	0.06	0.97	0.75	0.12	0.38

Daily dep. rate (mg cm^{-2} day^{-1})	07/2018	08/2018	09/2018	10/2018	11/2018	12/2018	01/2019	02/2019	03/2019	04/2019	05/2019	06/2019	07/2019
Mean	9.17	25.95	41.38	13.78	11.75	27.15	39.34	17.54	1.88	0.84	4.58	7.34	1.80
median	7.95	4.83	38.66	5.46	5.36	1.16	32.48	14.34	0.96	0.39	2.04	1.78	1.73
min	1.82	0.17	5.65	0.06	0.00	0.00	6.93	1.25	0.11	0.07	0.03	0.12	0.81
lower	4.56	1.78	20.77	2.59	0.00	0.00	16.47	7.49	0.69	0.18	0.70	0.60	1.06
upper	11.02	17.00	58.00	14.34	19.96	52.70	52.54	25.38	1.51	0.66	7.35	5.50	2.48
max	22.12	465.13	97.72	80.00	54.20	108.94	118.95	66.45	6.18	5.63	17.69	65.10	3.03

90th percentile	17.65	28.00	72.66	38.27	32.18	74.69	82.59	32.53	5.36	1.40	12.29	24.80	2.92
10th percentile	3.37	0.67	11.67	0.36	0.00	0.00	11.64	2.59	0.35	0.11	0.21	0.34	0.88
n	16	27	28	31	30	31	31	27	13	30	30	30	10
St. Dev	5.81	88.36	24.31	19.54	14.51	35.20	28.86	14.55	2.06	1.33	5.19	14.08	0.84
St. Error	1.45	17.00	4.60	3.51	2.65	6.32	5.18	2.80	0.57	0.24	0.95	2.57	0.27

RMS depth	07/2018	08/2018	09/2018	10/2018	11/2018	12/2018	01/2019	02/2019	03/2019	04/2019	05/2019	06/2019	07/2019
Mean	0.02	0.02	0.03	0.02	0.02	0.04	0.04	0.04	0.02	0.03	0.03	0.03	0.02
median	0.01	0.01	0.02	0.01	0.02	0.03	0.03	0.03	0.02	0.03	0.03	0.02	0.02
min	0.00	0.00	0.00	0.00	0.00	0.00	0.00	0.00	0.00	0.00	0.00	0.00	0.00
lower	0.01	0.01	0.01	0.01	0.01	0.02	0.02	0.02	0.01	0.02	0.02	0.01	0.01
upper	0.02	0.02	0.03	0.02	0.03	0.05	0.05	0.06	0.03	0.05	0.04	0.03	0.03
max	0.05	0.11	0.21	0.17	0.14	0.22	0.30	0.30	0.15	0.14	0.14	0.16	0.10
90th percentile	0.03	0.03	0.05	0.04	0.05	0.08	0.07	0.08	0.04	0.06	0.06	0.05	0.04
10th percentile	0.01	0.01	0.01	0.01	0.01	0.01	0.02	0.01	0.01	0.01	0.01	0.01	0.01
n	2448	4458	4320	4463	4243	4464	4462	4028	4463	4320	4242	4320	2016
St. Dev	0.01	0.01	0.02	0.02	0.02	0.03	0.03	0.03	0.02	0.02	0.02	0.02	0.01
St. Error	0.00	0.00	0.00	0.00	0.00	0.00	0.00	0.00	0.00	0.00	0.00	0.00	0.00

Temp. (°C)	07/2018	08/2018	09/2018	10/2018	11/2018	12/2018	01/2019	02/2019	03/2019	04/2019	05/2019	06/2019	07/2019
Mean	21.66	22.29	23.84	26.14	27.92	28.46	27.69	27.77	28.51	26.39	24.29	22.45	21.80
median	21.65	22.32	23.85	26.28	27.84	28.13	27.68	28.11	28.44	26.21	23.90	22.52	21.79
min	20.43	21.40	22.84	23.34	26.97	27.05	26.95	26.20	27.58	25.27	23.19	21.40	21.33
lower	21.23	22.01	23.58	25.04	27.52	27.70	27.45	26.63	28.09	25.84	23.56	21.86	21.64
upper	22.14	22.59	24.14	27.48	28.27	29.20	27.93	28.71	28.97	26.85	25.18	22.88	22.04
max	22.76	23.82	24.75	28.56	29.25	30.69	28.34	30.06	29.69	28.34	25.96	23.99	22.27
90th percentile	22.49	22.79	24.33	27.87	28.64	30.00	28.08	29.14	29.23	27.52	25.64	23.30	22.13
10th percentile	20.86	21.77	23.28	23.97	27.35	27.50	27.33	26.51	27.74	25.62	23.42	21.67	21.47
n	2448	4458	4320	4463	4234	4464	4462	4020	4457	4320	4242	4320	2016
St. Dev	0.57	0.37	0.40	1.45	0.50	0.93	0.29	1.12	0.54	0.72	0.86	0.62	0.24
St. Error	0.01	0.01	0.01	0.02	0.01	0.01	0.00	0.02	0.01	0.01	0.01	0.01	0.01

Light (mol quanta m^{-2} day^{-1})	07/2018	08/2018	09/2018	10/2018	11/2018	12/2018	01/2019	02/2019	03/2019	04/2019	05/2019	06/2019	07/2019
Mean	4.63	3.71	3.16	3.33	2.48	1.83	1.88	1.17	1.42	0.07	0.02	2.38	2.15
median	4.60	3.92	2.88	3.58	1.14	0.60	1.87	1.07	1.18	0.00	0.00	2.23	2.26
min	3.29	0.94	0.41	0.22	0.05	0.00	0.00	0.00	0.22	0.00	0.00	0.25	0.97
lower	4.23	2.87	2.19	2.93	0.29	0.09	0.51	0.02	0.76	0.00	0.00	1.87	1.92
upper	5.22	4.75	3.93	4.09	4.86	2.76	3.20	1.95	1.69	0.00	0.00	2.92	2.54
max	5.89	5.17	6.10	5.39	6.40	7.24	4.09	3.03	5.53	0.77	0.67	4.21	2.87
90th percentile	5.36	4.89	5.46	4.69	5.65	6.18	3.48	2.79	2.74	0.20	0.00	3.83	2.75

10th percentile	3.62	2.57	1.59	1.39	0.20	0.02	0.01	0.00	0.31	0.00	0.00	1.20	1.31
n	17	31	30	31	30	31	31	28	31	30	30	30	14
St. Dev	0.71	1.12	1.46	1.26	2.35	2.37	1.33	1.10	1.18	0.19	0.12	1.01	0.57
St. Error	0.17	0.20	0.27	0.23	0.43	0.43	0.24	0.21	0.21	0.03	0.02	0.18	0.15

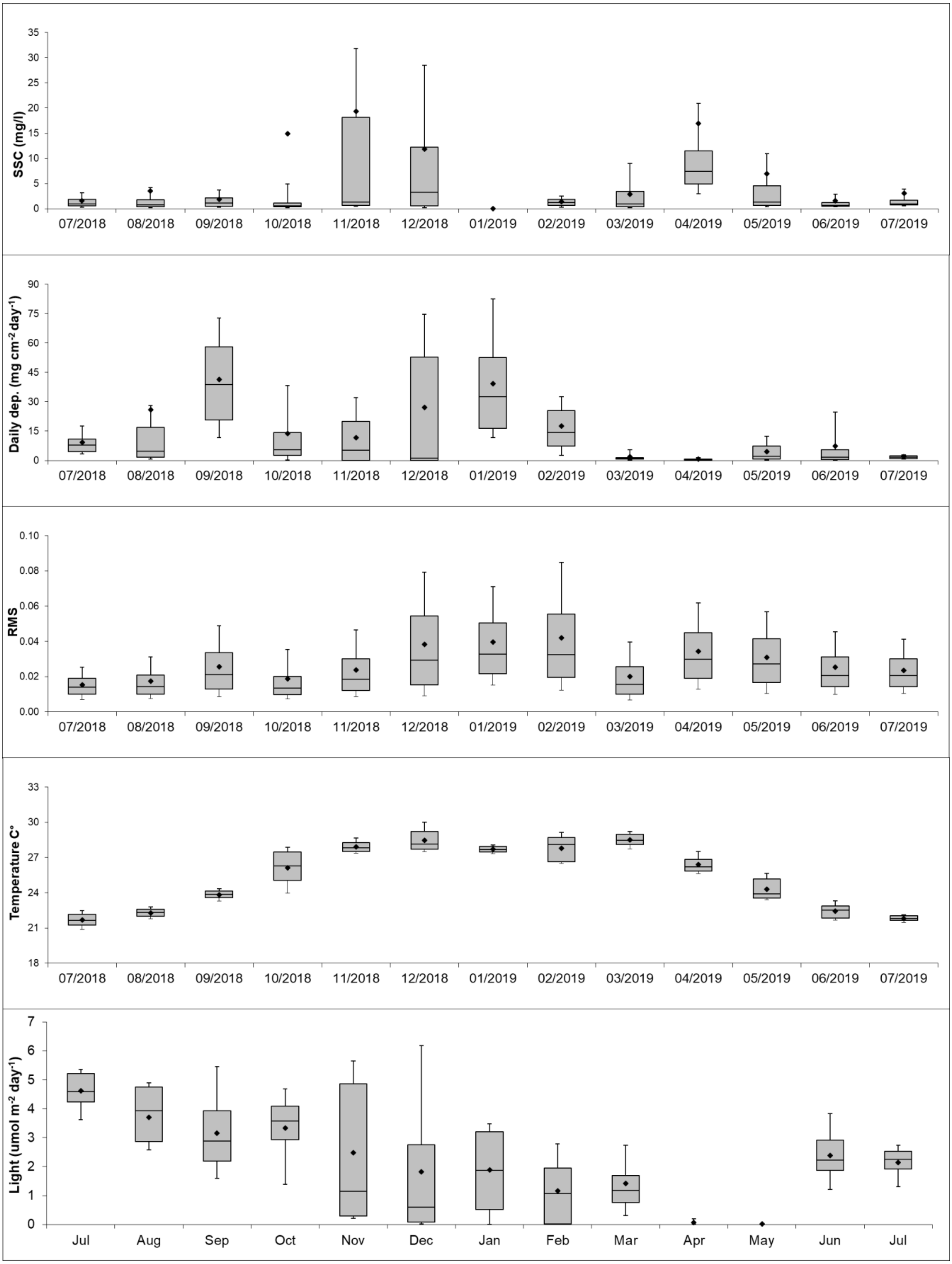
SSC (mg/l)
Daily dep. (mg cm⁻² day⁻¹)
RMS
Temperature C°
Light (umol m⁻² day⁻¹)
07/2018
08/2018
09/2018
10/2018
11/2018
12/2018
01/2019
02/2019
03/2019
04/2019
05/2019
06/2019
07/2019
Jul
Aug
Sep
Oct
Nov
Dec
Jan
Feb
Mar
Apr
May
Jun
Jul

A1.3.5 AMB 5: Holbourne

SCC (mg/L)	07/2018	08/2018	09/2018	10/2018	11/2018	12/2018	01/2019	02/2019	03/2019	04/2019	05/2019	06/2019	07/2019
Mean	9.67	1.49	5.54		0.28	0.90	0.57	1.07	2.53	4.15	7.62	5.61	16.40
median	0.46	0.26	4.41		0.16	0.61	0.49	0.73	1.08	2.81	6.20	3.08	11.92
min	0.00	0.00	0.00		0.00	0.00	0.00	0.00	0.00	0.19	1.63	0.00	0.00
lower	0.22	0.14	2.43		0.07	0.29	0.28	0.38	0.38	1.26	4.05	1.85	8.72
upper	3.95	0.63	7.13		0.35	1.24	0.70	1.34	2.64	5.05	9.03	5.24	17.60
max	398.24	169.55	35.63		3.97	4.02	3.93	16.15	31.62	91.96	69.88	546.13	444.23
90th percentile	25.78	1.77	10.64		0.62	2.17	1.02	2.41	6.83	8.78	13.15	9.08	27.31
10th percentile	0.08	0.07	1.48		0.01	0.11	0.11	0.16	0.12	0.80	3.08	1.21	6.85
n	2133	4446	1158	0	1695	4225	4418	3074	4405	4315	576	4313	2016
St. Dev	30.18	8.74	4.48		0.39	0.85	0.51	1.21	4.00	4.77	6.00	18.20	21.03
St. Error	0.65	0.13	0.13		0.01	0.01	0.01	0.02	0.06	0.07	0.25	0.28	0.47

Daily dep. rate (mg cm-^{2} day^{-1})	07/2018	08/2018	09/2018	10/2018	11/2018	12/2018	01/2019	02/2019	03/2019	04/2019	05/2019	06/2019	07/2019
Mean	0.20	0.26	0.91		5.90	19.07	17.10	13.38	0.47			3.22	3.85
median	0.02	0.13	0.91		3.25	16.62	16.40	0.02	0.07			2.81	3.12
min	0.00	0.02	0.78		0.14	1.52	5.93	0.00	0.00			0.85	0.77
lower	0.01	0.09	0.84		1.54	9.08	10.25	0.01	0.02			1.77	2.40
upper	0.05	0.29	0.98		6.39	24.24	22.60	15.57	0.68			4.51	5.30
max	2.59	1.34	1.05		30.53	53.12	38.41	116.12	2.63			8.25	8.77

90th percentile	0.20	0.62	1.02		11.78	34.31	28.10	20.07	1.39			5.36	6.36
10th percentile	0.00	0.05	0.80		0.43	5.75	7.03	0.00	0.00			1.34	1.90
n	17	29	2	0	13	31	31	21	25	0	0	30	12
St. Dev	0.62	0.29	0.19		8.17	13.01	8.40	31.47	0.72			1.93	2.29
St. Error	0.15	0.05	0.14		2.27	2.34	1.51	6.87	0.14			0.35	0.66

RMS depth	07/2018	08/2018	09/2018	10/2018	11/2018	12/2018	01/2019	02/2019	03/2019	04/2019	05/2019	06/2019	07/2019
Mean	0.009	0.010	0.014	0.022	0.017	0.024	0.021	0.025	0.012	0.022	0.016	0.019	0.017
median	0.009	0.009	0.012	0.019	0.011	0.018	0.018	0.021	0.010	0.019	0.015	0.016	0.015
min	0.000	0.000	0.000	0.003	0.000	0.000	0.004	0.003	0.001	0.003	0.003	0.003	0.000
lower	0.006	0.007	0.008	0.012	0.008	0.011	0.013	0.014	0.007	0.013	0.010	0.010	0.010
upper	0.011	0.012	0.017	0.030	0.019	0.032	0.027	0.031	0.015	0.028	0.020	0.023	0.021
max	0.030	0.068	0.107	0.448	0.181	0.176	0.106	0.124	0.061	0.103	0.065	0.090	0.063
90th percentile	0.015	0.017	0.024	0.038	0.036	0.048	0.038	0.044	0.023	0.038	0.026	0.034	0.029
10th percentile	0.004	0.005	0.006	0.007	0.006	0.007	0.009	0.010	0.005	0.009	0.008	0.008	0.008
n	2448	4455	4320	628	1725	4464	4462	3104	4461	4320	1464	4320	2016
St. Dev	0.004	0.005	0.008	0.021	0.017	0.018	0.012	0.015	0.008	0.012	0.008	0.011	0.009
St. Error	0.000	0.000	0.000	0.001	0.000	0.000	0.000	0.000	0.000	0.000	0.000	0.000	0.000

Temp. (°C)	07/2018	08/2018	09/2018	10/2018	11/2018	12/2018	01/2019	02/2019	03/2019	04/2019	05/2019	06/2019	07/2019
Mean	22.44	23.01			27.47	27.73	27.66	28.06	27.97	27.03	26.05	23.13	22.26
median	22.43	23.03			27.40	27.63	27.63	27.87	28.08	26.93	26.06	23.16	22.30
min	21.61	21.95			26.80	26.59	26.87	26.82	26.44	25.99	25.84	21.43	21.38
lower	22.12	22.91			27.13	27.47	27.54	27.74	27.59	26.58	25.97	22.75	22.19
upper	22.77	23.16			27.72	27.86	27.74	28.36	28.36	27.52	26.14	23.36	22.38
max	23.25	23.62			31.25	29.44	28.61	29.61	28.77	28.17	26.21	24.56	22.58
90th percentile	22.94	23.28			28.22	28.37	27.83	28.81	28.46	27.82	26.18	24.12	22.45
10th percentile	21.98	22.71			26.96	27.16	27.46	27.59	27.41	26.42	25.90	22.40	22.01
n	2448	2502	0	0	1725	4464	4249	3008	4461	4320	1422	4320	2016
St. Dev	0.38	0.23			0.44	0.51	0.22	0.48	0.43	0.53	0.10	0.59	0.18
St. Error	0.01	0.00			0.01	0.01	0.00	0.01	0.01	0.01	0.00	0.01	0.00

Light (mol quanta m^{-2} day^{-1})	07/2018	08/2018	09/2018	10/2018	11/2018	12/2018	01/2019	02/2019	03/2019	04/2019	05/2019	06/2019	07/2019
Mean	1.79	6.69	7.38		17.45	9.07	7.74	3.25	3.04	3.87	3.12	5.43	6.17
median	1.81	8.74	6.61		18.47	9.21	5.79	1.93	2.28	3.91	3.28	5.62	6.50
min	1.58	0.51	3.98		7.96	0.33	1.33	0.85	0.65	1.93	2.15	2.08	2.44
lower	1.75	1.61	5.32		15.75	5.36	3.19	1.64	1.86	3.27	2.78	5.06	6.02
upper	1.84	10.08	9.84		19.59	11.36	12.11	2.28	3.89	4.26	3.61	6.35	7.09
max	1.91	11.62	11.29		21.43	19.47	17.46	11.21	7.71	6.14	3.77	7.30	8.27
90th percentile	1.88	11.05	11.12		20.47	16.29	13.29	9.74	6.58	5.18	3.71	6.58	7.21
10th percentile	1.69	1.50	4.47		14.95	2.82	2.09	1.45	1.64	2.44	2.40	4.06	4.02
n	17	31	28	0	13	31	31	20	31	30	4	30	11
St. Dev	0.08	4.14	2.48		3.51	4.98	5.18	3.28	1.93	1.05	0.73	1.24	1.62
St. Error	0.02	0.74	0.47		0.97	0.89	0.93	0.73	0.35	0.19	0.36	0.23	0.49

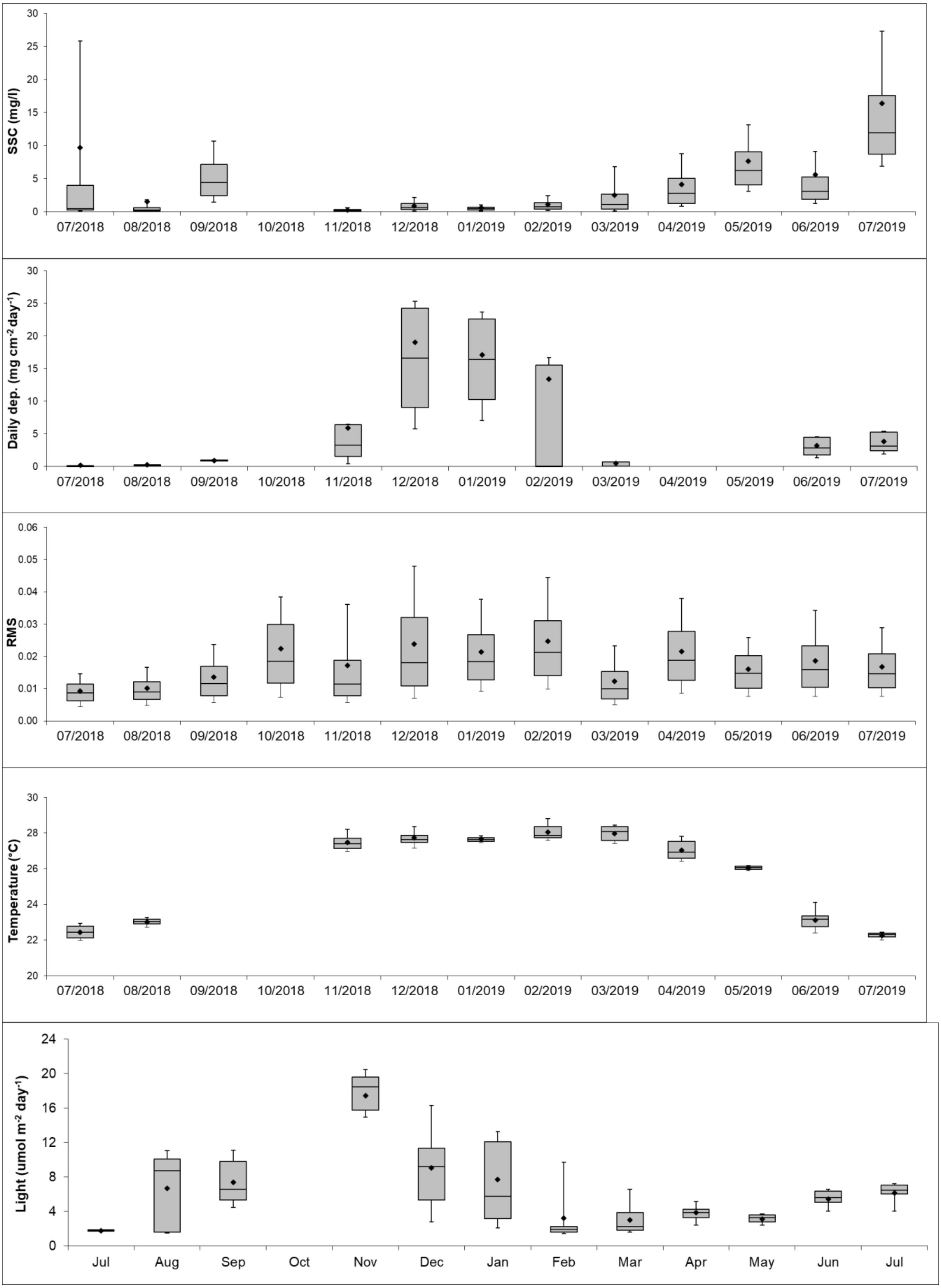
SSC (mg/l)
0
5
10
15
20
25
30
07/2018
08/2018
09/2018
10/2018
11/2018
12/2018
01/2019
02/2019
03/2019
04/2019
05/2019
06/2019
07/2019
Daily dep. (mg cm⁻² day⁻¹)
0
5
10
15
20
25
30
07/2018
08/2018
09/2018
10/2018
11/2018
12/2018
01/2019
02/2019
03/2019
04/2019
05/2019
06/2019
07/2019
RMS
0.00
0.01
0.02
0.03
0.04
0.05
0.06
07/2018
08/2018
09/2018
10/2018
11/2018
12/2018
01/2019
02/2019
03/2019
04/2019
05/2019
06/2019
07/2019
Temperature (°C)
20
22
24
26
28
30
07/2018
08/2018
09/2018
10/2018
11/2018
12/2018
01/2019
02/2019
03/2019
04/2019
05/2019
06/2019
07/2019
Light (umol m⁻² day⁻¹)
0
4
8
12
16
20
24
Jul
Aug
Sep
Oct
Nov
Dec
Jan
Feb
Mar
Apr
May
Jun
Jul

A1.4 Marotte current meter animations

Link to short video:

https://jamescookuniversity-my.sharepoint.com/:v:/r/personal/rachael_macdonald_jcu_edu_au/Documents/NQBP%20Ambient%20Marine%20Water%20Quality%20Monitoring%20Program/Bowen/Marotte%20video/bowen_cm_month.avi?csf=1&e=FQTmzI

Link to long video:

https://jamescookuniversity-my.sharepoint.com/:v:/r/personal/rachael_macdonald_jcu_edu_au/Documents/NQBP%20Ambient%20Marine%20Water%20Quality%20Monitoring%20Program/Bowen/Marotte%20video/bowen_cm_year.avi?csf=1&e=CFfuap

Centre for Tropical Water and Aquatic
Ecosystem Research (TropWATER)

ATSIP Building
James Cook University
Townsville Qld 4811

Phone: 07 4781 4262
Fax: 07 4781 5589
Email: TropWATER@jcu.edu.au
Web: www.jcu.edu.au/tropwater/